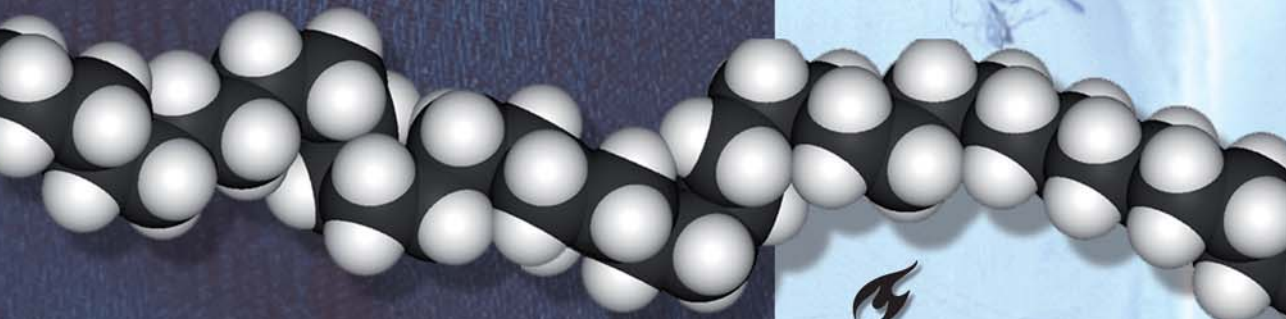


Béate D. Heru Utomo

High-speed Impact Modelling and Testing of Dyneema composite



High-speed Impact Modelling and Testing of Dyneema Composite

PROEFSCHRIFT

ter verkrijging van de graad van doctor
aan de Technische Universiteit Delft,
op gezag van de Rector Magnificus Prof. ir. K.Ch.A.M. Luyben,
voorzitter van het College voor Promoties,
in het openbaar te verdedigen
op maandag 21 november 2011 om 15.00 uur
door

Béate Deborah HERU UTOMO

ingenieur Luchtvaart- en Ruimtevaarttechniek
geboren te Dordrecht.

Dit proefschrift is goedgekeurd door de promotoren:

Prof. dr. ir. L.J. Ernst en Prof. dr. ir. D.J. Rixen

Samenstelling promotiecommissie:

Rector Magnificus	voorzitter
Prof. dr. ir. L.J. Ernst	Technische Universiteit Delft, promotor
Prof. dr. ir. D.J. Rixen	Technische Universiteit Delft, promotor
Prof. dr. ir. R. Marissen	Technische Universiteit Delft
Prof. dr. ir. R. Akkerman	Universiteit Twente
Prof. dr. E.P. Farenthold	University of Texas
Prof. dr. D.A. Cendón Franco	Universidad Politécnica de Madrid
ir. M.J. van der Jagt-Deutekom	TNO, adviseur

Copyright © 2011 by B.D. Heru Utomo

All rights reserved. No part of the material protected by this copyright notice may be reproduced or utilized in any form or by any means, electronic or mechanical, including photocopying, recording or by any information storage and retrieval system, without written permission of the copyright owner.

Printed in the Netherlands by *Ipskamp Drukkers B.V.*

Cover photography by S.J. Hebly

ISBN/EAN: 978-94-6191-023-3

Preface

Delft, November 2011

People like to throw an object and hit a target with it. Just think about children playing darts or about a teenage boy that throws a small paper aircraft to a girl in his class to draw her attention. When we become older, most of us still like to play ball games like hockey or football in which we score points if we are able to hit a target with a ball. Besides of all ages, throwing objects at targets is also of all times. An example of this is a hunter in the Stone Age that shoots an arrow on a pig in order to provide food for his family. Or more recently, hooligans that throw stones at a window.

These are all examples of impact, which is actually an interaction of one object with another. In the last couple of years, I studied impact phenomena. More specifically, I studied impact of a small projectile on a square Dyneema composite plate. This study is described in the thesis lying in front of you. I invite you to read further and hope that it will make impact on you in some way or another...

Béate Heru Utomo

Contents

Preface	v
Nomenclature	xi
Symbols	xi
Subscripts	xiii
Abbreviations	xiii
1 Introduction	1
1.1 Background	2
1.1.1 Ballistics	2
1.1.2 Viscoelasticity	3
1.1.3 Dyneema	7
1.2 Research framework	9
1.2.1 Earlier prediction approaches	9
1.2.2 Research objective	14
1.3 Research approach	14
1.3.1 Important phenomena in Dyneema laminates	14
1.3.2 Scaling issues	16
1.3.3 Property discretisation	16
1.4 Thesis outline	16
2 Terminal ballistics	19
2.1 Definitions	20
2.1.1 Impact conditions	20
2.1.2 Armour performance	22
2.2 Projectiles	26
2.2.1 Chemical Energy Projectiles	26
2.2.2 Kinetic Energy Projectiles	28
2.3 Dyneema targets	28

2.3.1	Armour requirements	28
2.3.2	Personal protection	29
2.3.3	Structural protection	29
2.4	Definition of impact in this research	30
2.4.1	Target	30
2.4.2	Projectiles	31
2.4.3	Environmental conditions	31
3	Dyneema behaviour	33
3.1	Built-up of Dyneema composite	34
3.1.1	Dyneema sheets	34
3.1.2	Production of Dyneema composite	35
3.2	Dyneema fibre response	36
3.2.1	Static fibre behaviour	36
3.2.2	Viscoelastic fibre response	38
3.2.3	Fibre response on projectile impact	40
3.2.4	Analysis of Dyneema fibre	46
3.3	Matrix behaviour	48
3.4	Dyneema composite behaviour	48
3.4.1	Dyneema composite processing	49
3.4.2	Static laminate behaviour	53
3.4.3	Composite impact behaviour	57
3.5	Discussion of Dyneema composite behaviour under projectile impact	60
4	Discretisation of Dyneema composite	63
4.1	Overall replacement models	64
4.2	Micro-mechanical replacement models	64
4.3	Layered replacement models	67
4.3.1	Orthogonal layered model	67
4.3.2	Lumped filament-bundle model	68
5	Approaches to study impact on Dyneema composite	71
5.1	Empirical methods	72
5.1.1	Empirical methods employed for impact on fibre reinforced composites	72
5.1.2	Discussion of empirical methods in impact problems	72
5.2	Simulation methods	72
5.2.1	Simulations of impact on fibre reinforced composites	73
5.2.2	Discussion of simulations in Dyneema impact problems	73
5.3	Used simulation software packages	73
5.3.1	Commercial code	73
5.3.2	Constitutive models	73
5.3.3	Element library	74
5.3.4	Integration schemes	74

5.3.5	Discussion of simulation software	74
6	Orthogonal layered model	77
6.1	Previous work on Layered modelling	78
6.2	Description of the Orthogonal layered model	79
6.2.1	Principle	79
6.2.2	Model description	80
6.3	Convergence test	89
6.4	Simulation results	95
6.4.1	Physical processes observed in real composite	96
6.4.2	Physical processes observed in simulations	97
6.5	Discussion of Orthogonal layered model	102
7	Lumped filament-bundle model	105
7.1	Description of Lumped filament-bundle model	106
7.1.1	Principle	106
7.1.2	Model description	109
7.2	Convergence tests	112
7.2.1	Tensile test	112
7.2.2	Ballistic test	117
7.3	Simulation results	120
7.3.1	Physical processes observed in simulation	120
7.3.2	Discussion of Lumped filament-bundle model	123
7.4	Discussion	128
8	Conclusions and recommendations	131
	Summary	135
	Samenvatting	141
	Acknowledgements	147
	About the author	153
	Bibliography	155

Nomenclature

Symbols

Symbol	Unit	Description
b	m	Width
c	N/m	Spring constant
c	m/s	Material wave velocity
\bar{D}	s^{-1}	strain rate tensor
f	Hz	Frequency
m	kg	Mass
p	N/m^2	Pressure
s	m	Distance
s_{proj}	m	Projected size of projectile on target
t	m	Thickness
t	s	Time
t_i	N/m^2	Traction in direction i
t_i^0	N/m^2	Threshold value of traction i -direction
u	m	Displacement
v	m/s	Velocity
x_j	m	Lagrangian coordinates
z	$-$	Number of filaments in truss element
A	m^2	Area
C_l	m/s	Longitudinal wave velocity
C_s	m/s	Transverse wave velocity
D	N/m^2	Creep compliance
E	N/m^2	Young's modulus
\bar{E}	N/m^2	Stiffness matrix
F	N	Force

Symbols (continued)

Symbol	Unit	Description
G_f	J/m^2	Fracture energy
I	Ns	Momentum
K_c	N/m^3	Spring stiffness of cohesive elements
L	m	Length
\bar{R}	m	Rotation matrix
S	m^2	Surface
T	$^{\circ}K$	Absolute temperature
T_0	N	Pretension force
T_c	m	Cohesive zone thickness
T_g	$^{\circ}K$	Glass transition temperature
T^{ν}	N/m^2	Surface traction
T_m	$^{\circ}K$	Melting temperature
U	J	Internal energy
$U_{kin,r}$	J	Residual kinetic energy
V	m^3	Volume
V_5	m/s	Projectile velocity (5% chance on perforation)
V_{50}	m/s	Projectile velocity (50% chance on perforation)
V_{95}	m/s	Projectile velocity (95% chance on perforation)
V_p	m/s	Projectile velocity
X	N/m^3	Body force
t	m	Thickness
α	deg	Total angle of attack
γ	deg	Total angle of attack
ϵ	-	Strain
ϵ	-	Logarithmic strain
λ	-	True strain
φ	deg	Roll
θ	deg	Pitch
ψ	deg	Yaw
$\bar{\epsilon}$	-	Strain tensor
μ	N/m	Tenacity
ρ	kg/m^3	Density
$\bar{\rho}_c$	N/m^2	Areal density of cohesive elements
σ	N/m^2	Stress
θ	deg	yaw

Subscripts

Subscript	Description
del	Delamination
mod	Modified
ov	Overall
1	In-plane direction
2	In-plane direction
3	Through thickness direction (out-of-plane)

Abbreviations

Abbreviation	Description
ADAMMO	Advanced Material Damage Model
AMMHIS	Advanced Material Models for Hypervelocity Impact Simulations
DMA	Dynamic Mechanical Analysis
EFP	Explosively Formed Projectiles
LFB	Lumped Filament Bundle
FSP	Fragment Simulating Projectile
HB	Hard Ballistics
OLM	Orthogonal Layered Model
PE	Polyethylene
PUR	Polyurethane Rubber
SB	Soft Ballistics
SEM	Scanning Electronic Microscope
STANAG	Standardization Agreement (NATO)
SVR	Still Video Range
UD	Uni-directional
UHMW PE	Ultra High Molecular Weight Polyethylene

Chapter 1

Introduction

Fibre reinforced armour materials, such as Dyneema composite, can give protection against projectile impact. It is important to know what happens inside the armour material due to impact, because this knowledge can help to further improve the performance of such materials. Current imaging techniques do not allow for a look inside the armour material during the impact process for every material. In order to obtain insight in the processes that occur within the material during an impact event, two numerical models are developed in this research that both offer the possibility to study the behaviour of Dyneema composite during impact in more detail.

This introductory chapter gives background information (1.1), a description of this research (1.2) and the research approach that is used to cope with the challenges that are posed by this research (1.3). In the subsequent chapters, the topics that are addressed here will be described in more detail.

1.1 Background

In this section some background information is given about the ballistics field. Because Dyneema is a viscoelastic polymer, the basic principles of viscoelasticity are described thereafter. This section will conclude with some general information about Dyneema, which is the material of interest in this research.

1.1.1 Ballistics

When you ask people what ballistics means, they will most probably answer that it is the science that studies the flight trajectory of a projectile. However, the ballistics field is much broader than that. The processes of the entire firing sequence are covered in the field of ballistics; from processes before the actual launch until the damage that the projectile does to its target due to impact.

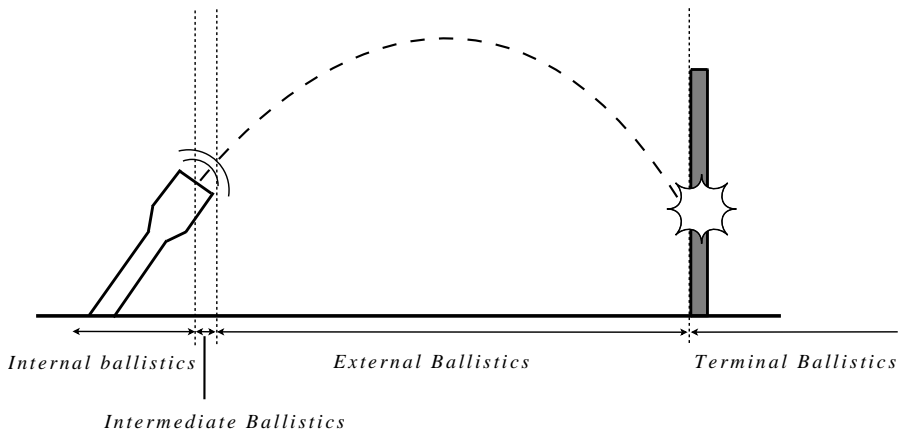


Figure 1.1: *Schematic representation of Ballistics field of study*

Figure 1.1 schematically shows what is covered by the ballistics field of study. The science of ballistics is often divided into four sub fields, namely internal ballistics, intermediate ballistics, external ballistics and terminal ballistics, see reference [1].

Internal Ballistics

The internal ballistics field studies the processes that take place prior to the moment that the projectile leaves the barrel; i.e. the processes that take place at the beginning of a firing sequence. Optimising the shape of gun powder propellants for maximising performance and studying pressure profiles of propellants are examples of subjects that are studied within this field.

Intermediate Ballistics

Just before the projectile starts its flight trajectory, phenomena such as shock waves and flash lights are observed in vicinity of the exit of the barrel. Intermediate ballistics is the scientific field that studies these phenomena. These phenomena influence the flight trajectory of the projectile and it is therefore useful to know what happens just before flight.

External Ballistics

When the projectile leaves the barrel, its flight trajectory starts. If it would be flying in vacuum, its trajectory would be a perfectly defined parabolic curve. Since projectiles do not usually fly in vacuum, their actual trajectories deviate from a parabolic one. The field of external ballistics studies the flight trajectory of a projectile, how it is influenced by external factors such as aerodynamic forces and how a smart projectile design can lead to a predictable and stable flight.

Terminal Ballistics

If a projectile impacts on a target, it interacts with it. Terminal ballistics studies the effect of projectile impact on a target. This thesis concerns the field of terminal ballistics and especially focuses on what happens within a flat Dyneema composite plate when it is impacted by a projectile with velocities between 200-500 m/s . More details on the terminal ballistics field are given in *Chapter 2 Terminal ballistics*.

1.1.2 Viscoelasticity

Dyneema is a viscoelastic material. The response of viscoelastic materials to loading are -unlike elastic materials- time dependent. For an elastic material, the stress-strain relationship is given by Hooke's law, see reference [2]:

$$\sigma = E \cdot \epsilon \quad (1.1)$$

If we have a sample of a perfect elastic material and apply a step stress σ_0 at time t_0 , the material will (theoretically) immediately respond with a strain ϵ_0 , see figure 1.2. As long as the applied stress is σ_0 , the strain in the sample will be ϵ_0 .

Creep

When we apply the same step stress σ_0 as shown in figure 1.2 a) to a viscoelastic material sample, the strain response in the sample is a function of time. This is schematically shown in figure 1.3. At time t_0 , there is an initial strain response. The amount of strain increases with time, while the stress remains constant.

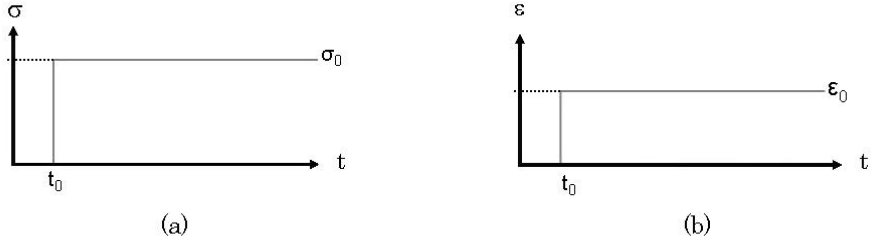


Figure 1.2: *Response of an elastic material to a step stress, a) step stress, b) strain response to step stress*

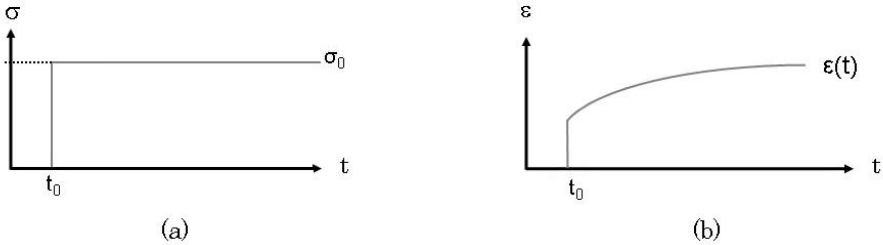


Figure 1.3: *Creep response of a viscoelastic material to step stress, a) step stress σ_0 at t_0 , b) strain response to step stress*

This time dependency, which is referred to as creep, implies that the Young's modulus of the material depends on the loading rate. The stress-strain relationship is then as follows, see references [3] and [4]:

$$\epsilon(t) = D(t - t_0) \cdot \sigma_0 \quad (1.2)$$

In this equation, $D(t)$ is the so-called creep compliance. $D(t)$ can be determined by putting a weight on a viscoelastic sample and monitor the increase in length as a function of time, see reference [5].

Stress Relaxation

If a strain step is applied to the same viscoelastic sample instead of a stress step, it also behaves differently compared to an elastic material. If a step strain is applied to a sample of elastic material, it will immediately give a stress response that is constant in time and we could just interchange graphs a) and b) from figure 1.2.

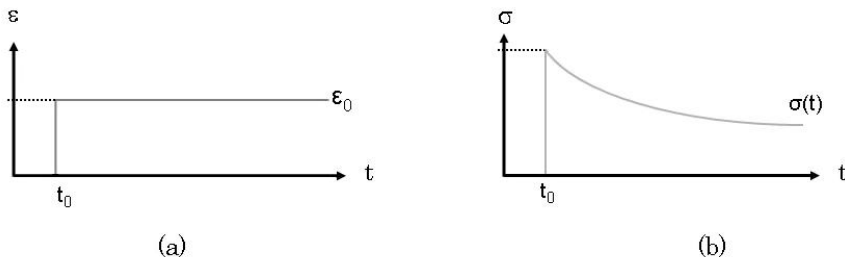


Figure 1.4: *Relaxation response of a viscoelastic material to a step strain, (a) step strain ϵ_0 at t_0 , (b) stress response to step strain*

The schematic stress response of a viscoelastic material sample to a strain step is shown in figure 1.4. At time t_0 , a step strain applied to the viscoelastic material is shown. Initially, the material responds to this strain step with a certain stress. This stress, however, decreases with time. This phenomenon is referred to as stress relaxation. The response of the viscoelastic material to a step strain can be described as in references [3] and [4]:

$$\sigma(t) = E(t - t_0) \cdot \epsilon_0 \quad (1.3)$$

$E(t)$ is the so-called relaxation modulus and can be seen as the time dependent version of the Young's modulus of a viscoelastic material. In stress relaxation experiments, a constant strain is applied to a specimen and the stress σ is measured as a function of time. From this, the relaxation modulus $E(t)$ can be determined.

Glassy and Rubbery state

In figure 1.5, the modulus E is plotted as a function of temperature T and loading time t . The modulus E is a function of both temperature and loading time. For low temperatures, the modulus E is high, which means that the material responds very stiff at low temperatures. The viscoelastic material is said to be in the glassy state and its response is generally brittle. If the temperature is increased, the modulus E drops and remains constant within a certain temperature range. This lower constant modulus is called the rubbery modulus and the material is said to be in its rubbery state. If the material is in the rubbery state, the material is less stiff and shows more ductile behaviour than in the glassy state .

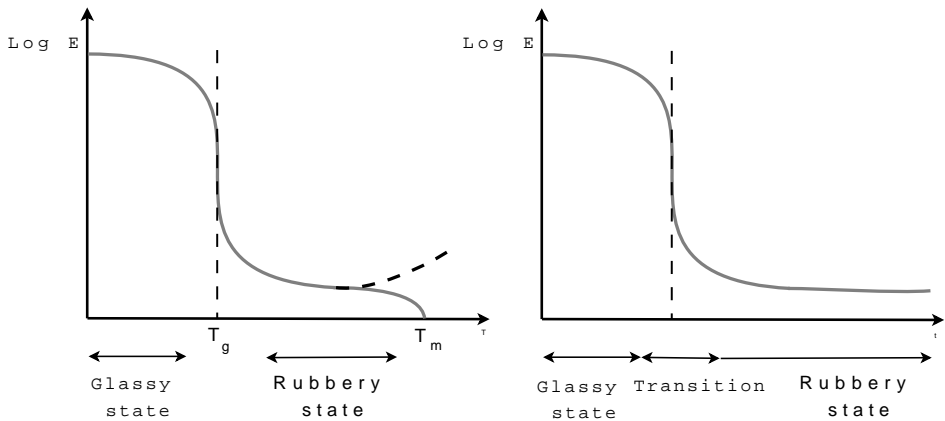


Figure 1.5: a) E modulus vs. temperature (dotted line represents a thermoset, solid line represents a thermoplastic), b) E modulus vs. loading time

Time-Temperature equivalence

In figure 1.5 b), the modulus E is plotted as a function of loading time. Again, a higher and a lower modulus can be distinguished. It is seen that for the larger part, the modulus E has a similar dependence on time and temperature. This equivalence is referred to as time-temperature equivalence and is used in the so called time-temperature superposition. Time-temperature superposition especially has a practical importance; an example is the determination of the glassy modulus by doing experiments at low temperatures for which the glassy modulus is almost the same as the modulus found at short loading times. If an entire range of E moduli should be determined, Dynamic Mechanical Analysis (DMA) is done in which a viscoelastic sample is loaded at various frequencies and/or temperatures. Here, the loading frequency is assumed to be the inverse of loading time, see reference [6].

Glass transition temperature

There is a temperature range in which a viscoelastic material undergoes a transition from the glassy state to the rubbery state and this is indicated with the glass transition temperature T_g . There are different definitions of T_g , but the definition that is most often used is the temperature at which the damping properties are the highest compared to the elastic properties. For more information, see reference [5].

The glass transition temperature T_g indicates a transition from a solid phase (glassy state) to another solid phase (rubbery state) and vice versa. The transition from the glassy state to the rubbery state is not a sharp transition, which is also shown in figure 1.5. The transition takes place within a certain

temperature range.

Melting temperature

If a viscoelastic thermoplastic material, such as Dyneema, is in the rubbery state and the temperature is further increased, the material will eventually become a fluid at the melting temperature T_m , see the solid line in figure 1.5 a). In the fluid phase, there is no longer a real stiffness and therefore, the modulus E decreases to zero.

Non-ideal viscoelastic behaviour

In figure 1.5, the solid lines represent the behaviour that is often seen with viscoelastic materials. This behaviour is considered ideal viscoelastic behaviour. There are however viscoelastic materials that show time dependent behaviour, which deviates from the $\log E$ vs. T curve shown in figure 1.5. If a viscoelastic material is in the rubbery state and the temperature is increased, viscoelastic thermoplasts become fluid. In the case of thermoset materials, e.g. natural rubber and some epoxies, the fluid state is not reached. Upon increasing the temperature of such samples, the modulus will increase again. This is indicated with the dashed line. Thermoset materials will therefore never reach a fluid state, but rather disintegrate.

Another example of non-ideal viscoelastic behaviour is that at very low temperatures, there is no real plateau for the glassy modulus. In some cases, the material can have a modulus that increases with decreasing temperature. The behaviour of most viscoelastic materials can be classified as ideal viscoelastic behaviour such as indicated with the solid line of figure 1.5.

1.1.3 Dyneema

Dyneema is a synthetic polyethylene (PE) $-\text{[CH}_2\text{]}-$ fibre that is produced using a patented gel spinning process, see reference [7]. Polyethylene gel gives a stacked lamellar structure that is oriented by stretching, see reference [8]. Because of this stretching, Dyneema fibres have a higher strength and stiffness than non-oriented polyethylene. Because of these properties, Dyneema is used in high performance applications, which are described hereafter.

Dyneema applications

Dyneema fibre is up to fifteen times stronger than steel, but has a much lower density, i.e. slightly lower than water. Its stiffness is in the order of 150 GPa . Because of these material properties Dyneema is applied in products in which both a high strength, a high stiffness and a low density is required, such as in sails, see figure 1.6.



Figure 1.6: *Dyneema sail (left), Air Cargo Container developed by DSM and DoKaSch (right). Courtesy of DSM*

Recently, at the beginning of 2008, a Dyneema Air Cargo Container is developed by DSM in cooperation with DoKaSch, see figure 1.6. This container consists of glass fibre combined with Dyneema. These glass fibres are concentrated at the outer side of the container, contributing to the bending stiffness of the container. Besides being lightweight, this combination of materials also protects the content against impact.

Dyneema is hard to process and protects very well against cutting. It is therefore very suitable for e.g. (butcher) gloves, in which cutting resistance is required. Other Dyneema applications are medical devices, such as surgical cables and orthopaedic structures, because of its low density, superior strength and stiffness and inertness to most materials. Because Dyneema can also absorb much energy, it is also applied in defence applications. For more information on Dyneema products, see reference [9].

Dyneema in defence applications

Defence applications based on Dyneema fibre-reinforced composites give protection against (small) bullets and fragments. Examples of this are helmets, vests, inserts and armoured vehicle panels.

Dyneema helmets and bullet resistant vests protect the human body against impact of small projectiles. Often, more protection is locally required, i.e. near the heart and lungs. These locations are the most lethal parts of the body, see reference [10]. Additional protection to those parts is often given by inserts that are placed in a vest. Inserts are (curved) plates that can be inserted in tailor made pockets in a bullet resistant vest. In figure 1.7, a Dyneema vest and helmet are shown on the left side and Dyneema inserts are shown on the right side. Dyneema composite plates are also used in armour vehicles. Because Dyneema shows creep behaviour, it is by itself not suitable for structural applications. Dyneema plates are therefore often used in combination with e.g. armour steel.



Figure 1.7: a) Dyneema vest and helmet, b) Dyneema inserts (right). Courtesy of TNO.

Armour steel is then used in the structural part of the vehicle and Dyneema is added to bring the protection to the required level. If the vehicle would only be made of steel, its weight would be much higher than if steel is combined with Dyneema. More information about Dyneema behaviour can be found in *Chapter 3 Dyneema behaviour*.

1.2 Research framework

In this section, an overview of earlier work is given. Thereafter, the research objective is given and how the objective could be met.

1.2.1 Earlier prediction approaches

Various attempts have been made in the past to cope with the prediction of the behaviour of Dyneema laminates. In most cases, the Dyneema laminate is simplified using homogenisation techniques to describe the response of the material. We also see that this homogenisation is quite crude, see reference [11]. The approaches that are used can be divided into three categories, namely analytical approaches, empirical approaches and numerical methods. These three prediction methods, with their advantages and disadvantages, are described hereafter.

Analytical methods

The behaviour of fibre reinforced laminates can be relatively easily described analytically if they are elastic. This is usually done by defining the properties of the laminates using an orthotropic stiffness definition:

$$\epsilon_{ij} = C_{ij} \cdot \sigma_{ij} \quad (1.4)$$

with $i, j = 1..6$

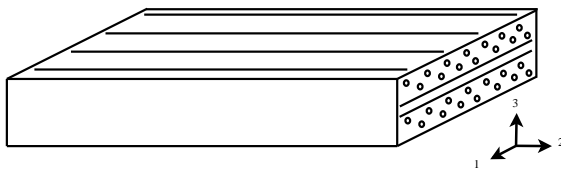


Figure 1.8: *Orientation in a laminate*

and

$$[C] = \begin{pmatrix} \frac{1}{E_{11}} & -\frac{\nu_{12}}{E_{11}} & -\frac{\nu_{13}}{E_{11}} & 0 & 0 & 0 \\ -\frac{\nu_{12}}{E_{11}} & \frac{1}{E_{22}} & -\frac{\nu_{23}}{E_{22}} & 0 & 0 & 0 \\ -\frac{\nu_{13}}{E_{11}} & -\frac{\nu_{23}}{E_{22}} & \frac{1}{E_{33}} & 0 & 0 & 0 \\ 0 & 0 & 0 & \frac{1}{G_{23}} & 0 & 0 \\ 0 & 0 & 0 & 0 & \frac{1}{G_{31}} & 0 \\ 0 & 0 & 0 & 0 & 0 & \frac{1}{G_{12}} \end{pmatrix} \quad (1.5)$$

The components ϵ_{ij} are the principle strain components, C_{ij} the entries of the stiffness matrix and σ_{ij} the directional stiffness components. The orientation that is used in this case is shown in figure 1.8. In the case of an anisotropic material, the entries C_{ij} are all different. For orthotropic fibre reinforced laminates, their behaviour can be summarised in $[C]$ as in equation 1.5, see reference [12].

The entries C_{ij} can be determined experimentally using dedicated tests. For many fibre reinforced materials, C_{ij} can also be approximated by combining the individual mechanical properties of the matrix and the fibres for fibre reinforced materials with a fibre volume content of 60% and lower using the so-called Halpin-Tsai equations, see references [13], [11] and [14]. Having a fibre volume content of more than 80 %, this theory does not apply to Dyneema laminates. We will therefore not describe the Halpin-Tsai equations in detail. It should be noted that equation 1.4 is still valid for Dyneema laminates in the elastic region, but a detailed response of Dyneema laminates cannot be determined from the Halpin-Tsai approximation. This is because Halpin-Tsai gives average values for the whole composite and does therefore not allow for studying the influence of fibre properties on the laminate. This is especially important if the failure behaviour of Dyneema laminates as a function of fibre material needs to be studied.

Describing failure in Dyneema composite analytically is more challenging than the description of the elastic behaviour. Some co-workers developed analytical formulations of more detailed behaviour such as the percentage of the material that is delaminated, see e.g. reference [15]. The percentage of the delaminated area gives an indication of how much material has failed, but does not give information on where it is exactly damaged or what it looks like (e.g. round

shaped, square shaped etc). An even more detailed, but also more complicated approach is developed by Leigh Phoenix et al. [16], who also give predictions of multi-layered systems. This model has many parameters that cannot always be experimentally determined and gives detail on a layer level. Details such as fibre failure can therefore not be predicted using this model. In a more general sense, an analytical solution for projectile impact on Dyneema fibre gives very complex methods, meaning having many parameters, with the smallest detailed predictions on a layer level. It is therefore not suitable for incorporating small details, see also *Chapter 4 Discretisation of Dyneema composite*.

Empirical methods

Empirical or semi-empirical approaches ¹ are often simpler than analytical approaches. The relation between different factors -such as impact velocity, density, stiffness etc.- are often summarised in a single formula, see reference [17]. Most researchers agree on the fact that the behaviour of a fibre reinforced composite target subjected to impact, depends on the material properties of the armour, the geometric built-up of the composite, the projectile impact velocity and the boundary conditions, see reference [18]. Most of the work in this field has been done in the 1990s and are semi-empirical methods rather than empirical methods. The difference between semi-empirical and empirical methods is that semi-empirical methods have an analytical basis but contain some experimentally determined correction factors; in empirical methods, a relation between different parameters is found using experimental data only. In general, (semi-)empirical approaches require numerous experiments. Much empirical work is done by P.M. Cunniff, who derived several relations, see for example references [17] and [19]. Most of the research in this area seems to be based on Cunniff's work, see for example references [20], [21] or [22]. Cunniff performs a dimensional analysis in which he finds the following two parameters for the analysis of a projectile-armour system:

$$\Phi \left(\frac{V_{50}}{(U^*)^{\frac{1}{3}}}, \frac{A_d \cdot A_p}{m_p} \right) \quad (1.6)$$

$$U^* = \frac{\sigma \cdot \epsilon}{2 \cdot \rho} \cdot \sqrt{\frac{E}{\rho}} = \frac{\sigma \cdot \epsilon}{2 \cdot \rho} \cdot C_l \quad (1.7)$$

Here, V_{50} represents a performance measure of the armour (see *Chapter 2 Terminal ballistics*), U^* is the product of specific toughness and longitudinal strain wave velocity C_l (see *Chapter 3 Dyneema behaviour*), A_d aerial density of the system, A_p contact area of the projectile and m_p the mass of the projectile:

¹In literature, some 'analytical' approaches can be found. Care should be taken here, because they are often semi-empirical rather than analytical

It is seen that these dimensional parameters indicate that the performance of the armour is independent of the projectile properties such as mass and density, see reference [17]. The use of dimensional analysis is often questionable, since parameters -such as areal density of the projectile and areal density of the armour- can appear more than once. If one of these parameters is more important, it will not be found using dimensional analysis. In addition, it is essential that all the parameters that influence each other are known and used in the dimensional analysis, which may not be known in advance. We find the outcome of this research questionable, because the geometric built-up and the shape of the projectile are not taken into account. Although limited in use, we do think that these relations can be used as a first approach.

Another approach including more parameters is described in reference [19], in which Cunniff predicts the ballistic limit velocity V_0 (see *Chapter 2 Terminal ballistics*) by the following relation:

$$V_0 = X_8 \cdot X_5^{\sec\theta-1} \cdot (e^{X_6 \cdot (\frac{A_D \cdot A_p}{m_p})^{X_7}} + X_9) \quad (1.8)$$

The obliquity, see also *Chapter 2 Terminal ballistics*, is represented by θ . A_p and A_D represent the contact area of the projectile with the target and the areal density of the target, respectively. The factors X_i are coefficients that should be experimentally determined. We will not discuss these factors further here. For more information, we refer to reference [19].

Empirical methods that we have seen in this field do not give information on for example a filament level, like for example filament fracture or sliding. Empirical methods treat these phenomena as a black box. That is why they are suitable for a first indication on what happens, but they are not suitable to study processes in Dyneema due to impact in detail.

Numerical methods

If we want to study details, analytical methods easily become too complicated and empirical methods are not suitable to study Dyneema processes due to projectile impact because these processes are, to our knowledge, usually considered as a black box. Numerical methods however offer the possibility to study these processes in more detail than can be done using empirical or analytical methods.

We see that numerical methods have gained importance over time. The general increase in computational capacity from the last decades allows for more possibilities in numerical approaches. From the beginning of the nineties of the twentieth century, people have become more and more interested in studying the failure phenomena of fibre reinforced composites in detail using simulations, see for example references [23], [24], [25] or [26].

In the eighties and nineties of the twentieth century, simulations were made that essentially function as a means to determine if a fibre reinforced material fails,

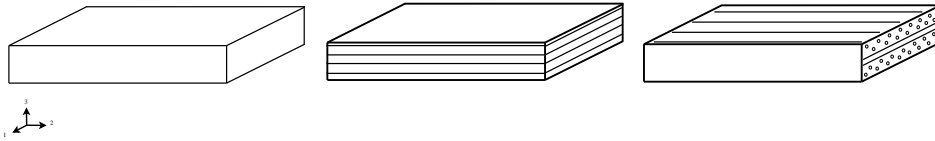


Figure 1.9: *Replacement models: a) Overall replacement model, b) Layered model, c) Micro-mechanical model*

see reference [27]. It all started with the implementation of laminate theory in numerical models, thus enabling to study average stresses, strains etc. in the fibre reinforced material at different places in the material. Fibre reinforced materials were mainly modelled using an overall replacement model, see figure 1.9 a). Different criteria for different phenomena (e.g. fibre fracture, matrix-fibre adhesion, delamination) are implemented and if one of these criteria is reached, the material is considered failed. Using an overall replacement model enables us to get an idea about the failure location, but does not allow for a detailed study, since the development of different phenomena is not shown². A deviation for fibre volume contents of more than 60 % can be explained by a different distribution of the matrix material in the composite.

For development purposes, we are not only interested in the occurrence of maximum stresses, but also in more detailed phenomena such as delamination or filament fracture. Knowledge about these kind of phenomena can facilitate the further development of materials. One of the pioneers that developed a more detailed model is Liu. Liu developed a model for delamination evolution in a fibre reinforced laminate using a layered approach, see reference [28]. In this model, it is no longer assumed that the material can be modelled with an overall replacement model, but as a number of interacting material layers, see figure 1.9 b). Modelling the material as a collection of different layers enables the assignment of different properties in different directions in each layer. This method is developed for static applications, but we believe that it is also suitable for dynamic applications. In this research, a layered model is developed for studying impact phenomena, see *Chapter 6 Orthogonal layered model*.

A layered model is very useful for studying delamination effects in fibre reinforced laminates. If more detailed phenomena on e.g. a filament bundle level need to be studied, a layered model is not suitable. Recently, it is discovered that phenomena on this scale play an important role in the material behaviour, see reference [29].

²As we have seen before, the application of laminate theory works well with fibre volume contents up to 60%, see references [13] and [14]

1.2.2 Research objective

Materials giving protection against projectile impact, such as Dyneema composite, are widely used in the defence industry. In general, defence products are improving continuously. Understanding the behaviour of such materials due to projectile impact is of crucial importance in order to be able to further improve the material.

However, it is nowadays still not possible to study the behaviour in Dyneema composite during an impact event. Acquisition systems are either too slow or too inaccurate. In this research, we are searching for a method that enables us to study effects in Dyneema composite due to projectile impact in the range of 200-500 m/s . We choose to apply simulation methodology for this purpose and our research objective is [30]:

‘to develop a simulation tool to predict the time response of flat Dyneema-composite plates that are impacted by small projectiles’

This simulation tool should give more insight into the processes that occur within a Dyneema laminate due to projectile impact. In the past, also some analytical and empirical approaches were used. Why we chose for developing a simulation tool will be described hereafter.

At TNO, simulation work has been done in the computer code Autodyn. This research is a follow up of the research done at TNO, see references [31] and [32]. In the future, the developed simulation tool could facilitate further development and improvement of Dyneema composite or any other fibre reinforced composites.

1.3 Research approach

For the development of the simulation tool, it is important to experimentally determine what phenomena take place in Dyneema composite due to projectile impact. From experiments, the most important phenomena are determined and described hereafter.

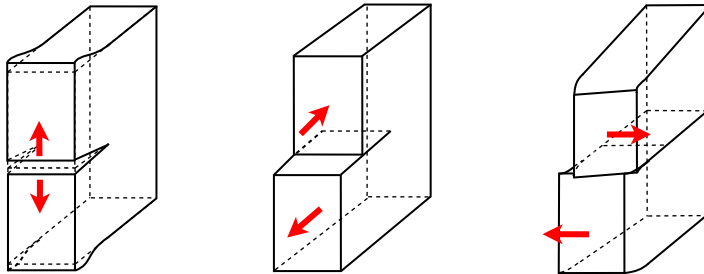
As we saw previously, earlier models did not show the details that we require for this research. This indicates that the simulation tool should be able to show more details than the aforementioned simulation models. Defining the scale on which the simulation tool should be able to describe the details is therefore important. Therefore, we will discuss on what scale the simulation tools should be developed and what approach is followed to incorporate them in the simulations.

1.3.1 Important phenomena in Dyneema laminates

If a Dyneema laminate is subjected to projectile impact, a number of processes within a few microseconds. From post impact analysis using visual inspection



Figure 1.10: *Delamination in Dyneema composite due to impact*



Mode I: Opening mode Mode II: Sliding mode Mode III: Tearing mode

Figure 1.11: *Delamination modes*

and microscopic techniques, we found that there are three phenomena that develop in Dyneema laminates due to projectile impact, namely *delamination*, *filament fracture* and *filament sliding*. On a much smaller scale, we also found some other phenomena, but they are considered less important, see also *Chapter 3 Dyneema behaviour*. The tool that is developed should therefore at least be able to describe delamination, filament fracture and filament sliding.

Delamination is defined as the debonding of layers within a laminate and an example of delamination of a Dyneema laminate after impact by 9 mm bullets is shown in figure 1.10. In this figure, we see a plate of Dyneema composite that originally has the following sizes: 400 mm by 400 mm by 5 mm . This plate has been impacted with four bullets and in figure 1.10, the effects on the rear side of the plate (opposite to the impact side) are shown. Before impact, the plate was (at least macroscopically) flat. After impact, the layers in the laminate are partially debonded and they cause the ‘hill shapes’ that are shown in the figure. These ‘hills’ are called delaminations or delaminated areas.

Debonding of layers can occur in three so-called delamination modes. The first mode is the so-called opening mode. The second and third mode are the in-plane shear mode and out-of-plane shear mode respectively, see figure 1.11. Post impact analysis shows that many filaments are broken, see *Chapter 3 Dyneema behaviour*. Due to the projectile impact, the filaments elongate and much of the projectile kinetic energy is taken up as strain energy. The interaction between the filaments and the layers determine the actual strength of the laminate. What can also be seen is that some of the filaments are not fractured, but are pushed aside from the projectile. This is the aforementioned filament sliding.

1.3.2 Scaling issues

Filament sliding, filament fracture and delamination are not correctly shown in earlier models as previously mentioned. Preferably, this should be shown by the simulation tool. However, current computational hardware puts limits on the amount of memory that is required to use the simulation tool. From experiments, it turns out that the phenomena on a layer scale are of considerable importance. Therefore, the simulation tools are developed to describe the phenomena in Dyneema composite on a layer scale.

1.3.3 Property discretisation

To incorporate delamination, filament sliding and filament fracture, properties are discretised. For this research, two simulation tools are developed. The first tool, the ‘Orthogonal layered model’, can be used to study delamination in more detail. The second tool, the ‘Lumped filament-bundle model’, can also be used for making a delamination study and can, in addition, describe filament sliding and filament fracture.

The Orthogonal layered model makes use of layered modelling, see *Chapter 6 Orthogonal layered model*. In the case of the Lumped filament-bundle model, the filament bundle properties are represented by truss elements and enables studying even more detailed phenomena than using the Orthogonal layered model. With these computer simulations, the physical processes in the Dyneema laminate due to projectile impact can be shown more accurately than with previously developed models. It is expected that these simulations can contribute to a more thorough understanding of Dyneema behaviour due to projectile impact.

1.4 Thesis outline

The goal of this research is to develop a method with which the behaviour of Dyneema composite, subjected to projectile impact, can be predicted. An

outline of this thesis is schematically shown in figure 1.12. In *Chapter 1 Introduction* and *Chapter 2 Terminal ballistics*, a framework for this research is given. Dyneema composite behaviour is studied by doing a variety of experiments. *Chapter 3 Dyneema behaviour* addresses the Dyneema (composite) behaviour under various loads. From this, the most important phenomena that are seen in Dyneema composite due to projectile impact are determined. There are several ways and different scales on which the impact problem can be described. Possible approaches are addressed in *Chapter 4 Discretisation of Dyneema composite* and *Chapter 5 Approaches to study Dyneema behaviour*. The two models, i.e. the Orthogonal layered model and the Lumped filament-bundle model, that predicted Dyneema composite behaviour due to projectile impact are described in *Chapter 6 Orthogonal layered model* and *Chapter 7 Lumped filament-bundle model*. Finally, the conclusions and recommendations are given in *Chapter 8 Conclusions and recommendations*.

Research objective

'to develop a tool to predict the time response of flat Dyneema-composite plates that are impacted by small projectiles'

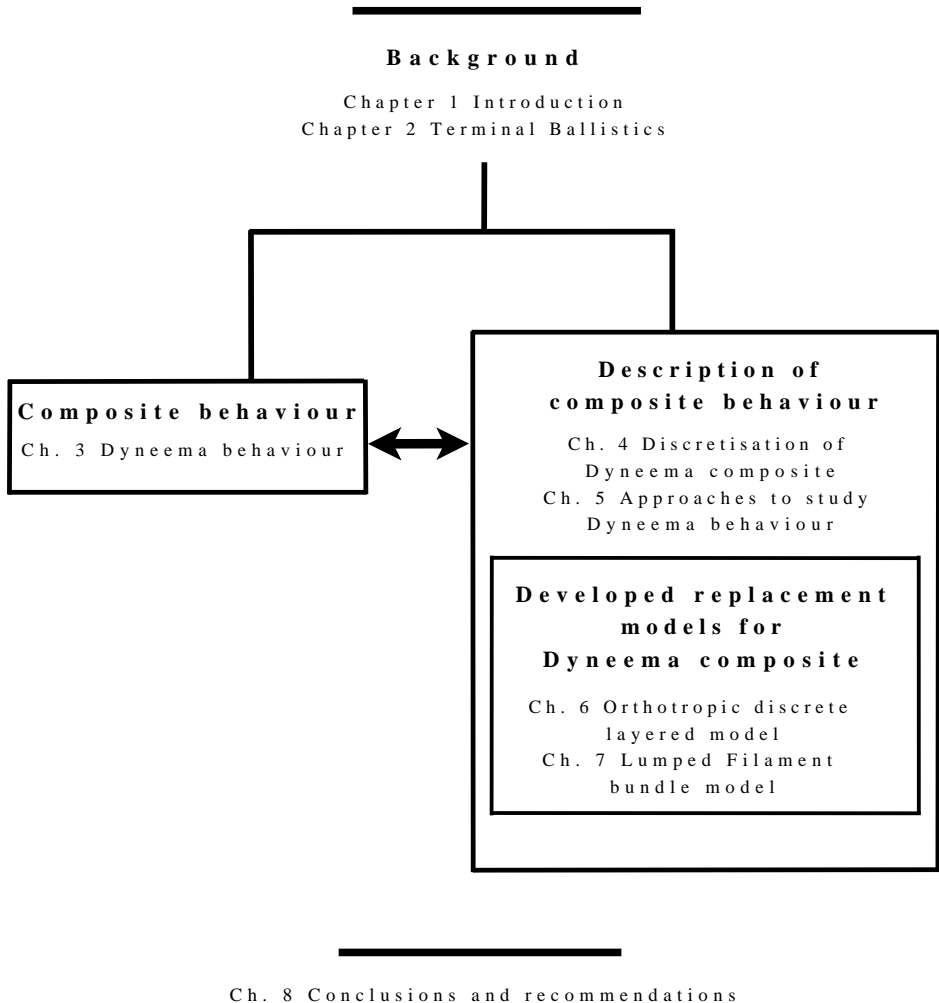


Figure 1.12: *Schematic thesis outline*

Chapter 2

Terminal ballistics

Chapter 1 Introduction states that this research is within the terminal ballistics field. In this chapter, this field is described in more detail, while keeping a focus on projectile impact on Dyneema composite. In section 2.1, often-used definitions in the terminal ballistics field are given. Terminal ballistics involves the interaction between projectile and target. An overview of commonly used projectiles and targets is given in section 2.2 and section 2.3 respectively. The combinations of target, projectile and impact conditions, which are considered in this research, are defined in section 2.4.

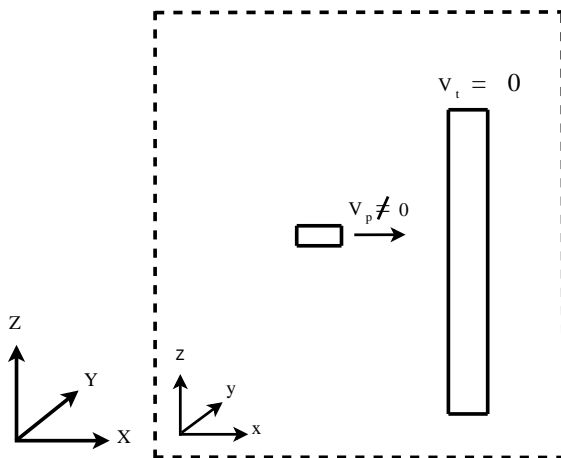


Figure 2.1: *Projectile and target*

2.1 Definitions

In this section, definitions that are commonly used in the terminal ballistics field are given. A distinction is made between definitions that are related to impact conditions and definitions that are related to armour performance.

2.1.1 Impact conditions

This research concerns the behaviour of Dyneema composite due to projectile impact. Its behaviour strongly depends on the impact configuration. It is therefore important to define the impact conditions to know about which configuration we are talking. Some commonly used definitions are given hereafter.

Projectile and target

Target and projectile interact with each other during impact. The target is usually defined as the object that is in rest in a local reference frame (x, y, z) . The projectile is then defined as the object that has a non-zero velocity with respect to that local reference frame, see figure 2.1. The target in this research is a Dyneema-composite plate, which is impacted by fragments.

The Dyneema composite studied here has a cross-ply lay-up. Changing the lay-up will influence the performance of the composite. Changing the lay-up from a cross-ply to a quasi-isotropic one, for example, will probably change the performance in terms of projectile resistance.

The projectile also influences the response of the target to impact. There are

many varieties in projectile geometry: the projectile can be tapered, have a straight body, can have a blunt or sharp nose etc. The penetration capability of the projectile depends, among others, on its geometry. A slender body is more suitable for penetrating a material than a thick body, because the energy is concentrated on a small area which allows for a high penetrability. A projectile body going from a small cross-sectional area to a bigger one can penetrate Dyneema composite relatively easy. First, a small area makes contact with the Dyneema composite and the filaments are pushed away (filament sliding) because the contact surface increases in time. If a projectile has sharp edges on the nose, the filaments directly in contact with the projectile are done more harm than if impacted by a blunt-nosed projectile. If a projectile has sharp edges, it can cut Dyneema filaments instead of only loading the filaments in tension. The deformability of the projectile, i.e. its elastic limit and its ductility, due to impact also influences the effect in the composite due to impact. This mainly depends on the ductility and the elastic limit of the projectile. If the projectile deformation causes a density increase, it can do more harm than a projectile of which the density remains the same or even decreases. In other words, a clear description of the projectile is essential.

Waves in the target

If Dyneema composite is impacted, waves start propagating through the material and they will reflect once they reach the boundaries of the composite. The waves that will initially run through the material can be described using elastic wave theory. Elastic wave theory applies to materials that follow Hooke's law, such as Dyneema. If the material is isotropic, two waves can be distinguished, namely a longitudinal (or dilational) wave and a transverse (or distortional or shear) wave, see reference [33]. The longitudinal wave velocity for an isotropic material, neglecting internal friction, is given by:

$$C_l = \sqrt{\frac{E}{\rho}} \quad (2.1)$$

and the transversal wave velocity by:

$$C_s = \sqrt{\frac{G}{\rho}} \quad (2.2)$$

Since Dyneema composite is not an isotropic material, the magnitudes of the longitudinal and transverse wave velocity can be locally different from equations 2.1 and 2.2. Note that these equations do apply within a single filament. The wave pattern at time t is determined by the interaction of the waves that propagate and their reflections. The reflection pattern is also a function of the geometry of the plate. The wave pattern depends on the geometry and material

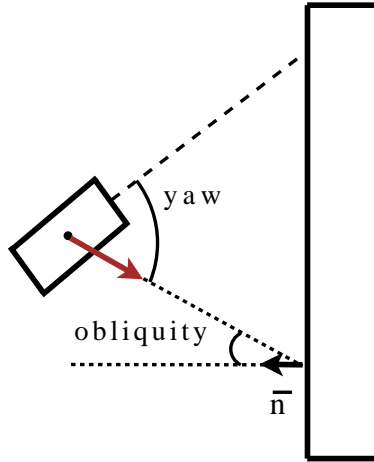


Figure 2.2: *Definition of obliquity and yaw (2D)*

properties of the target, which should both be defined to describe an impact problem.

Projectile orientation

In this research, projectile impact on a flat plate is considered. The orientation of the projectile is usually measured with respect to the normal of the plate. In ballistics, the orientation of a projectile is usually expressed using a single angle, the total angle of attack, see figure 2.2. The angle of attack α is defined as the smallest angle between the normal \bar{n} of the plate and the centreline of the projectile.

Impact velocity

The projectile impact velocity V_p is a vector. Its magnitude determines the amount of kinetic energy available to penetrate the target. It may be clear that the penetration ability increases with increasing kinetic energy of the projectile. But not only the velocity determines the penetrability of the projectile, it is often also a function of the orientation of the projectile with respect to the plate. The orientation of the velocity vector with respect to the plate is called the obliquity γ . The obliquity is defined as the smallest angle between the velocity vector and the normal of the target plate, see figure 2.2.

2.1.2 Armour performance

After impact has taken place, the ability of a Dyneema composite target to defeat projectiles can be determined. The effectiveness of the target, or armour

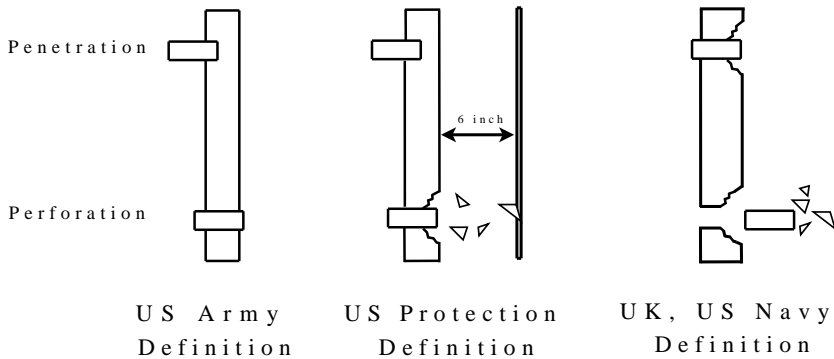


Figure 2.3: *Different definitions of penetration and perforation*

performance, can be described using the definitions given hereafter.

Penetration and perforation

If a projectile impacts on a target, the projectile may or may not go through the target. The target is said to be penetrated if the projectile is stopped by the target. This means that the projectile does not go through the target. If the projectile goes through the target, the target is said to be perforated. In literature, a penetration and a perforation, such as defined above, are often referred to as a *partial penetration* and a *complete penetration* respectively. In this text, we use the terms penetration and perforation for clarity's sake.

Among different countries and sometimes even within the same country, slightly different definitions are used for a penetration and a perforation, see figure 2.3.

The US Army defines a penetration as the case that no part of the projectile can be seen at the back of the plate, see figure 2.3 a). If part of the projectile can be seen at the back of the plate, the target is considered perforated.

The US Protection limit gives another definition for a penetration and a perforation, see figure 2.3 b). Targets are considered perforated if spall, which is caused by projectile impact, perforates a 0.5 mm thick Aluminium AL2024T4 witness plate that is placed a distance of 6" (152.44 mm) from the back of the target, see reference [34]. An example of such a witness plate is shown in figure 2.4. The white spots are areas on which spall has perforated the witness plate. By shining light on one side of the plate, these holes are projected on a screen behind the witness plate. If light spots are shown on the screen, the witness plate is considered perforated. Often, other material than AL2024 is used, because this type of aluminium is scarce and thus expensive. Each laboratory uses its own witness plate material, which is usually the same for all tests within the same laboratory. This enables making an objective comparison between targets.



Figure 2.4: *Witness plate. Courtesy of TNO*

The definitions of penetration and perforation that are used by the US Navy and in the UK are again different from the previous definitions, see figure 2.3 c). If the projectile has zero residual velocity after impact, the target is considered penetrated. The target is considered perforated if the projectile has a non-zero velocity after impact. It is seen that slightly different definitions of a penetration and a perforation exist. As a result, the performance of the same product may be different among different countries and even within the same country. In this thesis, the UK definitions for penetration and perforation will be used.

Ballistic limit (velocity)

The boundary between a penetration and a perforation case is indicated by the ballistic limit (velocity). The probability that a projectile perforates the target as a function of impact velocity is plotted in figure 2.5 for a certain projectile-target combination. In the case of a perforation, the projectile usually has a non-zero residual velocity \bar{V}_p ¹.

The highest velocity at which there is 0% chance on a perforation, meaning 100% chance on a penetration², is called the V_0 . Similarly, the V_{100} is the lowest velocity at which it is 100 % certain that the projectile perforates the target. If the projectile's impact velocity is between the V_0 and the V_{100} , it is unclear whether this will result in either a perforation or a penetration. In practise, the V_0 and the V_{100} are difficult to determine and the V_{50} is used to express the ballistic limit of a target, see reference [35]. The V_{50} is the impact velocity at

¹This depends on the used definition

²The subscript that accompanys V is in this case the % chance on a perforation

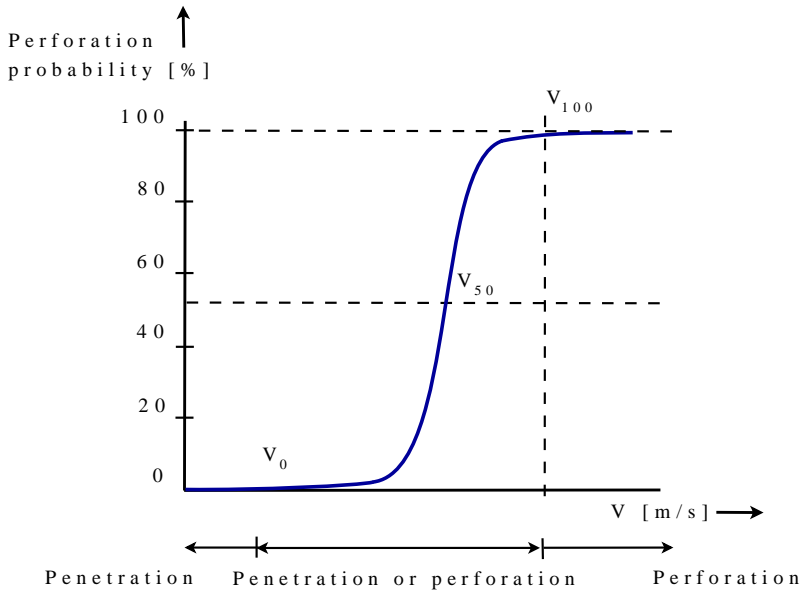


Figure 2.5: *Penetration and perforation of a target*

which the chances on a penetration and a perforation case are even; i.e. there is 50 % chance on a penetration and 50 % chance on a perforation.

The procedures to determine the V_{50} ballistic limit are described in the Standard NATO Agreement, or for short STANAG, defined by NATO countries. Still, most countries follow their own procedures to determine the V_{50} . In the Netherlands, STANAG procedures³ are usually adopted. STANAG 2920 and STANAG 4569 are usually applicable to terminal ballistic research. STANAG 2920 and is mostly used for determining the ballistic limit of Dyneema composite applications. STANAG 2920 defines a set of standards for ballistic test methods for personal armour materials and combat clothing. STANAG 4569 defines the procedures for evaluating the protection level of logistic and light armoured vehicles. To determine the V_{50} of a Dyneema composite panel, STANAG 2920 prescribes a six-shot experiment, which should result in three penetrations and three perforations. The maximum bracket of the projectile velocities in this experiment should not exceed 40 m/s. If an accurate determination of the V_{50} is required, this experiment is repeated for a number of panels and the average V_{50} values of separate targets are taken. Because the V_{50} is so often used, the term ballistic limit and the V_{50} are often used synonymously.

³New procedures to determine the ballistic limit of targets is forthcoming and are expected to come out in five years from now

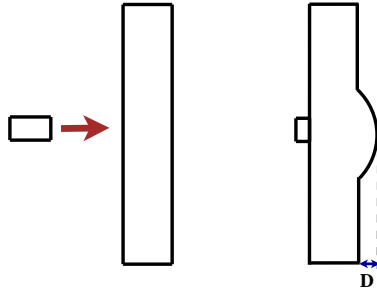


Figure 2.6: *Definition of maximum deformation of a target*

Maximum deformation

Due to projectile impact on the target, the target will deform. The maximum backside deformation, shown in figure 2.6, is a measure of target performance. In general, a small backside deformation is preferred for personal protection to minimize the seriousness of injuries.

Projectile residual velocity

If the target is perforated, the projectile continues to fly after impact with a certain velocity. This velocity is called the residual velocity. The residual velocity can, for example, be used to determine the amount of energy that is absorbed by the target. It should be noted that there are much more definitions on target performance available and only the most common definitions have been given here. The interested reader is referred to references [36], [35] and [37].

2.2 Projectiles

A wide range of projectiles is nowadays available. Projectiles are classified as either Chemical Energy (CE) based projectiles or Kinetic Energy (KE) based projectiles. In this section, we limit ourselves to projectiles that can be (partly) defeated by Dyneema composite applications.

2.2.1 Chemical Energy Projectiles

Chemical Energy projectiles⁴ require an internal explosive reaction prior to impact on a target. Due to the explosive reaction, CE projectiles obtain their final shapes. An example of a CE projectile is a grenade, which is mainly filled with explosives, see figure 2.7 a). The explosives are indicated with an arrow.

⁴Note that there is a distinction between chemical energy projectiles and chemical weapons. Generally, poisons or toxins are referred to as chemical weapons.

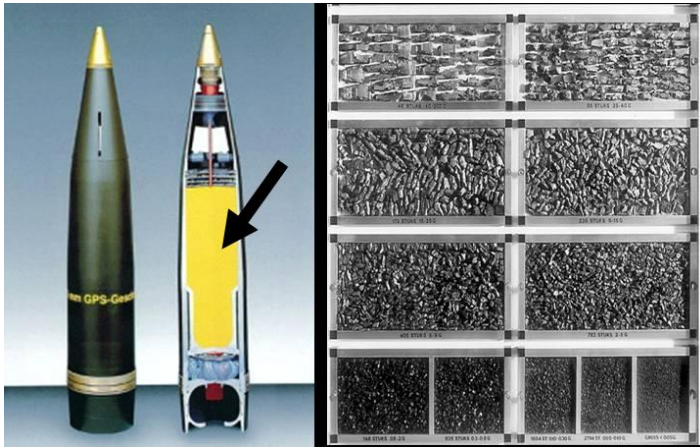


Figure 2.7: a) Grenade, b) Fragments coming from a grenade. Courtesy of TNO

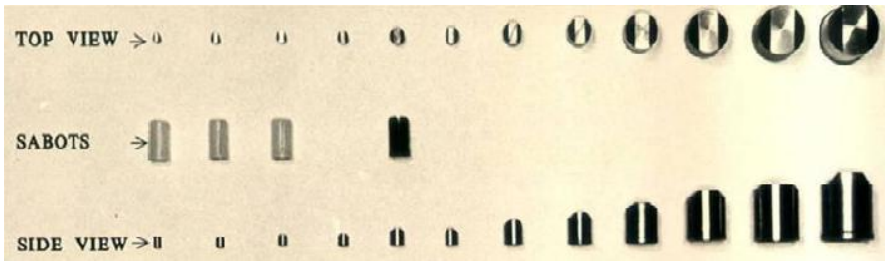


Figure 2.8: Fragment simulating projectiles. Courtesy of TNO.

The explosive reaction breaks the metal shell of the grenade up in fragments of different sizes, masses and velocities, see figure 2.7 b). Because of the large number of fragments, there is a good chance of hitting multiple targets, which makes grenade very effective weapons.

Dyneema composite can protect, to a certain extend, against fragments. Experiments, in which the performance of Dyneema composite against fragments is determined, often use standardised fragments called Fragment Simulating Projectiles (FSPs), see figure 2.8. The resistance of a target against FSPs can be done in single-shot experiments. Using FSPs gives more reproducible results than doing experiments with a grenade; otherwise the V_{50} of armours against such fragments would be hard to determine. Using FSPs is also a more economical solution than doing tests with grenades. Further, the impact location on a target can be predefined using FSPs .

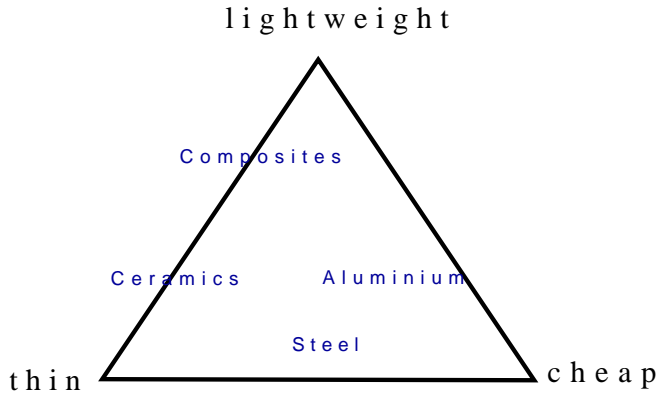


Figure 2.9: *Armour materials in requirements triangle*

2.2.2 Kinetic Energy Projectiles

In contrast to chemical energy projectiles, no explosion within the projectile is required for Kinetic Energy projectiles to obtain their final shapes. Some KE projectiles deform due to impact, but they keep their shapes from the beginning of the firing sequence until just before impact. Deformable KE projectiles contain a soft core-material such as lead. Deformable projectiles are used to achieve optimum stopping power by maximising their energy transfer to the target, meaning maximum lethality, to cut out persons or animals. Non-deformable projectiles contain a hard core-material such as tungsten carbide or hard steel. Non-deformable projectiles are used to achieve a penetration, which is as-deep-as-possible, to cut out aircraft or vehicles. Their shapes are almost unaltered after impact.

2.3 Dyneema targets

Dyneema (composite) is used in a variety of armour applications; i.e. there are various Dyneema (composite) armours. Each situation has its own requirements. Some general requirements are however distinguished and are described below. After this, some examples of Dyneema-composite armour applications are given.

2.3.1 Armour requirements

The requirements for armour depend on the projectiles that should be defeated, as well as on the specific application. Armour material should possess a certain strength, toughness or hardness. In some applications, it is required that the armour should be stable under impact conditions, see reference [38].

Dyneema composite is mainly used in armour applications that require high energy absorption and at the same time have a low weight. More general, armour should ideally be cheap, light and thin, see reference [39]. This is shown in figure 2.9. In general, materials used in armour do not fulfil all these three properties at the same time. Composite materials, and thus also Dyneema composite, give lightweight structures, but are not necessarily thin or cheap.

2.3.2 Personal protection

A low weight is especially important for personal protection applications. If the weight of personal armour is kept to a minimum, a person will have better mobility, which is desirable. Hereafter, two personal-protection applications, in which Dyneema composite are used, are described.

Helmets

Dyneema helmets protect the human head against fragments and bullets. The V_{50} against a 1.1 g FSP can, for example, be as high as 700 *m/s*. Dyneema helmets are produced by a deep-drawing process in order to realise the curvature required for a helmet. Dyneema helmets have a lower mass compared to other helmets that offer the same protection against projectiles. A weight reduction of up to $\pm 20\%$ can be realised with respect to the currently-used Induyco (type MVD) helmet if Dyneema helmets would be used.

Inserts

Bullet resistant vests alone do often not offer protection against heavier munition. Inserts, panels that can be placed in tailor-made pockets in the vest, can be used to solve this problem. Inserts can be made of only Dyneema or can be combined with armour steel and ceramics. Ceramics and/or steel protect against the heavier non-deformable projectiles such as Armour Piercing (AP) munition, see figure 2.10. If ceramics or steel is combined with Dyneema, Dyneema is used to stop the ceramic fragments which results from impact; in addition the shock on the human body due to impact can be distributed over a great area to minimise the damage in the human body.

2.3.3 Structural protection

Dyneema composite is also used in structural protection, e.g. in vehicles, aircraft and ships. Its high strength and low density come in useful in these applications. Because Dyneema composite is resistant against moisture, chemicals and UV light, Dyneema can be used in parts of the world in which the weather conditions are more severe than in Europe. Two common Dyneema composite applications, spall liners and armour panels, are described below.



Figure 2.10: *non-deformable 7.62 AP munition. Courtesy of TNO.*

Spall liners

Dyneema composite plates can also be used as spall liners. Due to projectile impact on a structure, spall can be generated. Spall is usually widely distributed in space. If a Dyneema composite plate is placed behind the actual (usually metal) armour, the space occupied by spall becomes smaller. In this case, Dyneema composite is not primarily used to defeat projectiles but to catch fragments, resulting from spall, and hence reduce the damage in the vehicle.

Armour panels

Dyneema armour panels are used to protect structures, such as police vehicles, helicopters and ships, against projectiles. There are various Dyneema armour panels, for example panels that protect against handgun ammunition, military ball ammunition, anti-tank ammunition and/or mines. Using Dyneema composite panels can save more than 50 % weight compared to conventional armour steel solutions. In this research, we investigate the effect of fragment impact on flat Dyneema armour panels.

2.4 Definition of impact in this research

From the above, it can be seen that there are many possible impact configurations. In this section, the specific impact case that we have studied in this research, is defined.

2.4.1 Target

In this research, projectile impact on a flat Dyneema HB25 composite plate, consisting of a number of Dyneema HB25 sheets, is studied. A Dyneema HB25 sheet is a non-woven cross-ply of which each uni-directional layer has a thickness of about four filaments. HB stands for Hard Ballistics and HB products are

used in cockpit doors or as inserts in bullet resistant vests to give extra protection. Composites made of this type are usually rather rigid in contrast to the SB (Soft Ballistic) type, which is a flexible composite that is used in for example bullet proof vests.

2.4.2 Projectiles

A Dyneema composite plate of the aforementioned dimensions can give protection against fragments and bullets. Since such a plate is mainly used to defeat 1.1 *g* FSPs, the impact of these projectiles on Dyneema composite is studied here. An impact velocity range of 200-500 *m/s* is considered, which lies around the V_{50} of the considered Dyneema plate against these projectiles. In this research, only perpendicular impact will be considered. This means that impact effects as a function of obliquity and/or yaw are not considered. Spin of the projectile will not be taken into account in this research.

2.4.3 Environmental conditions

It is assumed that the (properties of) Dyneema composite in this research are not affected by moisture, UV or other ageing effects. Further, the environmental temperature is assumed to be 293° *K* at all times. Relaxation in the material due to elevated temperatures are thus not considered in this research.

Chapter 3

Dyneema behaviour

For this research, a simulation tool should be developed, which is able to describe the behaviour in Dyneema composite caused by projectile impact. In order to develop such a tool, it is important to have knowledge about the behaviour of the constituents of Dyneema composite under different load cases. In section 3.1, general information about Dyneema composite is given. The material properties and behaviour of (the constituents of) Dyneema composite are determined with various experiments. The behaviour of Dyneema fibre and the PUR matrix, which are the constituents of Dyneema composite, is described in section 3.2 and section 3.3 respectively. The Dyneema composite properties and behaviour are discussed in section 3.4. In the last section, it is discussed which of the phenomena, observed in the various experiments, are most important and should be accounted for in the simulation tools, which are developed in this research.

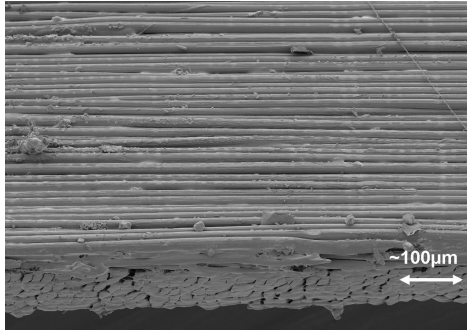


Figure 3.1: *Part of Dyneema sheet*

3.1 Built-up of Dyneema composite

3.1.1 Dyneema sheets

The manufacturer produces Dyneema fibre that consists of smaller units, which are called filaments. In a sheet (or ply), the fibres are equally distributed and flattened in unidirectional layers. In a layer, the fibres cannot be visually distinguishable and only the filaments can be seen. The layers are rotated by 90 degrees with respect to the adjacent layers; each sheet is a non-woven cross ply. The number of unidirectional layers in one sheet depends on the sheet type. In this research, we will only consider Dyneema composite that is made of sheets that contains two perpendicularly oriented layers, such as shown in figure 3.1. A non-woven cross-ply is also the most commonly used configuration for Dyneema composite; Dyneema angle ply composites are less common. A Dyneema composite plate is built up from a number of Dyneema sheets.

Dyneema filaments

The volume content of the filaments in Dyneema composite is typically more than 75 %. This percentage is higher than that of most fibre reinforced composites, which typically contain 40 % fibres or filaments by volume. The Dyneema filaments are a special grade of Ultra High Molecular Weight Polyethylene (UHMW PE) having the formula $-\text{[CH}_2\text{]}_n-$, see also references [40] and [41], with n in the order of 100.000. Dyneema filaments are produced by a patented gel spinning process, see reference [42]. During the gel spinning process, polyethylene chains are stretched and oriented in length direction of the filaments. By stretching, the filaments become very strong and stiff, see reference [7]. The behaviour of Dyneema fibre subjected to various load cases is described in the next section.

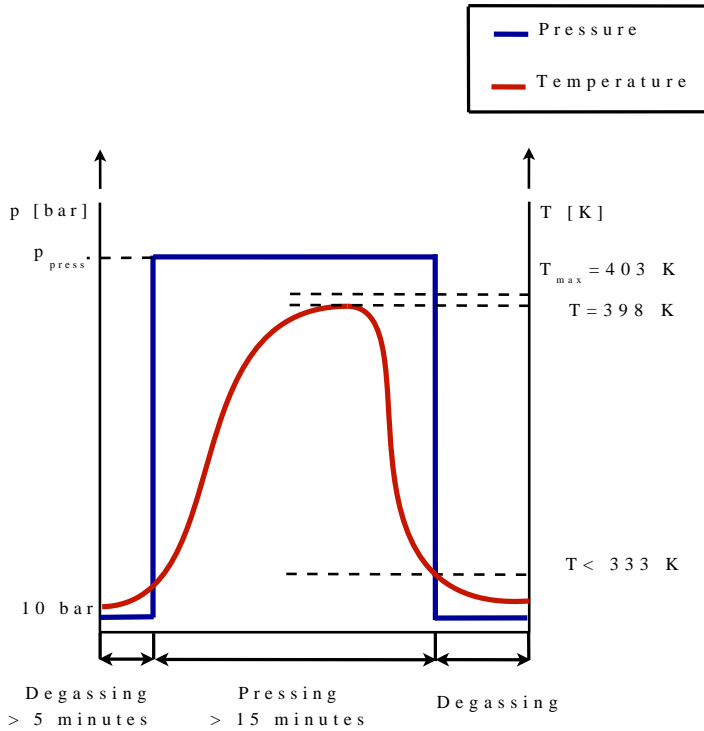


Figure 3.2: *Schematic pressure cycle of Dyneema composite*

Matrix material

The matrix material that is used in the Dyneema composite considered in this research is a Polyurethane rubber (PUR). The matrix material in this composite keeps the filaments together and also gives some rigidity to the composite. The properties of the matrix are more extensively described in section 3.3.

3.1.2 Production of Dyneema composite

In order to produce a Dyneema composite plate, a number of Dyneema sheets are cut in the desired dimensions and are pressed together. The actual number of sheets depends on the desired thickness of the plate and the required performance. The sheets are pressed together by applying a predefined pressure-temperature cycle.

A schematic pressure-temperature cycle is shown in figure 3.2. It is seen that a pressure-temperature cycle is divided into three subsequent phases, namely the degassing phase, the pressing phase and a second degassing phase. In the first

degassing phase, the sheets are heated to a temperature of $333\text{ }^\circ K$. By heating the sheets to this temperature, the air that is trapped between the sheets is removed. If many voids would be contained in the final product, local weak spots in the end product would be the result. This first phase typically takes a few minutes.

In the pressing phase, pressure is applied to the layers while the temperature is further increased to $398\text{ }^\circ K$. The higher the applied pressure, the higher the density of the sample will be and the higher its ballistic performance will be. For a good quality Dyneema composite, it is important that all layers have reached this temperature to assure good adhesion between the layers. At $403\text{ }^\circ K$ the filaments undergo a phase transition that causes a strength loss of the fibres and therefore care should be taken that the temperature in the sheets does not exceed this limit. This phase takes less time when the composite plate is thin, because there is less material to heat. When all the sheets have reached a temperature of $398\text{ }^\circ K$, the sheets are cooled down to $333\text{ }^\circ K$ again while maintaining the high pressure. When all the sheets have cooled down to $333\text{ }^\circ K$, the pressure is released and the second degassing phase starts.

During the second degassing phase, the sample is removed from the press and cooled down to room temperature. When the sample is removed, it is flexible. When it is cooled down to room temperature, the composite becomes more rigid and is ready for use.

3.2 Dyneema fibre response

Dyneema fibre is a viscoelastic material and its response is therefore a function of the applied strain rate. This means that the response of the fibres may be different for different load cases, see also reference [43]. Therefore, various experiments have been done at different strain rates and the observed behaviour is described in this section.

3.2.1 Static fibre behaviour

If a fibre is loaded in compression, it is seen that it is not able to resist this. However, Dyneema fibre is very strong in tension. The behaviour of the Dyneema fibre under quasi-static conditions is studied by doing tensile tests. Because the friction coefficient of Dyneema fibre is very low against most materials, a dedicated fibre clamp was used, which is shown in figure 3.3 a)¹. In order to overcome the problem with the low friction coefficient, the fibre is wound around the helical part of the clamping device, which makes it harder for

¹Dyneema's low friction coefficient is a drawback if it has to be clamped. Its low friction coefficient is, however, a very favourable property in medical applications such as surgical cables and prostheses

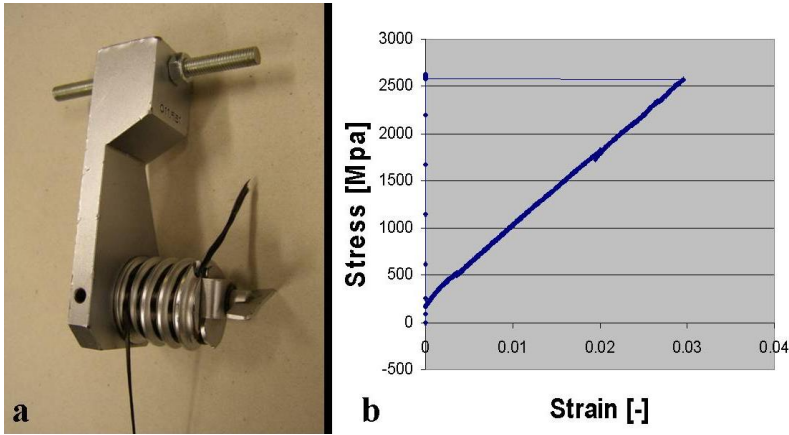


Figure 3.3: a) Clamping mechanism for fibre tensile test, b) Stress-strain diagram for Dyneema fibre

the fibre to slip away from the clamps. The end of the fibre is kept in place using an additional pin fixation.

A total of 28 tensile tests are done using these clamps at a loading speed of 100 mm/min at room temperature. At this loading speed, Dyneema is in its rubbery state, see reference [44]. The resulting stress-strain diagram for the Dyneema fibre is shown in figure 3.3 b). This figure shows one of the test results and is representative for all test results. It should be noted that the curve starts at a stress of 250 MPa while having zero strain. This is because a pre-force is applied to the specimen prior to the actual testing.

In every test, it is observed that the fibre specimen fails in the centre. It is seen that the fibre does not fail at once, but that the filaments in the fibre fail one after the other. The tensile modulus E of the Dyneema fibre that is determined with the tensile tests, averaged over 28 experiments, is 120 GPa with a standard deviation of 18 GPa . The accompanying average failure strain ϵ_{max} is about 0.022 with a standard deviation of 0.0058. A relatively large standard deviation for the failure strain is found compared to the tensile modulus. This may be explained by uncertainty in production; the filaments in the fibre do not all have exactly the same cross sectional size. The weakest filament, the filament with the smallest cross-section, in the fibre fails first. The variation in the failure strain can then be explained by the fact that the weakest link is different for each fibre that is tested.

The fibre shows a linear relation between the engineering stress and strain up to failure. If a tensile load is applied that is close to the failure load and the load is removed again, there is no residual strain in the fibre. This indicates that the Dyneema fibre behaviour is not only linear, but also elastic up to failure.

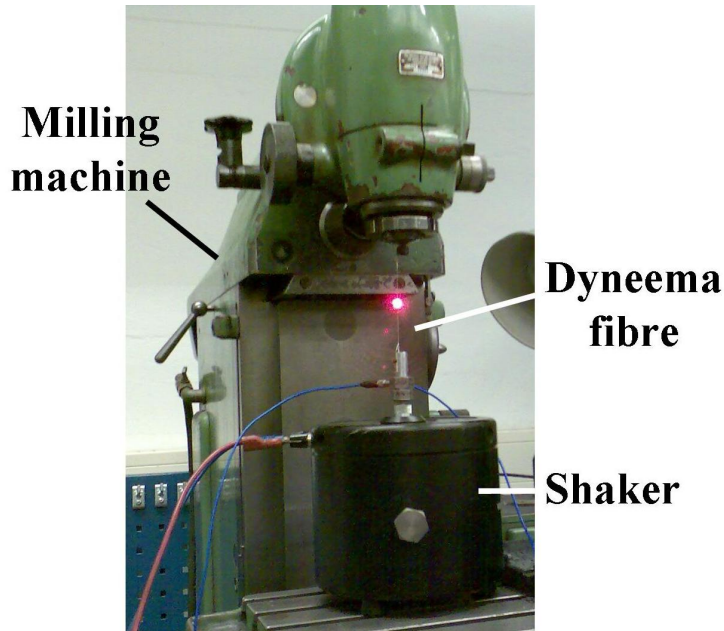


Figure 3.4: *Set-up of Dyneema fibre in a Milling Machine for a frequency response analysis*

3.2.2 Viscoelastic fibre response

The tensile tests give a value for the tensile modulus, the strain at failure and information on the qualitative behaviour of the Dyneema fibre subjected to a quasi-static tensile load. This response is however different when the material is subjected to dynamic loads.

Dynamic Mechanical Analysis of Dyneema fibre

Because there are high strain rates involved in projectile impact, we are especially interested in the response of the fibre if it is subjected to high strain rates. If standard Dynamic Mechanical Analysis (DMA) would be done, the maximum frequency at which the Dyneema fibre can be tested is about 100 Hz . Testing beyond this frequency gives problems with eigenfrequencies of the apparatus. Even when applying a low temperature (223 °K) combined with an 80 Hz frequency, the Dyneema fibre is still in its glass transition phase, see reference [44]. DMA experiments do not seem to be suitable to determine the glassy modulus of the Dyneema fibre.

To determine the glassy modulus, an alternative DMA experiment is done with a shaker that is combined with a (very stiff) milling machine, see figure 3.4. The

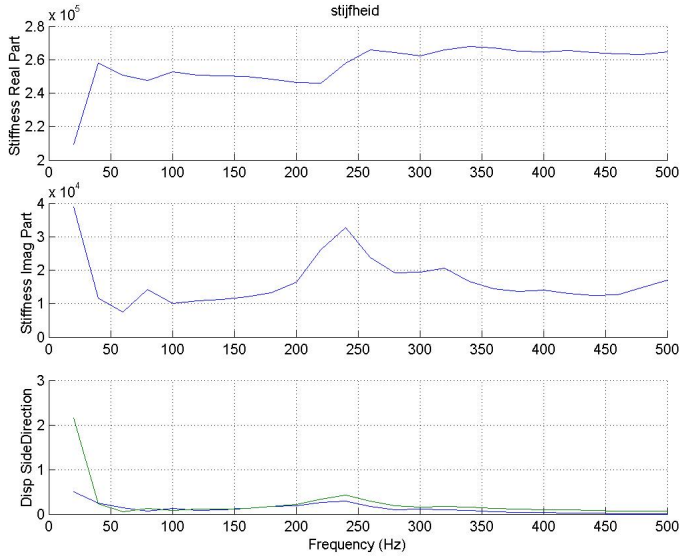


Figure 3.5: *Results of Dynamic Mechanical Analysis*

lateral displacements of the Dyneema fibre are measured by a laser. The shaker and the Dyneema fibre are clamped on the milling machine to keep them in place. Because the set-up has a higher system stiffness than conventional DMA machines, higher frequencies can be achieved. The measured fibre stiffness in this experiment as a function of the loading frequency is shown in figure 3.5. It is seen that the results give realistic values up to 500 Hz and that the tensile modulus is more or less constant from 60 Hz . If we look at the top figure, we see that the real part of the stiffness shows a jump at a frequency of 250 Hz . This jump is also shown by the imaginary part of the stiffness. This jump is probably an eigenfrequency of the machine. In the lower part of figure 3.5, displacements in two lateral directions are shown in mm as a function of the frequency (these directions are perpendicular to each other and to the actual loading direction). In this figure, it is shown that the lateral displacements are small compared to the applied displacement in loading direction (lower part of the figure). If the lateral displacements would be of the same order of the applied displacement, the results would be influenced and a wrong value for the stiffness would be measured.

However, we still need to convert the values to the tensile modulus E , since we actually measure the spring constant c in N/m with this set-up. Since the spring constant c is calculated by:

$$c = \frac{F}{u} \quad (3.1)$$

with F the applied force and u the displacement. Since $\epsilon = \frac{u}{L}$, the tensile modulus E is related to the spring constant c as follows:

$$c = \frac{F}{u} = \frac{F}{\epsilon \cdot L} = \frac{F}{A} \cdot \frac{A}{\epsilon \cdot L} = \frac{\sigma \cdot A}{\epsilon \cdot L} = E \cdot \frac{A}{L} \quad (3.2)$$

with A the area of the fibre (value obtained from the manufacturer) and L the length of the fibre. Now, we can calculate the tensile modulus of the fibre at high strain rates according to:

$$E = \frac{c \cdot L}{A} = \frac{2.6 \cdot 10^5 \cdot 0.10}{0.1702 \cdot 10^{-6}} = 160 \cdot 10^9 Pa \quad (3.3)$$

which is a higher value than measured using tensile tests, as expected. This value of 160 GPa , is the value at a frequency of 250 Hz or higher. If we do the same calculation for the stiffness between 80 and 220 Hz , we see that the modulus is about 120 GPa .

3.2.3 Fibre response on projectile impact

To determine the behaviour of Dyneema fibre when it is subjected to projectile impact, a dedicated impact experiment - the single fibre impact experiment - is further developed, see references [45], [46], [47], [48], [49], [50], [51] and [52] for earlier work. In this experiment, a projectile impacts on a fibre, which is schematically shown in figure 3.6. From this experiment, the Young's modulus E and the qualitative behaviour of Dyneema fibre under impact conditions is determined.

Experimental set-up

The used experimental set-up is shown in figure 3.7. It is seen that the fibre is placed vertically in front of the barrel. At the higher end of the fibre, the clamping is similar to the one used in the fibre tensile test; the fibre is wound around the clamps. A mass is attached to the lower end of the fibre to prevent it from moving during impact (not shown in the figure).

The projectile is accelerated in the barrel, which is driven by a pneumatic system that uses helium gas, see figure 3.7 a). The velocity of the projectile is controlled by the pressure of the helium, see reference [53]. The fibre is placed very close to the end of the barrel, so that the projectile can be aimed at the fibre accurately see figure 3.7 b). The impact on the Dyneema fibre is recorded using the high speed camera shown in figure 3.7 c). This camera has a maximum recording speed of $5.000.000$ images per second and is a so called Still Video Range (SVR) camera. The SVR camera projects sequential frames on

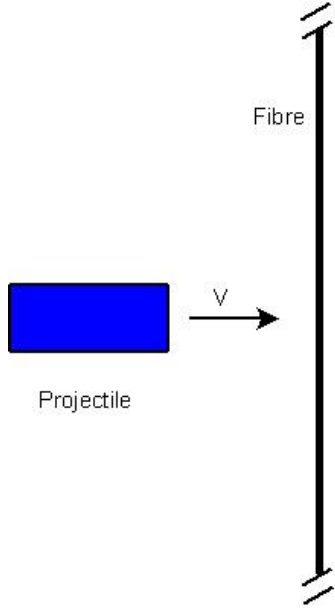


Figure 3.6: *Projectile impact on fibre (schematic)*

top of each other in one image with a maximum of 16 frames per image. This enables close following of an event in time. The time between two sequential projections is called the interframe time and is used as input in the experiments. In these experiments, the interframe time is chosen such that the distance s , see also figure 3.8, travelled by the projectile is the same. In all experiments, s is 8 *mm*, which is somewhat bigger than the projectile length, which is 6.35 *mm*. The interframe can, after the experiment, be checked with the following formula:

$$t = \frac{s}{v} \quad (3.4)$$

with v the impact velocity of the projectile and t the interframe time.

Determination of the dynamic tensile modulus

Before the projectile impacts on the fibre, the fibre is positioned vertically. When the projectile makes contact with the fibre, the fibre will locally move in the direction of the projectile, which is schematically shown in figure 3.8. At time t_0 , the projectile is in free flight and is not in contact with the fibre. At time t_1 , the projectile has already touched the fibre and the fibre has a triangle shape. At time t_2 , the projectile has moved somewhat further away from its initial position. As long as the response of the fibre is not plastic, the triangle will theoretically continue if the fibre has an infinite length. The velocity C_s is

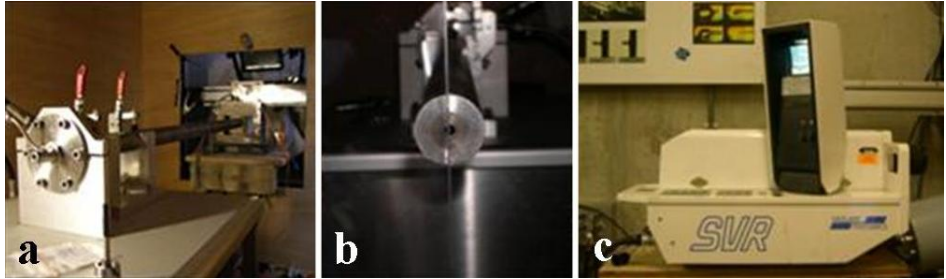


Figure 3.7: a) Barrel, b) Fibre in front of barrel, c) Still Video Range Camera (SVR)

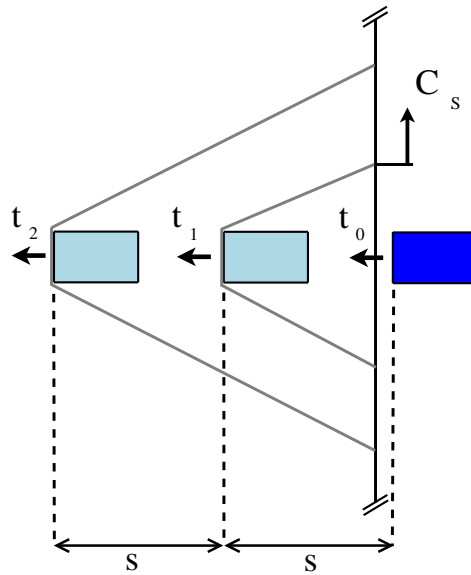


Figure 3.8: Fibre movement caused by projectile impact (schematic)

the velocity at which the end of the triangle moves further away from the impact point can be determined from experiments.

From the SVR images, both the projectile velocity V_p and the velocity C_s can be determined. Together with the tenacity μ , which is the spring stiffness of a fibre expressed in N/m , the density ρ and the pre-tension T_0 , the longitudinal wave velocity C_l in the fibre and the tensile modulus E can be calculated, see reference [54]:

$$C_l = \frac{1}{2} \cdot \left(B + \sqrt{B^2 - 4 \cdot \frac{T_0}{\mu}} \right) \quad (3.5)$$

$$E = \rho \cdot C_l^2 \quad (3.6)$$

with the parameters B and W :

$$W = C_s \cdot \left(\sqrt{1 + \left(\frac{V_p}{C_s} \right)^2} - 1 \right) \quad (3.7)$$

$$B = \frac{C_s^2}{W} + 2 \cdot C_s - \frac{T_0}{\mu \cdot W} \quad (3.8)$$

Results of impact experiment for Dyneema fibre

In figure 3.9, SVR records are shown for different impact velocities. In these images, the projectile moves from right to left. In the beginning, a triangle is seen in these figures. Prior to failure, the fibre no longer takes on a perfect triangle shape. This is caused by the fact that in this experiment, the filaments fail one by one. These images are used to calculate the tensile modulus at different impact velocities. In figure 3.10, the dynamic tensile moduli are shown as a function of impact velocity.

From figure 3.10, it can be seen that the modulus E is almost constant for impact velocities between 100 m/s and 450 m/s and the average modulus is about 200 GPa . From these results, it may be expected that E is constant within this velocity range, because the material acts as if it were in the glassy state. The value of 160 GPa , determined with the DMA experiment, and the 200 GPa that is determined from this experiment differ with 20 %. The fibre is believed not to be fully in its glassy state in the DMA experiments yet.

Two projectiles with different geometries are used in the experiments, namely a cylinder and a saddle projectile, see reference [55]. The cylinder has sharp edges and the saddle has no sharp edges that will be in contact with the projectile.

The two projectiles are used to study the influence of the projectile on the behaviour of Dyneema fibre. In figure 3.10, it is shown that the use of a different projectile geometry does not affect the value of the tensile modulus E . This is because the elastic behaviour is not influenced by the projectile geometry.

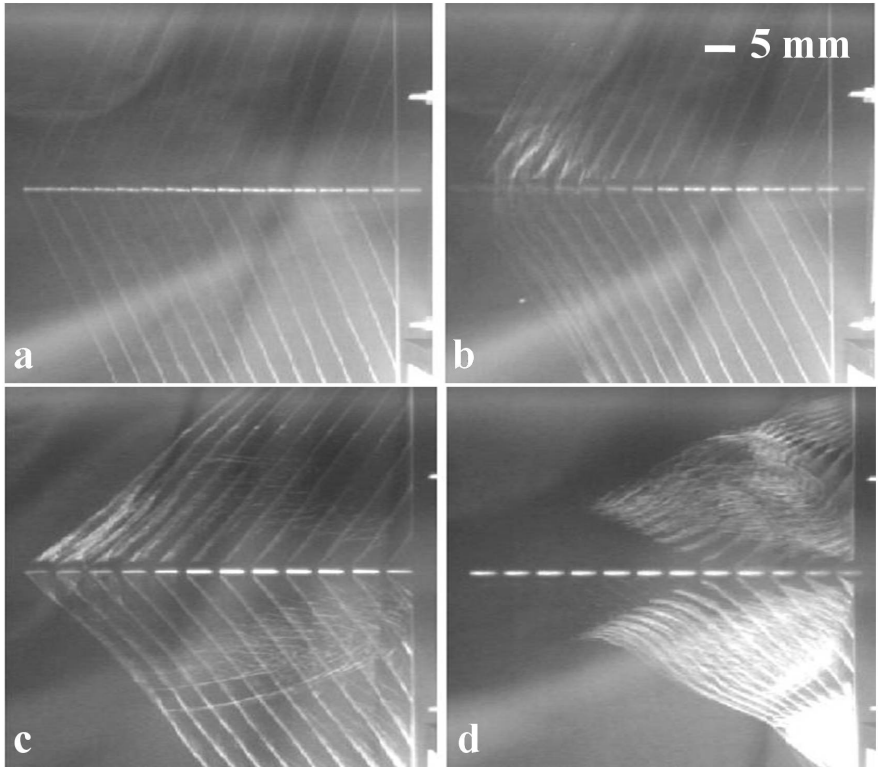


Figure 3.9: *Single fibre impact images at different impact velocities, a) 200 m/s, b) 300 m/s, c) 400 m/s, d) 500 m/s*

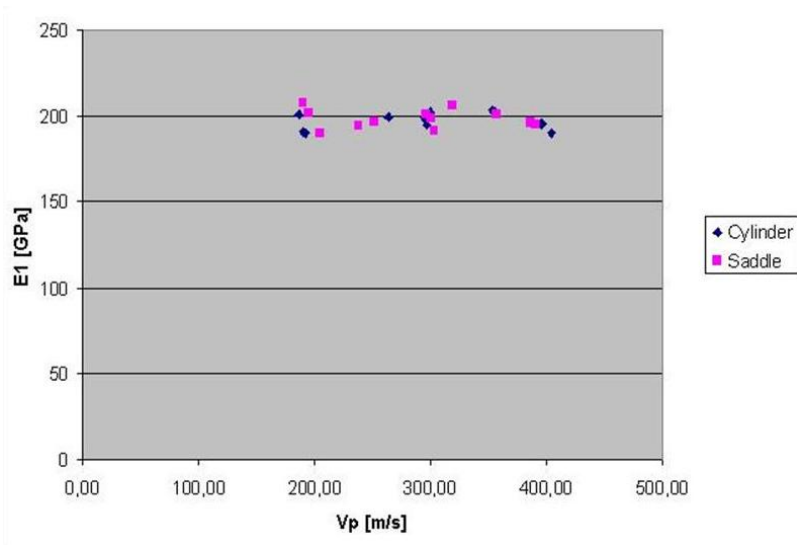


Figure 3.10: Modulus of Dyneema HB25 fibre as a function of projectile impact velocity

However, the moment of failure is different for the two projectiles. Using a cylindrical projectile, the fibre fails at a smaller displacement than when a saddle projectile with the same velocity and mass is used. In other words, the kinetic energy for both projectiles is identical. Cylindrical projectiles have sharper edges than the saddle projectiles. In the case of the cylindrical projectile, the fibre is cut by the edges of the cylinder projectile. The fibre fails at a larger displacement of the projectile using a saddle projectile, since it fails because the ultimate strain is reached.

The failure stress and strain cannot be directly determined using these experiments. Therefore, simulations are used to estimate these properties. Dyneema fibre fails if it is impacted by a saddle projectile having a velocity of 450 m/s . Assuming that the fibre also behaves linear up to failure under impact conditions, the failure stress and strain can be estimated using simulations. If we assume that the fibre fails instantaneous, we can model the fibre using truss elements with elastic properties only. In the simulation, we look at the stress at the failure location at the time that the fibre fails in the experiment. This stress can then be assumed to be the failure stress of the fibre. The failure stress is equal to 2.8 GPa and is again somewhat higher than the stress that is determined in the quasi-static tensile tests.

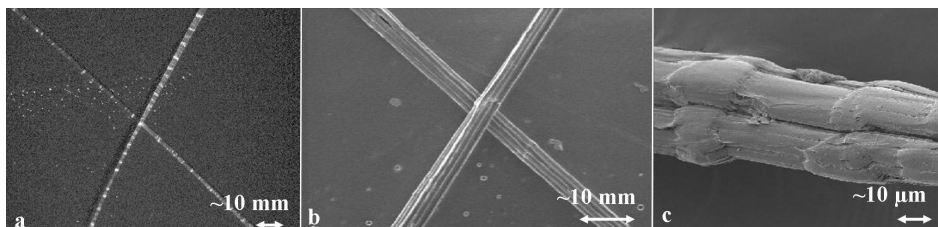


Figure 3.11: *a) Photo of a part of Dyneema fibre seen by an optical microscope, b) Part of Dyneema fibre seen with a SEM, c) Detail of Dyneema fibre seen with a SEM*

3.2.4 Analysis of Dyneema fibre

It is illustrative to study the Dyneema filaments before and after impact to get a feeling of which failure mechanisms occur. A study of both cases is presented below.

Fibre analysis before loading

In figure 3.11, three images of a part of undamaged Dyneema fibre are shown. Figure 3.11 a) shows an image taken with an optical microscope and figure 3.11 b) shows a magnification of the same filaments using a Scanning Electron Microscope (SEM). It is seen in figure 3.11 a) that the translucency varies within the filaments, indicating that the density of the filaments varies with location in the filament. It can also be seen that there are some local thicker spots in the filaments. From figure 3.11 b), the individual filaments can be seen more clearly. A SEM can show smaller details of the filaments compared to an optical microscope. Before analysing filaments with the SEM, the samples are coated with carbon particles. Carbon is chosen here, because it allows for studying the filaments at high magnifications. In figure 3.11 c), part of the filaments is magnified. On this scale, we see that the Dyneema filaments have an irregular surface with thicker and thinner cross sections. The thicker parts in the filaments are referred to as kink bends, see reference [56]. More kink bends occur when Dyneema filaments have been subjected to bending. The filaments shown in 3.11 directly come from the manufacturer. In this figure, some kink bends are already present. They may be introduced during the gel-spinning process, during which the filaments go over some roles.

Fibre analysis after impact

When studying the effects of projectile impact on Dyneema composite, it is hard to distinguish between the effects of projectile impact on the filaments and the matrix material. Therefore, a separate study of an impacted fibre is made. In figure 3.12, three distinct filaments are shown, which come from the same

impacted fibre. The fibre failed due to impact of a cylindrical projectile at 450 m/s . In figure 3.12 a), the left filament looks like it has been stretched and moved back to its original position after failure. Most of the failed filaments in an impacted fibre look like this filament. If the ultimate strain in a filament is reached, the filament fails subsequently and moves back to its original position. In figure 3.12 b), another filament from the same fibre is shown. Its surface looks different from an undamaged filament and from the filament in figure 3.12 a). This filament is believed to have undergone a phase transition due to a local temperature increase, which is probably caused by friction between projectile and filaments. Very few filaments in the fibre have undergone such a phase transition.

In figure 3.12 c), another filament from the same fibre is shown. This filament is curled and its surface is somewhat uneven like the filament in figure 3.12 b). The uneven surface of the filament again indicates that a phase transition has taken place, although the surface did not change as much as shown in figure 3.12 b). The phase transition may not have been completed in this fibre. The curling is caused by one-sided straining of the filament. This filament probably failed under a combined tension load and local heating.

As mentioned before, most of the filaments that have failed due to impact look like the left filament in figure 3.12 a). The number of filaments that have undergone a phase transition are small and are concentrated near the impact point. These filaments have been in direct contact with the projectile, which caused local heating due to friction between the projectile and the filaments. Since the number of filaments that have undergone a phase transition is small, heat effects are believed to play a negligible role in filament failure due to projectile impact.

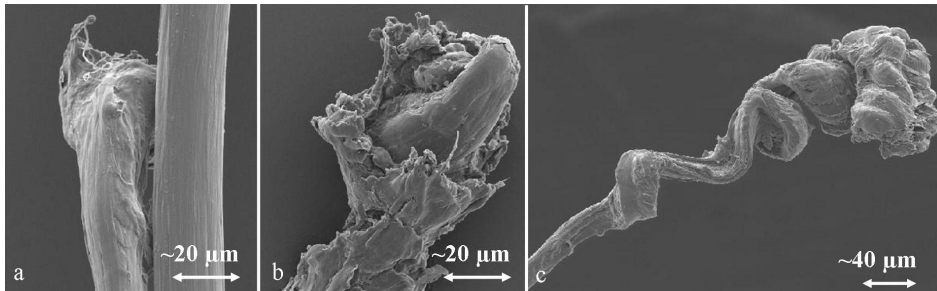


Figure 3.12: SEM images of failed filaments after projectile impact, a) Filament failed due to tensile load, b) Failed filament due to local heating, c) Failed filament due to a combination tensile load and local heating

Failure of filaments due to projectile impact is a very local phenomenon. About 5 mm away from the impact point, the filaments are visually undamaged and have probably only been loaded in their elastic regime.

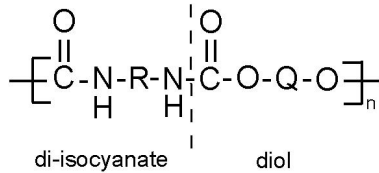


Figure 3.13: *Chemical composition of PUR*

3.3 Matrix behaviour

The matrix material used in Dyneema composite is a Polyurethane rubber (PUR). PUR consists of rigid di-isocyanate parts and more flexible di-alcohol parts that are alternately placed, see figure 3.13. R and Q depend on the specific PUR type. Matrix material in Dyneema composite is essential if loads between the filaments are to be distributed. If there would be no matrix material between the filaments, the ballistic performance of the composite drastically decreases, see reference [57].

PUR is a viscoelastic material, just like the Dyneema fibre material. The viscoelastic material properties are determined using a temperature scan². The glassy modulus is 4 *GPa* and the glass transition phase takes place from 225-423 °*K*. At a temperature T of 423 °*K*, the modulus becomes steady again and the value of the rubber modulus is 0.1 *GPa*. It is expected that the value of the tensile modulus of the matrix is between 0.1 *GPa* (value at room temperature) and 1 *GPa* (value at 223 °*K*) when it is subjected to projectile impact. The function of the PUR matrix is, besides transferring loads between filaments, to prevent the filaments from freely moving with respect to each other.

Only little is known about the plasticity, fracture and failure behaviour of the matrix material. This is considered to be of minor importance, since only a small amount is used in the composite. We believe that by studying the composite properties and the fibre properties, the matrix properties can be derived. For more information on this, see *Chapter 7 Lumped filament-bundle model*.

3.4 Dyneema composite behaviour

In this section, the behaviour of Dyneema composite is described. Dyneema has some characteristics that make doing experiments challenging. One of the characteristics is that Dyneema composite is hard to process. Correct processing of Dyneema is essential if it comes to producing specimens for experiments. In the first part of this section, it is described how Dyneema reacts on different processing mechanisms. In the remaining part of this section, a description is given of the mechanical behaviour of Dyneema composite.

²data given by manufacturer

3.4.1 Dyneema composite processing

Dyneema composite has a high resistance against plastic deformation, which makes it hard to process. Hereafter it is described how Dyneema composite behaves using different processing methods and which method is considered to give an optimal specimen.

Specimens

If a cut is made in a 5 mm-thick Dyneema-composite panel, tools typically wear after making three to four cuts of 200 mm length.

Specimen quality

Dyneema composite has a high fibre volume content. This means that not much matrix material is there to serve as an adhesive between the filaments and between the sheets in Dyneema composite. When Dyneema composite is processed, the adhesive layer is loaded very heavily and filament pull-out and delamination are often seen after processing. For the experiments with Dyneema composite, a good-quality specimen is essential. Since producing good-quality Dyneema composite specimen is not a straightforward process, a study is made on how Dyneema composite specimen should be produced.

If a metal sheet is processed, the quality of the cut is characterised by the roughness of the cutting surface and the number of burrs. Surface roughness and burr formation are however not relevant for the quality of a Dyneema-composite cut. A 200 mm cut with a milling machine (a method that is often used to process metals) has been made and is used as a reference case and from this, quality criteria for Dyneema composite have been determined. The cutting surface is compared with the surface of Dyneema composite that has not been processed, see figure 3.14.

The images in figure 3.14 are all made using an optical microscope. In figure 3.14 a), a section of Dyneema composite is shown that has not been processed yet. It is seen that filaments are not pulled out and that the alternating unidirectional layers have about the same thickness. Figures 3.14 b), c) and d) are images of Dyneema composite after processing. In figure 3.14 b), the same section of Dyneema composite is shown after processing. It is seen that filaments are pulled out of the composite due to milling. In addition to this, delamination of the sheets has taken place, indicated by a change of translucency, which is shown in figure 3.14 c). It should be noted that the thickness of the composite locally seems to increase due to the delamination. If we zoom in at the edge of the cut section of the composite, it is seen that the ends of the filaments are molten together, see figure 3.14 d). This is caused by melting due to frictional forces encountered during processing between the milling machine and the composite. Summarising, the number of molten or loose filaments, the delamination width, the thickness increase and tooling wear

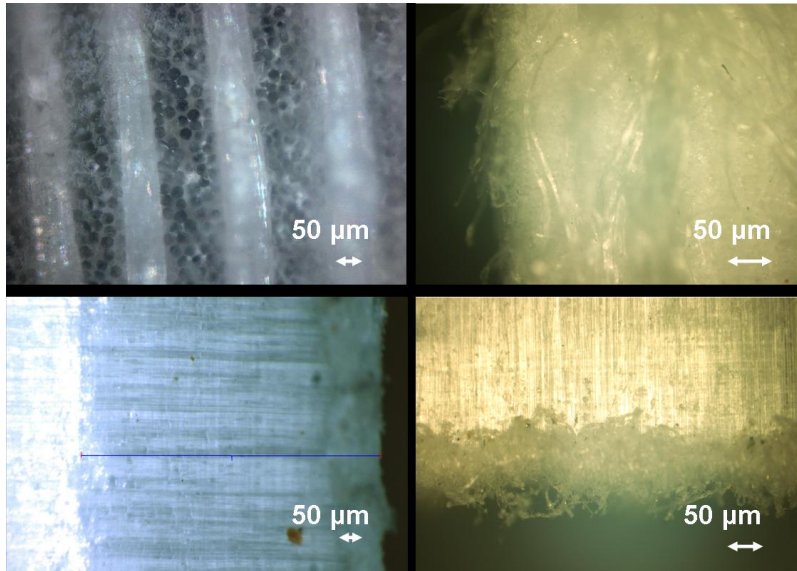


Figure 3.14: a) Section of unprocessed Dyneema composite, b) Section of processed Dyneema composite, c) Top view of processed Dyneema composite, d) Edge of processed Dyneema composite

occur due to processing with a milling machine and will be used to determine the quality of a cut in order to be able to compare different processing methods.

Processing methods

Dyneema composite is processed with a diamond saw, a band saw, circle saw, a punch, an abrasive water jet cutter, a miter saw and a knife to determine the optimum processing method. With each tool, a cut of 200 mm length is made in a 5 mm thick plate Dyneema composite plate. After processing, the quality of a cut is determined using the aforementioned criteria.

The quality of a cut is compared in pairs, circle saw and miter saw, circle saw and band saw, band saw and circle saw etc. Weight factors are assigned on a scale from 1-4 (1 being an unimportant criterion and 4 being an important criterion) to the different quality criteria and are shown in 3.1.

We believe that molten or loose filaments will influence the mechanical properties of a cut specimen most in terms of strength and stiffness.

Delamination of the layers is also believed to influence the strength of the specimen, although less than the presence of loose or molten fibres. The tooling wear and the processing speed influence the costs for making a specimen from Dyneema composite. Because the quality of the specimen is considered more important, the tooling wear and processing speed are given a lower weight factor

Table 3.1: Scores of processing methods

Quality criterion	Relative importance
Molten or loose filaments	4
Delamination width	3
Maximum thickness increase	3
Tooling wear	2
Processing speed	2

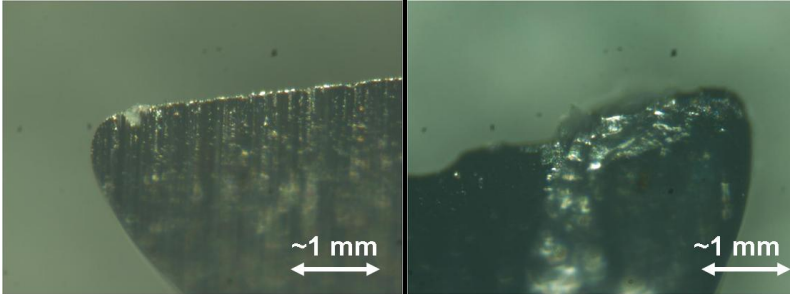


Figure 3.15: a) Undamaged knife, b) Knife after cutting Dyneema composite

for the trade-off.

Making a cut of 200 mm with a surgical knife in Dyneema composite was not possible. The knife already wears after making a cut of 40 mm length, see figure 3.15. In figure 3.15 a), a part of the knife is shown before cutting and in figure 3.15 b) the same part of the knife is shown after cutting 40 mm of 5 mm-thick Dyneema composite. Cutting a 3 mm-thick Dyneema composite gives the same results. Using a surgical knife for processing purposes is therefore not further considered.

An enormous force is required to punch through 5 mm Dyneema composite. At the maximum force of the bench (11 kN), only a small dent is seen in Dyneema composite and none of the layers has actually been perforated. Using a punch for processing purposes is therefore also not further considered in the processing method trade-off.

Processing method trade-off

Looking at the remaining processing methods, we see that milling causes the biggest delamination area (70 mm · 200 mm) followed by the diamond saw (41.2 mm · 200 mm). Abrasive water jet cutting gives a delamination area of a 1 mm · 200 mm.

The biggest thickness increase is seen with the specimens that are produced using the diamond saw, which gives a thickness increase of 63 % (the average of

all methods is 40 %). If a miter saw is used, it is seen that the Dyneema composite has been locally heated at the cutting edge. After cutting 200 mm, a lot of material has piled up and the tool could not be used anymore. Because of this pile of molten material, the thickness increase due to delamination cannot be reasonably determined. The measurements would be disturbed by the molten, piled up material. Abrasive waterjet cutting gives a thickness increase of 8.16 % and the increase in thickness using the rest of the methods typically lies within 25-35%.

The highest processing speed, namely 20 mm/s, can be obtained using a band saw. Using a diamond saw and a miter saw, cutting speeds of 0.25 mm/s and 0.15 mm/s are achieved respectively. A milling machine has a cutting speed of 6 mm/s and using water jet cutting a cutting speed of 2.5-10 mm/s can be achieved (an increase in cutting speed can be achieved, but will result in a larger thickness increase). Except for the band saw and the abrasive water jet cutter, the tools are typically worn after making the first cut of 200 mm.

As stated above, the quality of a cut using the aforementioned processing methods is translated to an objective score in which the methods are compared pairwise. The scores of the different processing methods are summarised in table 3.2.

Table 3.2: *Scores of processing methods*

Processing method	Score
Diamond saw	19
Band saw	47
Circular saw	35
Miter saw	12
Abrasive waterjet cutting	68
Milling	12

From table 3.2, it is seen that water jet cutting is the most favoured processing method, because it has the highest score. The success of this processing method lies in the fact that a very high, concentrated load is introduced, which results in high, local stresses in the material. Therefore, the material barely delaminates. Since water jet cutting gives the optimum result, the Dyneema composite specimens used for experiments are produced using abrasive water jet cutting. The standard settings for the abrasive water jet cutter are shown in table 3.3. These parameters are varied on the waterjet cutter, described in reference [58]. It should be noted that these variables could eventually be changed to obtain an even better result. Since these variables suffice, finding an alternative set of variables, is considered to be beyond the scope of this research.

Table 3.3: *Characteristics of abrasive water jet cutting*

Abrasive feed	200 g/mm
Water pressure	3700 bar
Cutting speed	150 mm/min
Abrasive	Australian desert sand

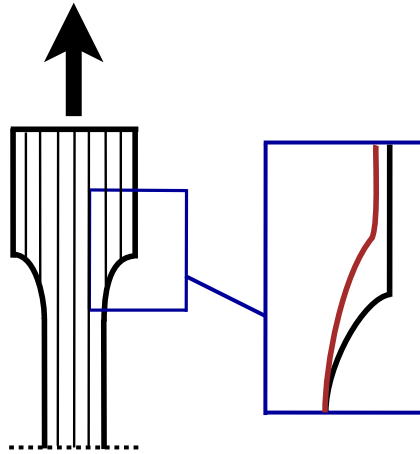


Figure 3.16: *Schematic representation of deformation of Dyneema dogbone specimen*

3.4.2 Static laminate behaviour

As mentioned before, especially the dynamic properties of Dyneema composite are important. However, the behaviour of Dyneema composite in tension and bending is hard to determine dynamically. Therefore, also some (quasi-static) experiments are done to get an idea of the behaviour under tensile and bending loads.

Tensile test

The specimens used for the tensile tests are rectangular and have sizes of $90\text{mm} \cdot 10\text{mm} \cdot 1.5\text{mm}$. The exact dimensions of the specimens vary within a range of a few tens of a millimetre and are measured before each test. Often, dog-bone shaped specimens are used for tensile tests to ensure a good clamping, see figure 3.16. This is however not applicable to Dyneema composite. The vertical lines in this figure represent the direction in which the filaments are oriented in this specimen. If a dog bone shaped specimen would be used, the edges start to deform in shear as shown in figure 3.16. If a tensile test is done using a dog bone specimen, the area near the edges start to deform first. At the same time, the layers are pulled off each other (due to shear). To avoid this,

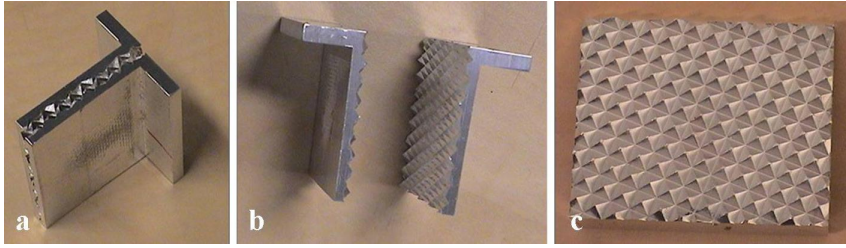


Figure 3.17: *a) Two clamps fitting into each other, b) Two separated clamps, c) Clamping surface with the pyramid bases rotated over 20 degrees*

rectangular Dyneema composite specimens are used.

Dedicated clamps are designed to prevent the rectangular samples from slipping during the experiment, see figure 3.17. A Dyneema specimen is clamped between two clamps on its upper and lower side. Each clamp, made of aluminum, has a pyramid-covered surface on which the pyramids are rotated over an angle of 20 *deg*. This angle is experimentally determined. If this angle would be smaller or larger, the specimen still slips out of the clamps. The specimen is placed between pneumatic clamps in the tensile bench, together with the pyramid clamps. The pneumatic clamps exert a pressure of 500 *bar* on the clamps. Although this clamping pressure is quite high, the clamps do still not show significant wear after ± 30 tests.

The Dyneema composite specimen consists of layers with two orientations. The first orientation is in the length direction of the specimen and the second orientation is perpendicular to the length direction, namely in width direction. In figure 3.18, the tensile test results (averaged) are shown.

During the first part of the tensile test, the strain in every layer is the same, although it is seen that the filament layers at the free edges are damaged first. In the layers that are oriented in the length direction the filaments are loaded. In the width-oriented layers, the bond between the filaments is loaded. The strength of this bond is much weaker than the failure strength of the filaments. The bond between the filaments fails first. After failure of this bond, the load is immediately transferred to the layers with filaments in length direction. This behaviour is shown in figure 3.18. In first instance, the slope of the curve is high (about 11 *GPa*) and almost immediately levels off. Before generating this curve, a 1 *kN* pre-force is applied. During this pre-load, the bond between the filaments probably breaks. The results of the tensile tests therefore indicates a lower initial stiffness than would be expected from the fibre and filament properties. This is because the bond between the filaments in the width orientated layers fails at an early stage. At the same time, the bond between the layers fails in shear. The stiffness of Dyneema composite using a tensile test consists partly of the adhesion between filaments and layer failure caused by tension and shear loads.

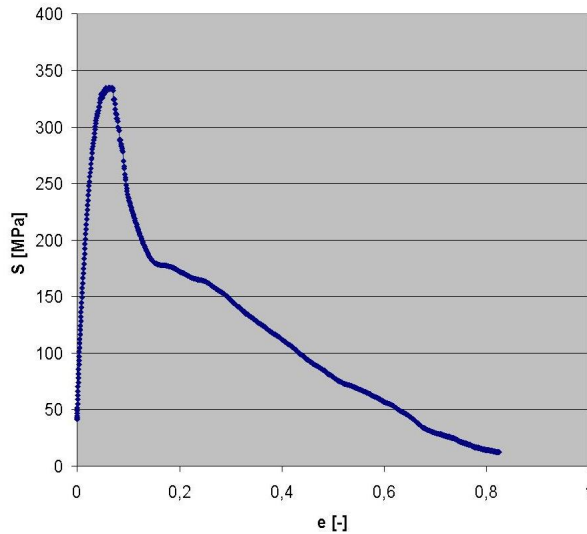


Figure 3.18: *Stress vs. strain of 5 mm Dyneema composite sample*

Three-point bending test

In order to determine the inter-laminar shear strength, a three-point bending test has been done. A schematic representation of the three-point bending test is shown in figure 3.19. A beam of material is balanced on two points and is loaded in the centre by a downward force F . The distance between the two points is 50 mm . This test is displacement driven, which means that the downward displacement of the Dyneema specimen increases as a linear function of time. The downward displacement is applied at a loading rate of 50 mm/min . The specimens used for this test have the same geometry as the tensile test specimens, and are rectangles of size $90\text{ mm} \cdot 10\text{ mm} \cdot 1.5\text{ mm}$. The exact dimensions are again measured before each test.

Delamination first occurs in the middle of the specimen, which is observed for ten out of eleven specimen. One of the test results is shown in figure 3.20, which is representative for all three-point-bending tests (for the first part of the test). For some specimens, it is seen that at the beginning, there is little resistance against the applied displacement. Some of the specimen have a small amount of curvature and first become straight, which can be seen from the small slope of the curve of the figure. After a constant slope, a higher resistance against bending is observed, which can be recognised by the steeper slope of the curve. After this, the curve levels off again and delamination growth is seen. After some softening behaviour, the curve remains more or less constant. In three of the eleven tests, some hardening is seen after softening.

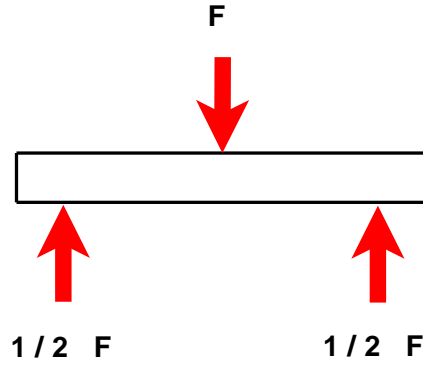


Figure 3.19: Schematic representation of three point bending test

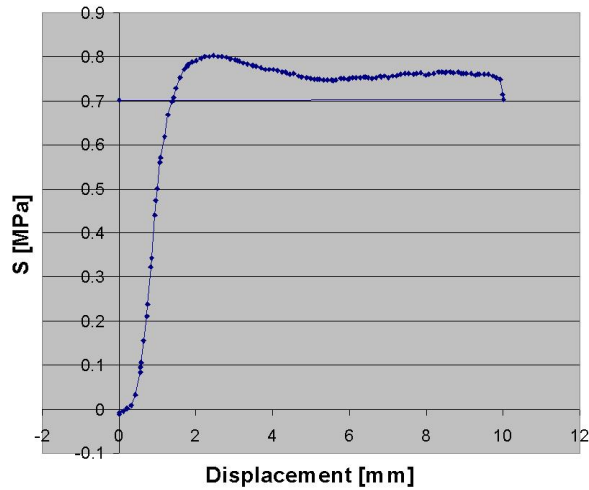


Figure 3.20: Results of three point bending test

The delamination strength is defined here as the maximum strength that occurs after the first time that hardening takes place. The average strength of eleven tests is 0.79 MPa . The standard deviation of the strength is 0.14 MPa , which is quite high. It should be noted that strength is not a pure material property and therefore it has a higher standard deviation than e.g. the stiffness of a material. The delamination strength of Dyneema composite that is found here should therefore be considered as an approximation of the inter-laminar strength. The displacement u at failure is 2.5 mm which is again averaged over 11 tests. The standard deviation is 0.67 mm , which is again high for the same reasoning stated earlier. This maximum displacement should be seen as an approximation of the maximum displacement.

3.4.3 Composite impact behaviour

Dyneema composite plates of 5 mm thickness can stop small projectiles. Upon stopping these projectiles, (damage) phenomena occur in such plates and are described hereafter.

Filament effects

If a projectile impacts on the panel, distinct phenomena can be seen at the filaments. The first thing to be seen is that due to impact, the filaments are loaded in tension. Some of them break during this process, because their ultimate tensile stress is reached. The filaments close to the projectile are not only loaded in tension. Depending on the geometry of the projectile, the filaments perform so-called sliding behaviour, see figure 3.21. The mechanism of filament sliding is demonstrated in figure 3.21 a) and b). Figure 3.21 a) shows two filaments before projectile impact. The projectile, in this picture an apple, is somewhat bigger than the space between the two filaments. However, the projectile is still able to move between the filaments without letting the filaments fail in tension, because they slide away from their original position, see figure 3.21 b). In figure 3.21 c), the same mechanism is shown for filaments in a Dyneema composite plate. Filament sliding does not directly cause filament failure. However, since some filaments slide away from the projectile, the filaments that are directly taken in the direction of the projectile are more heavily loaded. If fibre sliding would not occur, more filaments are available to directly take up the energy of the projectile.

Delamination

Delamination is caused by projectile impact, which exerts a load on the Dyneema composite target. If the interface is loaded too heavily, part of the sheets will detach, which is called delamination. Delamination can be easily

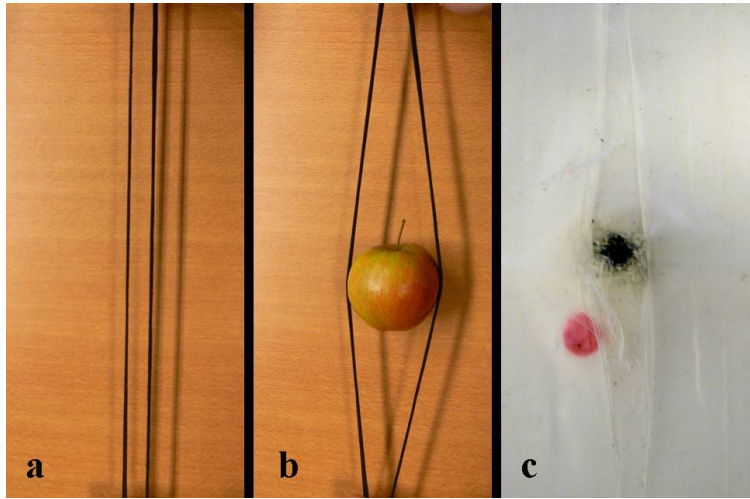


Figure 3.21: a) Two 'filaments' in rest b) Two 'filaments' sliding away c) Filament sliding in Dyneema composite

recognised by a thickness increase of the panel after impact, such as shown in figure 3.22 a).

In figure 3.22 a) the back side of a plate, which is impacted by a 9mm bullet at 400 m/s , by is shown. In figure 3.22 b) the front side of the same plate is shown. It is seen that the delamination pattern of the front and back of the plate differ significantly. The delamination at the back of the plate looks like a hill, while the delamination at the front is a star-shaped.

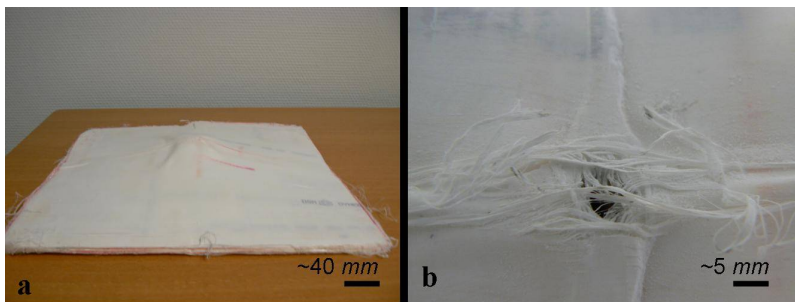


Figure 3.22: a) Backside of delaminated plate, b) Front side of delaminated plate

Heat effects

Just like for the fibre, a microscopic analysis of Dyneema composite before and after impact is made. In figure 3.23, three images are shown of a part of undamaged Dyneema HB25 composite. In figure 3.23 a), a section of Dyneema HB25 is shown. The sample is prepared by embedding a piece of Dyneema composite in epoxy resin and finished by planing and polishing the sample. In a single unidirectional layer is four to five filaments thick. This is even better seen in figure 3.23 b), in which a section of a unidirectional layer is shown using a SEM. In this figure, it is seen that the section is covered with a smooth layer. Due to cutting the sample using a surgical knife, some matrix material is spread over the filaments. In figure 3.23 c), a top view of a Dyneema HB25 layer is shown. It is seen that the unidirectional layers alternate and that they are oriented 90° with respect to the adjacent layers.

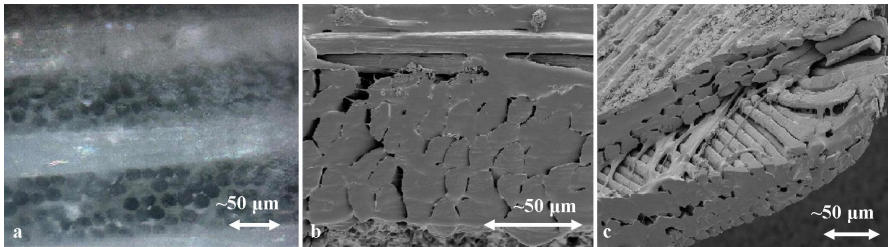


Figure 3.23: a) Section of Dyneema HB25 (optical microscope), b) Section of Dyneema HB25 (SEM), c) Top view of Dyneema HB25 (SEM)

Small parts of impacted Dyneema fibre were affected by local heat effects. Therefore, some heat effects are expected in Dyneema composite after impact as well. To be able to distinguish heat effects from other possible effects, the composite was heated to $353^\circ K$ locally. The filaments melt at a temperature of $403^\circ K$, so heat effects at $353^\circ K$ are expected to be matrix dominated. In the heated HB25 sample, three phenomena were seen and they are shown in figure 3.24. In figure 3.24 a), a phase transition of, mainly, filaments are shown. In figure 3.24 b) a network is shown and in figure 3.24 c), some bead-shaped material is shown. The network and beads are not seen after impact in the fibre and are probably a result of matrix melting.

Impacted Dyneema composite is compared with the heated and undamaged HB25 samples. The impacted composite is also analysed using a SEM and three images of this are shown in figure 3.25. Here, a phase transition, a network and beads, can be seen. Most of the filaments failed due to tensile loading, see figure 3.25 a). A small number of filaments has undergone a phase transition due to heating, which causes the network formation shown in figure 3.25 b). In figure 3.25 c), something similar to the earlier shown beads from figure 3.24 c) is seen. The beads in figure 3.25, however, have smaller diameters and the diameter of

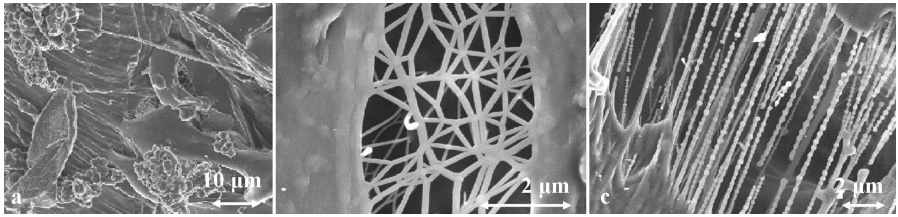


Figure 3.24: SEM images of heated HB25, a) Phase transition, b) Network, c) Beads

the connecting wire is also smaller. The beads in figure 3.25 c) seem to be part of a network. This has neither been found in the heated specimen of Dyneema HB25 composite nor in the impacted fibre. We expect that this matrix material that is heated and at the same time has been mechanically loaded. In the SEM images of the impacted composite, it was not possible to clearly distinguish between matrix material and filaments after impact. Only a small part, a few μm away from the impact point has been found to be affected by heat.

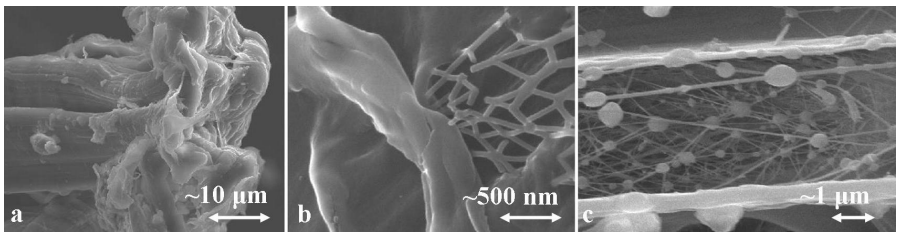


Figure 3.25: SEM images of impacted HB 25, a) Phase transition, b) Network, c) Beads

From the microscopic analysis, it turns out that some heat effects occur in Dyneema composite due to projectile impact. However, we may conclude that the majority of the filaments fail due to mechanical loads. It is nevertheless hard to conclude what the influence on the matrix material exactly is from this study due to heating or projectile impact, because it is hardly distinguishable from the filaments.

3.5 Discussion of Dyneema composite behaviour under projectile impact

In this chapter is shown that various processes occur in Dyneema composite due to projectile impact. Delamination, filament sliding and filament fracture can be detected by visual inspection. Heat effects can only be visualised using (electron) microscopy.

The areas influenced by local heating are typically concentrated within a sphere with a radius of a few μm from the impact point. Delamination, filament sliding and filament fracture are typically seen within a sphere with a radius of 100 mm from impact point. Heat effects are therefore considered negligible compared to the other phenomena that occur in Dyneema composite. Therefore, heat effects are not taken into account for the development of the simulation tool in this research.

Chapter 4

Discretisation of Dyneema composite

The goal of this research is to develop an appropriate tool for simulating perpendicular projectile impact on Dyneema composite plates. The simulations done with this tool should not only give a global visualisation of the impact and penetration or perforation of the projectile, but should also give more detailed information on the governing physical phenomena. As mentioned before, experimentally observed phenomena such as delamination, filament sliding and filament fracture should be included. Possible modelling concepts for the simulation of perpendicular projectile impact will be considered in this chapter. In section 4.1, overall replacement models are discussed. After that, we zoom in on a smaller scale and we will address micro-mechanical models in section 4.2. In section 4.3, we will address two layered replacement models, which are developed for this research.

4.1 Overall replacement models

In literature, there are currently no simulation tools available, by our knowledge, that can describe physical phenomena in a Dyneema composite plate due to perpendicular projectile impact on both a global and on a more detailed level. For other types of fibre reinforced polymer (FRP) plates only few simulation models are found for perpendicular projectile impact. These models, in general, simplify the composite too much for our research goal, see for example references [59], [60], [61] or [62]. FRP plates are often described with an ‘overall replacement model’ with anisotropic properties, see figure 4.1. In this figure is shown that there are various ways to describe the impact problem on Dyneema composite in terms of sizes. Note that other possibilities, such as multi-scale (domain decompositions) or stochastic models. These methods are however not considered here. The interested reader is referred to, e.g. reference [63].

The idea of such a overall discretisation is that the intricate local structural behaviour can be disregarded completely and that the replacement model gives a sufficiently accurate description of the impact and penetration or perforation processes. The anisotropic stiffness properties are generally found from simple bending and stretching experiments on FRP plate material and/or from ‘mixture rule’ considerations. If penetration or perforation should be described, adequate contact algorithms are required. In most commercially available simulation packages such algorithms are readily available.

The most challenging part of using an ‘overall replacement model’ is the creation of an adequate failure model. This is the essential part that is necessary to simulate the penetration or perforation of the projectile through the Dyneema composite target. After reaching a failure criterion, the material is in general either considered as void or its stiffness properties are extremely reduced. In this way, delamination phenomena could be described if a delamination is considered as a volume of ‘void material’. However, it appears to be hard to confine delamination in the filament directions or between Dyneema sheets only, such as is often observed in impact experiments. Simulated delaminations often cross the sheet layers or the filaments, which is generally not realistic (apart from some filament bridging). The intricate phenomenon of filament sliding can also not be described, because filaments are not physically present in this replacement model. Because of the reasons mentioned above, it is decided not to build an ‘overall replacement model’ for Dyneema composite. In this research, we aim at developing more sophisticated models than an overall replacement model.

4.2 Micro-mechanical replacement models

In our search towards more sophisticated models, it is essential to realise that the Dyneema composite is built-up from filaments and matrix material on a micro scale, see figure 4.2. We can see that on a micro scale we distinguish

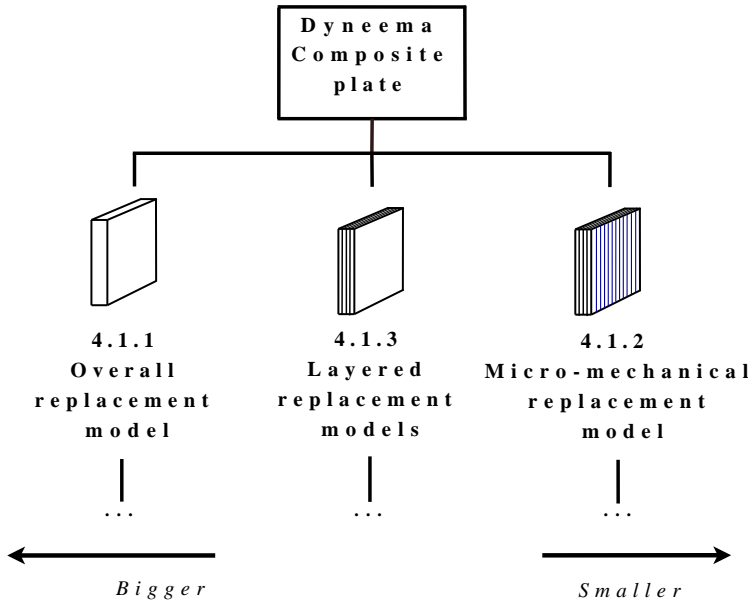


Figure 4.1: Possible scales to study a Dyneema composite plate

between the following three constituents or phases:

- filaments
- matrix material
- interfaces between filaments and matrix material

If we are able to establish appropriate mechanical models for each of these phases, including appropriate failure models, we could *in principle* build very detailed ‘micro-mechanical replacement models’ for a Dyneema composite plate. In such a model, all three phases could probably be well described by dedicated continuum descriptions. However, the restriction *in principle* is mentioned here on purpose, because we need to deal with severe problems if a micro-mechanical model would be developed. Two problems that could be encountered if appropriate mechanical models for each phase should be made are:

- We do not know the actual filament distribution, which is highly dependent on the location in the composite on a micro scale. This means that assumptions should be made for the filament distribution. From other attempts of micro-mechanical modelling for FRP, e.g. reference [64], [65] or [66], we have learnt that the actual mechanical behaviour of the composite very much depends on the assumptions made.

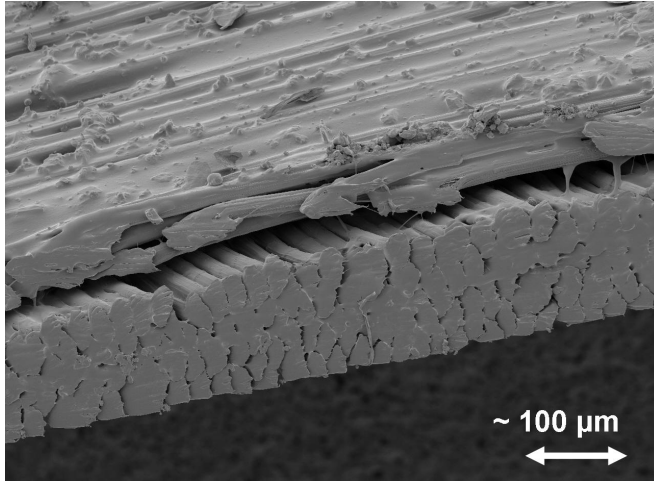


Figure 4.2: *Phases in Dyneema composite on a micro-scale. In this figure, filaments and matrix can be distinguished*

- The interfaces between filaments and matrix material are not perfect or are at least subject to variability. We should therefore, again, make assumptions for the failure models and variability.

Both problems make it hard to create an adequate micro-mechanical model. An additional problem is that if each individual filament with its surrounding matrix material would be modelled, the modelling of the whole plate will result in an extremely detailed and large model because of the enormous number of individual filaments in the Dyneema composite plate. If, for example, a FE method for the discretisation would be used, this would result in a model with such a large number of elements and nodes that the actual simulations cannot be performed with the currently available computers.

As a result, we decided to develop a simulation tool for Dyneema composite plates subjected to perpendicular impact of which the complexity is somewhere in between that of ‘overall replacement models’ and the ‘micro-mechanical replacement models’ mentioned above. By doing so, we will still be able to meet the pre-defined requirements and at the same time, we expect to be able to use a finite element discretisation leading to simulation times and memory requirements that are economically and practically feasible. Such models are discussed in the next section.

4.3 Layered replacement models

Examples of models that fall, in terms of complexity, between overall replacement models and micro-mechanical replacement models are ‘Layered replacement models’. Layered replacement models consist of a number of layers, which can have different properties, and an interface between these layers. In this section, two Layered replacement models, namely the *Orthogonal layered model* and the *Lumped filament-bundle model*, that are developed for this research are discussed.

4.3.1 Orthogonal layered model

If we approach the impact problem on a meso-scale instead of on a micro-scale, it is observed that the Dyneema composite plate is built-up from a number of uni-directional (UD) layers. These layers cross each other perpendicularly. A logical suggestion would therefore be to build a layered replacement model, in which each physical layer is replaced by a layer with anisotropic properties, which is in analogy with the earlier discussed ‘overall replacement model’ that was used for the whole plate. If a layered replacement model is to be built, we should deal with creating:

- an adequate continuum replacement model to describe the mechanical behaviour of single UD layers, which also includes failure criteria. This model will be referred to as the ‘UD-layer replacement model’
- an adequate model describing the contact between two adjacent (crossing) layers, including the failure development due to delamination. This model will be referred to as the ‘interface model’.

The development of both the UD-layer replacement model and the interface model will be challenging. If we build a ‘layered replacement model’ for the whole Dyneema composite plate, we see that because of the thickness of physical layers, about $17\ \mu m$, we will end up with quite a large amount of layers over the plate thickness, namely about 300 UD layers. Using finite element modelling, each layer should be discretised with several elements over its thickness. Furthermore, the size ratio of an element should preferably be close to one. This means that we will again end up with a FE model, which consists of too many elements and nodes. This will probably result in unrealistic simulation times and amount of memory usage. An alternative, at first sight, is to use layers of shell elements. However, we suspect that shell elements would simplify the model to a too large extent. From this, it can be concluded that this layered replacement model, where each UD-layer is replaced with an equivalent UD-layer replacement model and the connection between these layers is described by the interface model cannot be used for practical applications.

A possible improvement for this model, would be ‘orthogonal replacement models’, which describe the equivalent mechanical behaviour of two crossing UD-layers. In this case, however, the required number of layers over the plate thickness would only be reduced by a factor two. Consequently, the improvement in terms of simulation run time and memory usage would still be insufficient to become of practical use. Therefore, the idea rises to replace more physical layers with an orthogonal replacement model. In that case, the number of orthogonal replacement layers can be chosen over the plate thickness freely. Of course, convergence tests must be performed to establish the advisable numbers of layers over the plate thickness and to proof the validity of this idea. The actual description of this type of layered model, together with the creation of an adequate ‘orthogonal layer replacement model’ with matching failure criteria will be discussed in *Chapter 6 Orthogonal layered model*. In this chapter the applied interface model is also discussed.

It appears that the delamination phenomena can quite well be described with the above described orthogonal layered replacement model. The effects of filament sliding and filament fracture are, however, not considered. This is caused by the fact that no filaments are actually discretised in this model, because their reinforcements are taken into account in the orthogonal properties of the layers. This is the reason that an improvement of the layered replacement model is sought. The attained improvement is discussed in the next section.

4.3.2 Lumped filament-bundle model

The above described layered replacement model does not account for filament sliding and filament fracture, because actual filaments are not discretised in the model. The reinforcement effects of the filaments are only included by the appropriate orthogonal properties of the layers. To be able to include filament sliding and filament fracture, the filaments and their (failure) properties should be modelled separately. But as discussed previously a model which contains all physical filaments is currently not feasible for the same reasons, see also section 4.2. It was therefore decided to ‘lump’ filament bundles from each replacement layer towards the (inter-)faces of these layers, while correcting the orthogonal properties of the layers by simply subtracting the reinforcing effects of the filaments. In the FE model, this results in layers of ‘discrete filament bundles’. Between these layers of discrete filament bundles, three-dimensional elements with modified orthogonal properties are used. This modification should be done, because the filament reinforcing effects are subtracted from the rest of the composite. The details of this type of modelling will be discussed in *Chapter 7 Lumped filament-bundle model*.

With discrete filament bundle layers with relatively weak three-dimensional elements in between, using an interface model has become super fluent. We can now describe delamination phenomena by ‘voiding’ the relatively weak layers between the discrete filament bundles, after reaching a failure criterion. In this

case, delaminations will automatically be controlled to run in between the space of the discrete filament bundle layers.

If sufficient numbers of ‘discrete filament bundles’ in thickness as well as in lateral directions are chosen, it is expected that the ‘Lumped filament-bundle model’ will show the equivalent mechanical behaviour of the real Dyneema composite during impact. The number of discrete filament bundles crossing the path of the projectile should, of course, be adequately chosen. For this purpose, various convergence studies should be performed. These studies and some obtained results are reported in *Chapter 7 Lumped filament-bundle model*.

Chapter 5

Approaches to study impact on Dyneema composite

It is outlined in *Chapter 3 Dyneema behaviour*, that a Dyneema composite plate subjected to impact can be discretised on different levels, namely on a plate, layer, constituents, an atomic or even smaller level. In addition to different discretisation levels, various methods are available with which Dyneema behaviour can be studied. We submit that the methods that are applicable to this research are empirical (or phenomenological) or simulating in nature. Both methods are addressed in this chapter and it turns out that simulation methods are most suitable to use for our research goal stated in *Chapter 1 Introduction*. A variety of (commercial) software is available for making computer simulations and therefore a trade-off is made between ABAQUS, Autodyn and LS Dyna. In the ballistics field, there is a trend towards using one of these three software packages, which have all shown to be suitable for modelling impact events. As described hereafter, ABAQUS, of these packages, is the most suitable for our research.

5.1 Empirical methods

Empirical methods, in general, are used to find a relation between parameters. In other words, a relation between the input and output should be found. The required data is usually generated by carrying out a number of experiments in which the input parameters are varied. By performing curve fitting, regression analysis or dimensional analysis, the input is related to the output.

5.1.1 Empirical methods employed for impact on fibre reinforced composites

Empirical methods have proved to be a useful means to explore the ballistics field. They have been established in the ballistics field because it was believed that describing impact events was technically so complex that it triggered the possibility of using other methods that researchers have at their disposal, such as simulation methods.

As stated above, if a relationship between parameters should be found, the input parameters are varied to find a relation between input and output. In this specific case, the input variables are the (material) properties of the target and projectile, projectile velocity, and projectile orientation are varied. The output parameters to which a relation should be found are the projectile residual velocity, projectile orientation, maximum deformation of the target or delaminated area.

5.1.2 Discussion of empirical methods in impact problems

Empirical methods are especially useful if much data is already available, for example in test laboratories. Employing empirical methods for impact problems is rather costly, since a large number of test specimens and also a large number of experiments are required. Despite the fact that empirical methods give insight in how the results depend on the input parameters, a serious drawback is also revealed. Empirical methods do not give information on what happens in the Dyneema composite plate; this is treated as a black box. Since the present research goal is to visualize what happens in Dyneema composite, empirical methods will not be considered in this research.

5.2 Simulation methods

Governing equations can often not be solved analytically, because of the size and complexity of the problem. The solutions to these equations are therefore usually approximated numerically or, in other words, simulations are made.

5.2.1 Simulations of impact on fibre reinforced composites

If simulations of projectile impact on Dyneema composite are made, reality is approximated such that the behaviour of both the composite and the projectile can be described by the governing equations. Whether the simulation is realistic depends on the assumptions that are made and the applied discretisation level. Simulations allow for determining the relation between input parameters and results, but in addition allow for studying the processes inside Dyneema composite during impact.

5.2.2 Discussion of simulations in Dyneema impact problems

Simulation methods can serve as an aid towards a good understanding of what happens in the material due to projectile impact. Developing a simulation tool may however be time-consuming; the appropriate discretisation level should be determined; it should be determined what properties and governing equations are relevant; the relevant properties should be (experimentally) determined etc. The possibility of being able to study what happens in the material is nevertheless crucial for this research and therefore a simulation tool is developed in this research.

5.3 Used simulation software packages

5.3.1 Commercial code

In response to the need for a simulation tool in industry, a commercially available software package is selected to attain the goals of this research. In commercial packages the most common governing equations and element formulations have already been implemented. In the terminal ballistics field, there is a tendency towards using LS Dyna, ABAQUS or Autodyn for impact simulations. A deliberate choice is made between these three packages for which the available constitutive models, element-library and integration schemes are considered.

5.3.2 Constitutive models

In ABAQUS and Autodyn, the constitutive behaviour of a material, from the elastic region up to final failure, is built up by the user. For this research, an elastic constitutive model should be combined with a constitutive failure model. Both ABAQUS and Autodyn offer the possibility to combine an elastic constitutive model with a failure constitutive model, although the number of constitutive models in Autodyn is limited compared to ABAQUS.

LS Dyna, by contrast, offers ready-to-use constitutive models, which describe the behaviour from the elastic region up to final failure. It is impossible to implement the material behaviour by making different combinations of elastic and failure models such as in ABAQUS and Autodyn. Despite the absence of the option to freely combine elastic constitutive models with failure constitutive models, many constitutive models are available in LS Dyna. If the available constitutive models do not suffice, ABAQUS, Autodyn and LS Dyna all offer the possibility to implement constitutive models by user-defined Fortran routines.

5.3.3 Element library

In *Chapter 3 Dyneema behaviour*, it is stated that two layer-level models are developed in this research. To be able to build different models and to experiment with the various modelling possibilities, various elements are required. Examples are cohesive elements or some other type of interface elements for describing the interaction between the layers, truss elements to represent the filaments and three-dimensional elements for the remainder of the composite.

Three-dimensional elements are available in all three software packages. Elements to model the behaviour between the layers are available in LS Dyna and ABAQUS, but not in Autodyn. Elements such as rod or beam elements for modelling the filament behaviour, are not available in Autodyn either.

5.3.4 Integration schemes

In high-speed impact problems, defined as cases in which the projectile impact velocity exceeds 10 m/s , an explicit integration scheme is, in general, used to solve the governing equations. If an implicit scheme is used, the time steps would become too large and higher order effects, which play a role in especially dynamic problems, would not be taken into account. Since higher order modes are important for events that are dominated by high strain rates, an explicit integration scheme is more suitable for our problem to describe Dyneema impact, see also reference [67].

In all three software packages, an explicit integration scheme is available. In ABAQUS, an implicit scheme is also available, which enables the user to simulate quasi-static load cases using the same simulation model. An example could be a load case in which a pre-stress is applied and impacted after that.

5.3.5 Discussion of simulation software

Summarising, using Autodyn is abandoned because of the limited number of available constitutive models. Reinforcing this view is the absence of elements to represent the interface and the filaments. Both ABAQUS and LS Dyna offer

sufficient possibilities to experiment with various replacement models. An extra advantage of ABAQUS over LS Dyna is that in ABAQUS material models can be built up from different standard modules. This gives a flexibility in using material models without directly having to write a material user subroutine. Further, it is seen that in ABAQUS both implicit and explicit calculations can be made on the same model (under certain conditions). Since these kinds of calculations may be needed in the future, the simulation model is developed in ABAQUS to take full advantage of its possibilities ¹. Later in this research, it has turned out that contact definitions are essential in modelling impact problems. Since this was not clear in the early phase of this research, contact definitions have not been taken into account when choosing simulation software.

¹It should be noted that these software packages have been studied in 2005. Since the development of software is an ongoing process, the information given above may be outdated

Chapter 6

Orthogonal layered model

One of the effects that occurs in Dyneema-composite plates due to projectile impact is delamination. Delamination, amongst others, should be described by the simulation tool that we developed. Recently, quasi-static delamination development caused by shear loads in (notched) composite specimens has successfully been modelled using a layered modelling approach, see reference [28]. This has been done by representing a fibre-reinforced cross-ply composite with a replacement model that consists of a set of UD layers with an interface layer between the layers. A summary of this work is given in section 6.5. In this research, a layer discretisation is also used to develop a simulation tool that is able to show delamination development in Dyneema composite that is impacted by a rigid projectile. The developed model is called the *Orthogonal layered model* and is described in section 6.2. The convergence test of the ballistic simulations done with this model are described in section 6.3. Finally, the results obtained with the Orthogonal layered model are given in section 6.4 and discussed in section 6.5.

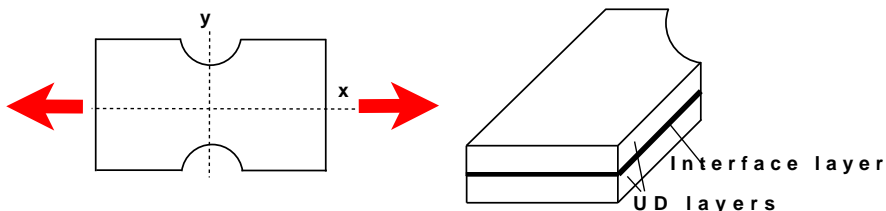


Figure 6.1: Notched specimen

6.1 Previous work on Layered modelling

Continuous fibre-reinforced composites are, still, often represented by overall replacement models. As discussed in *Chapter 4 Discretisation of Dyneema composite*, overall replacement models only allow for a description of the composite's average behaviour. Liu developed a more detailed model that can describe delamination development in notched composites, see reference [28]. This work inspired us to represent a Dyneema composite panel as a set of discrete layers with interface layers between these discrete layers.

Liu modelled a cross-ply, glass-epoxy composite with a layered model and simulated delamination development in specimens such as shown in figure 6.1, see also reference [28]. The specimens that he modelled are built up from unidirectional (UD) layers, both in reality as well as in the model. These layers together form a $[0_n/90_{2n}/0_n]$ composite. The UD layers are strong and stiff in the fibre direction and are weaker and less stiff in the directions perpendicular to the fibres. The glass-epoxy composite is modelled by a number of UD layers having interface layers in between. The interface layers represent the bonding between the UD layers. By making such a discretisation, (notched induced) delamination development in fibre-reinforced composites can be described in more detail than if the composite would be represented by an overall replacement model.

We will now explain the statement about a discrete layered model being able to show more detail than an overall replacement model. Let us therefore focus on the failure behaviour of a composite material. A composite material, by definition, consists of at least two materials. In overall replacement models, failure behaviour of the composite material is uniquely defined, i.e. by a single material model, while it may be a result of interacting phenomena, see *Chapter 4 Discretisation of Dyneema composite*. Since it is difficult, if not impossible, to define a single criterion that captures all interrelating failure mechanisms, the way a composite material fails in a simulation done with an overall replacement model can deviate tremendously from what is found in experiments. The way that a composite fails is a result of (the interaction of) failure of its components rather than a single mechanism. Liu's model, consisting of crossing UD layers

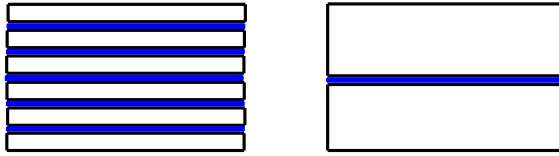


Figure 6.2: *Discretisation of layers. Composite consisting of 6 sheets (left), discretisation of the 6-layer composite into two layers with an interface in between (right)*

and interface layers, allows for a definition of different failure mechanisms and interactions between these failure mechanisms; this is the main reason why more realistic results are obtained with a layered model than would ever be achieved using an overall replacement model.

6.2 Description of the Orthogonal layered model

6.2.1 Principle

In the Orthogonal layered model, failure is considered as a function of different failure mechanisms of individual components of the composite. In the Orthogonal layered model, we choose to model Dyneema composite by discrete layers (having properties of orthogonal Dyneema layers) and interface layers between them. The Orthogonal layered model can therefore show failure of Dyneema layers, failure of interfaces and the interaction between these failure mechanisms. In an overall replacement model, a composite would simply be modelled as a material with orthotropic properties and accompanying failure criteria. In other words, it would not be possible in an overall replacement model to distinguish between different failure mechanisms.

From the discussion above, it may be understood that not every real Dyneema sheet is modelled separately. The reason for this is that the size of the model would become too large. Therefore, a number of Dyneema sheets are modelled together as a orthotropic layer, see also *Chapter 4 Discretisation of Dyneema composite*. Replacing multiple plies with a single layer is schematically shown in figure 6.2. In the left of figure 6.2, a six-ply composite with interface layers between the plies is shown. If it would be represented by a replacement model consisting of two orthotropic layers and an interface layer in between, it would look like what is shown in the right of figure 6.2. The requirement for the replacement model being an appropriate one is that the behaviour, such as maximum displacement or failed area, at least approaches that of the original six-layered composite.

By modelling Dyneema composite as described above, we think that it is possible to obtain more detailed simulation results than with an overall replacement

model. Hereafter, the components of the Orthogonal layered model, namely the *Orthogonal layers* and the *Interface layers* are described in more detail.

Orthogonal layers

The orthogonal layers in this model refer to the Dyneema sheets in the composite. In this model, the layers are described with an orthotropic material model. The adhesion properties will be projected on the interface layers, which will be discussed after this. This discretisation decouples the better properties of the composite, namely strength and stiffness, from one of its weaker properties being the adhesion between the sheets in the Orthogonal layered model.

Interface layers

The adhesive properties between the orthotropic Dyneema layers are modelled with cohesive elements in the Orthogonal layered model. The cohesive elements describe the interface behaviour, which is mainly detaching of layers that result in delamination. Cohesive modelling is similar to fracture mechanics in the sense that both methods can describe crack development. The difference comes from the fact that in fracture mechanics methods, a crack area must be assumed before loading occurs, whereas in cohesive modelling no preliminary assumption of the place of the crack is required. This means that crack initiation *and* development can be modelled by using cohesive elements as opposed to fracture mechanics methods, in the sense that a crack location does not need to be defined at the beginning of the simulation.

6.2.2 Model description

In this part, we will describe the Orthogonal layered model that we have developed. The material properties, used in the models, is based on the data of our own experiments. The overall replacement material properties are obtained from reference [68]. The data stated in this reference is property of to TNO and is confidential.

Geometry

The model that has been used for analysis consists of six Dyneema layers and five cohesive layers. The three-dimensional elements in the Dyneema layers have sizes 0.5 mm by 0.5 mm by 0.16375 mm and the cohesive elements have sizes of 0.5 mm by 0.5 mm by $1.4 \cdot 10^{-3}\text{ mm}$.

Initial conditions

A velocity \bar{V} , is posed on the projectile as an initial condition. Prior to impact, the projectile has a velocity of 300 m/s in positive z-direction; this is the

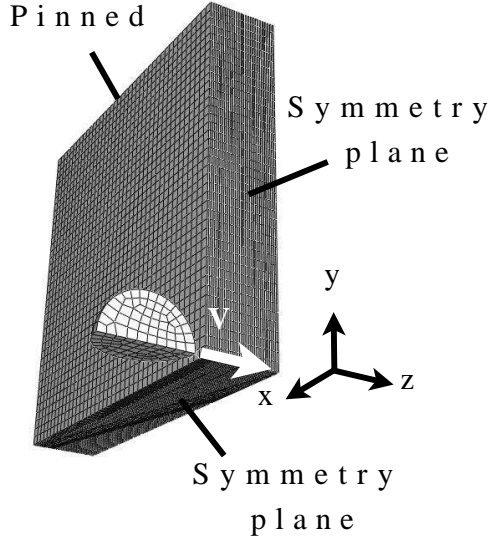


Figure 6.3: *Impact case.*

direction, normal to the Dyneema composite plate just like in the test case shown in figure 6.3, in which the impact case is shown. The other velocity components (in x-direction and z-direction) are zero.

Boundary conditions

Boundary conditions are applied to the Orthogonal layered model. The boundary conditions are posed on the upper and lower edges of the plate. Boundary conditions, amongst others, determine the way that waves are reflected at the border of the plate and thus influence the wave pattern in the composite that result from a projectile impact. The boundary conditions are applied at the xz -plane shown in figure 6.3 (indicated by ‘pinned’). These pinned boundary conditions are applied in all simulations and means that the displacements u_x, u_y, u_z , are equal to zero.

In addition to a pinned boundary condition on the outer edges of the plate, symmetry conditions are posed on two faces, see also figure 6.3. Both the projectile and the Dyneema composite plate are symmetric about the xz -plane and the yz -plane. On the xz -plane, the symmetry conditions are $u_y, \theta_x, \theta_z=0$ and on the yz -plane the symmetry conditions are $u_x, \theta_y, \theta_z=0$. By doing so, only a quarter of a plate needs to be modelled instead of the whole model. We assume that the deformation pattern caused by projectile impact follows the same symmetry.

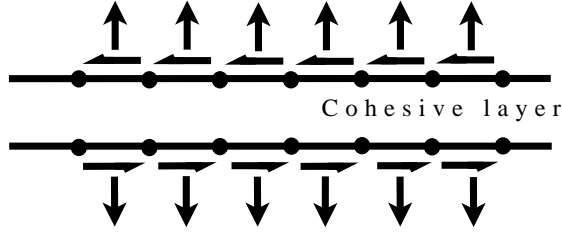


Figure 6.4: Load cases that can be described by a layer of cohesive elements

Constitutive models

The simulations done with the Orthogonal layered model contains two bodies, namely the projectile and the Dyneema composite plate and the latter is modelled with the Orthogonal layered model). The projectile is modelled as a rigid body, because the projectile's deformation is assumed to be negligible, which is in accordance to experiments for steel projectiles and with the velocities until at least 500 m/s .

The adhesive layers between the discrete layers are described using cohesive elements. Cohesive elements can take up through-thickness tension and shear stresses, see figure 6.4. The presence of the cohesive elements will therefore affect the matrix $[C]$ (see formula 6.3); more specifically values C_{33} , C_{55} , C_{66} , C_{31} and C_{23} in the discrete layers as compared to an overall replacement model, see section 1.2.1. The value of C_{33} in the discrete layers will be higher than that in an overall replacement model, since the Dyneema layers themselves have a very high resistance against deformation in that direction. For the same reason, C_{55} and C_{66} are higher for the discrete Dyneema layers than for in overall replacement model. Additionally, also the terms associated with Poisson contractions, i.e. C_{31} and C_{23} , will be lower, because the discrete layers will have less contractions.

The constitutive model of the interface is shown in figure 6.5 (not on scale). The constitutive response of the interfaces, or rather adhesive layers, is assumed to be linear in first instance as shown in this figure. In the elastic regime, the constitutive response is described with a linear elastic traction-separation law as follows:

$$\bar{t} = \begin{pmatrix} t_n \\ t_s \\ t_t \end{pmatrix} = \begin{pmatrix} K_{nn} & K_{ns} & K_{nt} \\ K_{ns} & K_{ss} & K_{st} \\ K_{nt} & K_{st} & K_{tt} \end{pmatrix} \cdot \begin{pmatrix} \epsilon_n \\ \epsilon_s \\ \epsilon_t \end{pmatrix} \quad (6.1)$$

In equation 6.1, s and t are the in-plane directions and n the out-of-plane direction that is in the direction perpendicular to s and t , see figure 6.6. Here, \bar{t} represents nominal traction with components in n , s and t direction. Here, \bar{t} is expressed in force per unit area. The \bar{t} is the result of an applied strain $\bar{\epsilon}$ and

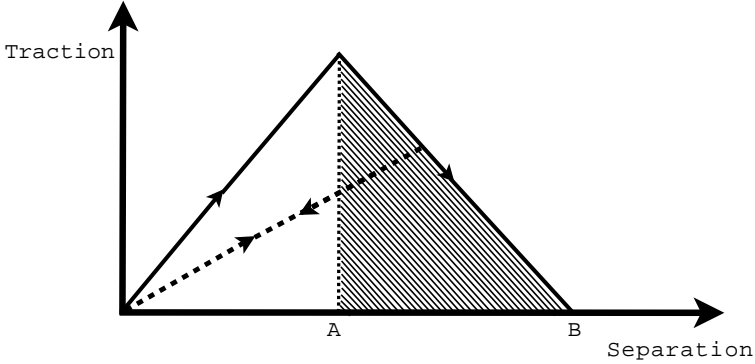


Figure 6.5: *Constitutive behaviour of cohesive zones (not on scale)*

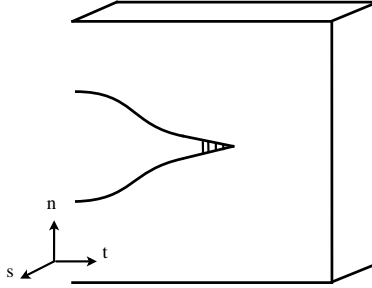


Figure 6.6: *Cohesive zone reference frame*

K_{ij} is the matrix that relates traction \bar{t} to strain $\bar{\epsilon}$. The delamination development in Dyneema composite is mainly determined by K_{nn} . Permanent debonding of layers occurs if the Dyneema composite is loaded beyond its elastic limit, i.e. beyond point A in figure 6.5. The elastic part is small for Dyneema and the elastic stress-strain response can be assumed to be linear. For Dyneema, the elastic limit is reached if:

$$\left\{ \frac{\langle t_n \rangle}{t_n^0} \right\}^2 + \left\{ \frac{t_s}{t_s^0} \right\}^2 + \left\{ \frac{t_t}{t_t^0} \right\}^2 = 1 \quad (6.2)$$

Here, t_i is a traction in a certain direction and t_i^0 are the accompanying maximum stresses. Note that $\langle t_n \rangle$ has the value t_n if the value is positive and zero otherwise; this means that the cohesive elements can only fail in tension. If the left side of the equation is equal to one, the interface is assumed to have reached its elastic limit and delamination development starts if the interface is further loaded in tension. In our model, it is assumed that the interface has the same stiffness in all directions (because the matrix material has isotropic

properties), but is stronger in the in-plane direction than in the out-of-plane direction, which is also what would be expected from a layered composite material, see reference [69]. We choose for this failure model, because we assume that failure occurs as a function of bending loads that are induced by projectile impact. These bending loads cause both normal loading of the interface as well as shear loads. We believe that it is the interaction between shear and normal load that eventually determine whether delamination occurs or not. This is the standard interactive criterion available in ABAQUS and because we did not do experiments that show a different relationship, we choose what is available in ABAQUS, see formula 6.2. The properties of the cohesive elements, such as used in our simulations, are stated in table 6.1.

If the composite is loaded beyond its elastic limit, debonding of the Dyneema sheets becomes permanent. The way from the elastic limit until final rupture can occur in different ways, e.g. linear, exponential etc. From reference [70], we know that the critical energy release rate rather than the shape of the softening curve determines the final failure of the interface. In this research, we choose a linear softening curve and failure (indicated with point B in figure 6.5) that is based on energy. If we relate this to figure 6.5, this means that the adhesive bond is failed if the hatched area is equal to the specified critical energy release rate.

Table 6.1: *Properties of cohesive elements*

Property	Value	Unit
ρ	980	kg/m^3
K_n	850	MPa
K_s	850	MPa
K_t	850	MPa

The behaviour of Dyneema composite is schematically shown in figure 6.7 (not on scale) for a single material direction. Although the properties are direction-dependent, the shape of the stress-strain curve is the same. In first instance, the Dyneema sheets respond elastically to loading. As described in *Chapter 3 Dyneema behaviour*, Dyneema sheets consist of matrix material and Dyneema filaments and the properties of the layers therefore represent the average behaviour of the matrix material and the filament material. In this case, they form a material that has orthotropic properties that can be described by the matrix $\overline{\overline{C}}$ ¹:

¹The values of C_{ij} are confidential and property of TNO and can hence not be given in this thesis. For more information, see reference [68]

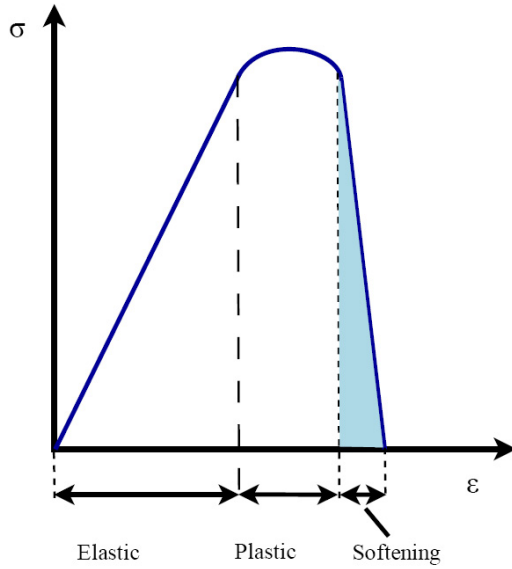


Figure 6.7: Schematic stress-strain behaviour of Dyneema sheets (not on scale)

$$\bar{\bar{C}} = \begin{pmatrix} C_{11} & C_{12} & C_{13} & 0 & 0 & 0 \\ C_{12} & C_{22} & C_{23} & 0 & 0 & 0 \\ C_{13} & C_{23} & C_{33} & 0 & 0 & 0 \\ 0 & 0 & 0 & C_{23}^s & 0 & 0 \\ 0 & 0 & 0 & 0 & C_{31}^s & 0 \\ 0 & 0 & 0 & 0 & 0 & C_{12}^s \end{pmatrix} MPa \quad (6.3)$$

Beyond the elastic limit, an orthotropic Hill surface is used to implement direction-dependent plastic and failure behaviour in these layers. Hill's surface is given in reference [71]:

$$f = \sqrt{\frac{F(\sigma_{22} - \sigma_{33})^2 + G(\sigma_{33} - \sigma_{11})^2 + H(\sigma_{11} - \sigma_{22})^2}{+2L\sigma_{23}^2 + 2M\sigma_{31}^2 + 2N\sigma_{12}^2}} \quad (6.4)$$

with

$$F = \frac{\sigma_p}{2} \left(\frac{1}{\bar{\sigma}_{22}^2} + \frac{1}{\bar{\sigma}_{33}^2} - \frac{1}{\bar{\sigma}_{11}^2} \right) \quad (6.5)$$

$$G = \frac{\sigma_p}{2} \left(\frac{1}{\bar{\sigma}_{33}^2} + \frac{1}{\bar{\sigma}_{11}^2} - \frac{1}{\bar{\sigma}_{22}^2} \right) \quad (6.6)$$

$$F = \frac{\sigma_p}{2} \left(\frac{1}{\bar{\sigma}_{11}^2} + \frac{1}{\bar{\sigma}_{22}^2} - \frac{1}{\bar{\sigma}_{33}^2} \right) \quad (6.7)$$

$$L = \frac{3}{2} \left(\frac{\tau_p}{\bar{\sigma}_{23}} \right)^2 \quad (6.8)$$

$$M = \frac{3}{2} \left(\frac{\tau_p}{\bar{\sigma}_{13}} \right)^2 \quad (6.9)$$

$$N = \frac{3}{2} \left(\frac{\tau_p}{\bar{\sigma}_{12}} \right)^2 \quad (6.10)$$

$$(6.11)$$

In these equations $\bar{\sigma}_{ij}$ is the yield stress in the specific direction, σ_0 is the pressure yield stress and $\tau_p = \sigma_0/\sqrt{3}$. Damage is initiated if the plastic strain treshold ω_D is equal to one. The plastic strain treshold is given by:

$$\omega_D = \int \frac{d\bar{\epsilon}_p}{\bar{\epsilon}_p^D} \quad (6.12)$$

with $\bar{\epsilon}_p^D$ the threshold strain value for onset of damage (or elastic limit). We use a Hill surface, because the constitutive model that we used for the elastic part of the Orthogonal layers, require that we define a direction dependent behaviour for the plastic regime. However, the plastic strain is taken a thousand times smaller than the maximum elastic strain. This ensures that there is almost no plastic behaviour before actual failure occurs.

This onset threshold is again different for each direction using a Hill surface f . Once damage is initiated, the material starts to degrade. From reference [70], it is known that the failure of materials can be best characterised by their failure energies, which is similar to the approach used for the cohesive layers. From his research, it turns out that the failure behaviour (linear, quadratic etc.) has almost no influence on the outcome. Our choice for a linear failure behaviour is therefore quite arbitrary. After this energy is taken up by an element, the element is considered failed and taken out of the computation. The mass of the element is however retained.

Mesh

The Dyneema plate has six orthogonal layers, each having a thickness of 0.66 mm with four elements through the thickness. The Orthogonal layers are

modelled with C3D8 elements, which are three-dimensional elements with eight nodes. Between the Dyneema layers, interface layers are placed that are modelled with cohesive elements. In these simulations COH3D8 elements are used, which is an acronym for a three-dimensional cohesive element with eight nodes. The mesh of the cohesive elements match with the mesh of the three-dimensional elements; the cohesive elements only differ in thickness compared to the three-dimensional elements. The thickness of the cohesive elements are 0.008 mm , which is close to zero. The thickness value of the cohesive elements is chosen close to zero, because in the reality there is no distinct physical adhesive layer. The purpose for using cohesive elements is therefore to have the possibility to resemble the adhesive properties between the orthogonal layers. In our opinion, this can best be approximated by choosing a very thin adhesive layer. The value for the thickness could even be smaller, but then the computational time will also increase accordingly. The mentioned value is therefore a compromise between being as closely as possible to zero thickness and computational time².

Contact definition

In the ballistic simulations, the projectile impacts on the Dyneema composite plate. Once the projectile touches the plate, the projectile interacts with the plate and a contact definition is required to describe this interaction. A contact definition is also required to describe the interaction between the layers in the Orthogonal layered model. This contact definition is needed in the case that cohesive elements fail and the orthogonal layers can come in contact with each other. This contact definition should fulfill the requirements stated hereafter. The contact algorithm should be able to describe contact between rigid bodies, deformable bodies and self-contact. If the contact between bodies would result in a penetration, this should be prevented by the algorithm. Usually, the outer surfaces of the bodies that can potentially interact with each other or with themselves are defined as the contact surface in contact algorithms. These surfaces are defined by the edges of the elements at these surfaces and the nodes of the elements. An appropriate contact definition should preferably exclude node into surface and edge to edge penetration to prevent penetration of two bodies. It may be clear that multiple contact with an element should be possible. Because the relative displacements on the contacting surfaces can be quite large, a ‘finite-sliding’ formulation is used. This so-called ‘finite-sliding formulation’ should be used for large displacement problems. In addition to this, if an element fails (and is hence removed from the simulation) the contact surface of the body that contained the failed element should be redefined by the algorithm. In ABAQUS/Explicit, there are two algorithms that can be used to define contact between objects, namely the general contact algorithm and the contact

²in ABAQUS, the geometric thickness is used to determine the time-step

pair algorithm. In addition, there is also a possibility to define an own contact formulation, see references [72] and [73]. Because the general contact algorithm seemed to fulfill all the requirements above, it is used in these simulations. Because the contact pair algorithm allows self-penetration of a body and does not allow for a redefinition of a contact surface if a failed element is removed, this algorithm is not used here.

In the simulations, the contact between the bodies is assumed to be frictionless. The friction coefficient from Dyneema on steel is $\mu = 0.01$, which is very low and can therefore be said to be frictionless compared to most materials. Furthermore, if the simulated ballistic experiments are performed, there is no measurable temperature at the point of impact, see also *Chapter 3 Dyneema behaviour*. This indicates that the energy loss of the projectile due to friction effects is negligible and therefore friction is not taken into account.

In essence, the used contact algorithm in this case checks if there is a gap h between the different bodies. If two (or more) bodies are not in contact, $h > 0$. There are hence two possibilities, the gap between the bodies can be either open or closed:

$$p = 0 \cap h > 0 \text{ open} \tag{6.13}$$

$$h < 0 \cap p > 0 \text{ closed} \tag{6.14}$$

with p the pressure that the bodies exert on each other. If $h < 0$, the bodies that are interacting are penetrating each other. This is not acceptable and the algorithm calculates what pressure p should be applied to the bodies to get back to the condition $h=0$. This is done by taking the average of the required pressure p required to push back the bodies by taking the bodies in turn to be the master surface. Summarising, the requirements that we put on the contact definition are covered by the used general contact algorithm in ABAQUS.

Stable time increment

Simulations should preferably run as fast as possible. The simulation run time depends, amongst others, on the type of elements that are used in the simulation (in which the smallest time increment is the limiting factor). The simulations, done with the Orthogonal layered model, contain three different elements, rigid body elements, cohesive elements and three-dimensional solid elements. The stable time increment, and thus the total simulation run time, is determined by the smallest stable time increment in the simulation. In this case, it will be determined by the three-dimensional solid elements and the cohesive elements, because rigid elements have a large stable time increment. The stable time increment Δt is given by reference [72]:

$$\Delta t = \frac{T}{C_l} \tag{6.15}$$

Here, T is the characteristic element length and C_l the longitudinal wave velocity $\sqrt{\frac{E}{\rho}}$ in the element. Preferably, the stable time increment of the elements in the same simulation and that of the surrounding elements should have the same value. In this (ideal) case, none of the elements would be limiting the speed of the calculation and the ratio of the stable time increments should be close to one:

$$\frac{\Delta t_c}{\Delta t_m} = \sqrt{\frac{\bar{\rho}_c \cdot K_m}{\bar{\rho}_m \cdot K_c}} \approx 1 \quad (6.16)$$

Δt is the stable time increment; $\bar{\rho}$ is the areal density; the indices c and m indicate a composite layer and a matrix property respectively. With K , the stiffness of the specific elements according to:

$$K_i = \frac{E_i}{T_i} \quad (6.17)$$

The stable time increment of the three-dimensional solid elements is in the present simulations in the order of milliseconds, whereas the stable time increment of the cohesive elements is in the order of microseconds. This is caused by the much smaller thickness of the cohesive elements compared to that of the solid elements. At the same time, E_i is smaller while the densities of both elements are about the same. From this, it may be clear that the stable time increment of the simulations is clearly determined by the cohesive elements.

6.3 Convergence test

Liu's model, is developed for quasi-static load cases. Therefore, we assume that the Orthogonal layered model converges for (quasi-) static load cases. A difference, however, between Liu's model and the Orthogonal layered model is that his model is built up from UD layers and that our model consists of orthotropic layers.

In this section, projectile velocity V_p at $t = 20\mu s$, maximum displacement of the nodes in the composite plate in shooting direction u_{max} and delaminated area A_{del} ³ at $t = 20\mu s$ as a function of mesh size, mesh pattern and size of the plate are reported. For all models, a quarter of a Dyneema composite plate is modelled and the initial and boundary conditions in the model are defined according to the reference frame as shown in figure 6.3. The upper part of the plate is pinned, i.e. $u_x = u_y = u_z = 0$. On the xy symmetry plane, $u_z \equiv 0$ and on the xz symmetry plane, $u_y \equiv 0$. The projectile has an initial velocity of 300 m/s in positive z -direction and is placed 0.5 mm in front of the plate at the

³The delamination area is defined as the area of the projection of delamination in the plate on the xy -plane

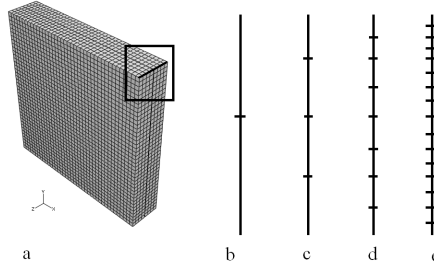


Figure 6.8: Models used to study the influence of the number of cohesive layers to the simulation results. a) Whole model b) Projection of corner of model with 1 cohesive layer, c) Projection of corner of model with 3 cohesive layers, d) Projection of corner of model with 7 cohesive layers, e) Projection of corner of model with 15 cohesive layers

beginning of the simulation. Unless stated otherwise, the plates are 20 mm by 20 mm.

Number of interface layers

To study if the number of interface layers influences the simulation results, four simulations are done. These simulations all have the same outer dimensions, but have a different number of interface layers, namely 1, 3, 7 and 15 interface layers, see figure 6.8. In this figure, the horizontal lines represent the location of the interface. The simulations with 1, 3, and 7 interface layers have eight three-dimensional elements through the thickness, while the simulation with 15 interface layers has 16 elements through the thickness. The critical energy release rate is the same for the cohesive layers in the different simulations.

Table 6.2: Summary of study to the influence of the number of interface layers in a 4.007 mm Dyneema composite plate. The result data is given at $t = 20\mu\text{s}$

Coh. layers	V_p	u_{max}	A_{del}
1	237.9 m/s	3.8 mm	349 mm ²
3	237.9 m/s	3.8 mm	352 mm ²
7	238.1 m/s	4.1 mm	354 mm ²
15	238.2 m/s	3.7 mm	351 mm ²

The results of these four simulations are summarised in table 6.2. From this

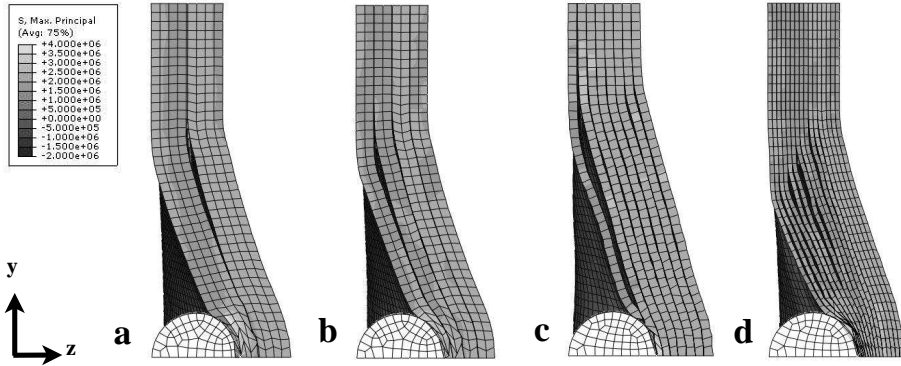


Figure 6.9: *Delamination of models in which the number of cohesive layers is varied at $t = 20\mu\text{s}$ seen from the side. a) model with 1 cohesive layer, b) model with 3 cohesive layers, c) model with 7 cohesive layers, d) model with 15 cohesive layers*

table, we see that the maximum displacement in the shooting direction, we see that the maximum displacement in the simulation with seven layers is higher (4.1mm) than in the other simulations (3.7mm and twice 3.8mm). However, we accept a 10% difference in results and this result falls within this range. It is seen that the projectile velocity at $t = 20\mu\text{s}$ ranges between $237.9\text{--}238.2\text{ m/s}$ in all simulations and that the delaminated area lies between 349 and 353 mm^2 . From the above, we can conclude that the simulation results are, for us, close together and that the influence of the number of interface layers on the results is small for this impact case.

On a qualitative basis, there are some difference in delamination patterns between the simulations, see figure 6.9. In the simulation with 7 cohesive layers, we see that delamination occurs closer to the projectile than is the case in the other simulations. Also, the delamination seems to run over the entire length of the plate. This can also be seen from a bigger delaminated area, although this effect is minor. From this, we tend to think that the number of elements through the thickness in the orthogonal layers is too small compared to the ratio between thickness of the layer and length of the layer. This is obviously smaller in the other simulations and the influence of the number of elements on the simulation results is described hereafter. This indicates that care should be taken in how many three-dimensional elements should be used in the simulations and that this cannot be seen independent of the number of cohesive layers. However, we can conclude that the simulation results seem to be consistent and seem to have a low dependency on the number of cohesive layers.

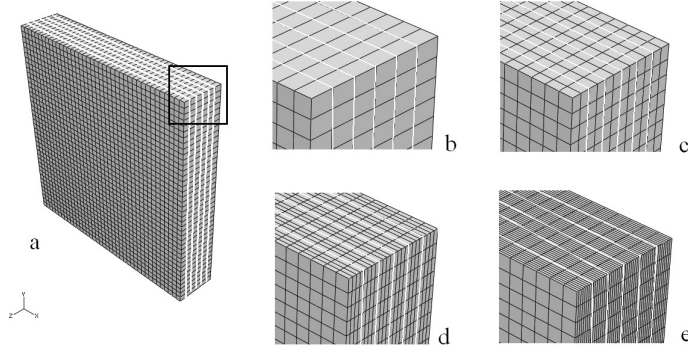


Figure 6.10: *Models used to study the influence of number elements through the thickness of the plate to the simulation results. a) Whole plate, b) model with 1 element in a layer, c) model with 2 elements in a layer, d) model with 4 elements in a layer, e) model with 8 elements in a layer*

Mesh size

In order to see if the mesh size influences the simulation results, four simulations are done with different mesh definitions. All simulations have five interface layers. In these simulations, the mesh size of the Dyneema layers is varied in thickness direction. In the directions perpendicular to the thickness direction (i.e. in-plane), the elements have dimensions of 0.5 mm by 0.5 mm . In the thickness direction, the number of elements in each Dyneema layer is varied and simulations done with Dyneema layers that contain 1, 2, 4, and 8 elements in the thickness direction of the plate, see figure 6.10.

In table 6.3, the results for the mesh sensitivity study are summarised. In this table it is seen that the velocity of the projectile at $t = 20\mu\text{s}$ varies between 239.2 and 243.0 m/s . The maximum displacement in the Dyneema composite plate lies between 3.72 and 3.84 mm and the delaminated area varies between 353 and 359 mm^2 . From the results in this table, we see that the results of the projectile velocity V_p varies most as a function of the number of elements through the thickness in the orthogonal layers. A higher u_{max} and A_{del} as a

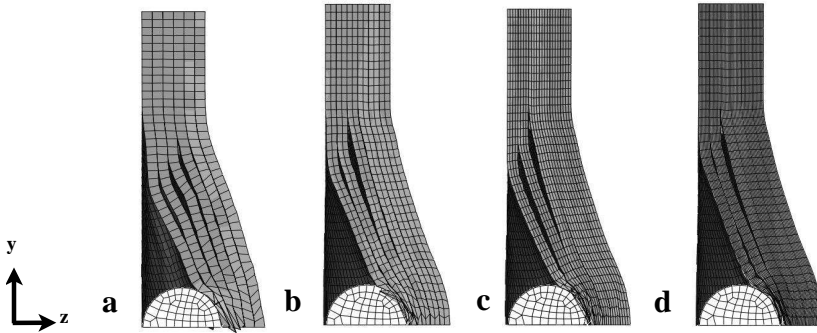


Figure 6.11: *Delamination of models in which the number of elements through the thickness in a Dyneema layer are varied at $t = 20\mu s$ seen from the side. a) model with 1 element through a Dyneema layer, b) model with 2 elements through a Dyneema layer, c) model with 4 elements through a Dyneema layer, d) model with 8 elements through a Dyneema layer*

function of number of elements through the thickness is, however not seen here unlike in the convergence test with number of cohesive elements. However, in these simulations, the number of cohesive layers is not varied and it is expected that the results are a function of both number of cohesive elements and number of three-dimensional elements through the thickness of an orthogonal layer. From table 6.3, it is seen that the lowest and highest value vary 5% from each other for V_p , which is a deviation that we accept. From this, we can conclude that a smaller mesh affects the results for these simulations at most by 5%, which is well acceptable for us.

Table 6.3: *Summary of study to the influence of the mesh size in a 4.007 mm Dyneema composite plate. The result data is given at $t = 20\mu s$*

No. elements	V_p	u_{max}	A_{del}
1	243.0 m/s	3.79 mm	353 mm ²
2	240.9 m/s	3.72 mm	356 mm ²
4	240.2 m/s	3.74 mm	359 mm ²
8	239.2 m/s	3.84 mm	359 mm ²

Qualitatively, we seen that the delamination shapes look alike, see figure 6.9. In this figure, it is seen that delamination occurs at the same location for all simulations. We can, therefore, conclude that the simulation results are within 5 %, while the number of elements through the thickness in an orthogonal layer is varied between one and eight.

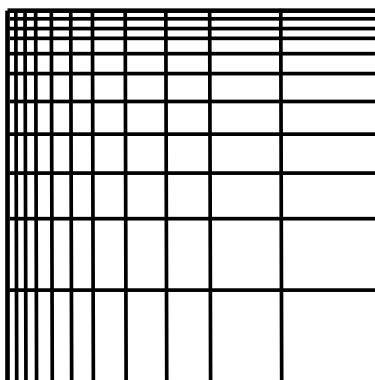


Figure 6.12: *Example of a mesh gradient*

Mesh gradient

To reduce the number of elements in a simulation, a so-called mesh gradient can be used. This can possibly decrease the computation time, because the model is made of less elements with different sizes opposed to a model that consists of small elements of all the same size. The stable time increment in simulations made with the Orthogonal layered model depends primarily on the thickness of the cohesive elements; if a smaller thickness of the cohesive elements is chosen, the stable time increment also decreases and, as a result, the computation time increases, see also 6.2.2.

For this part of the study, a Dyneema composite with five interface layers is used. The mesh gradient is applied in two (in-plane) directions, as schematically shown in figure 6.12. In each simulation, five interface layers are modelled and each Dyneema layer contains four elements through the thickness. Three in-plane gradient ratios, namely 1, 2 and 4, are used in the simulations, while keeping the number of elements constant. The maximum ratio of 4 is used here, because higher ratios are normally not used. The summary of the results can be found in table 6.4. In this table, a maximum ratio is also stated, which is different from the in-plane ratio. The maximum gradient ratio is the ratio between one of the in-plane sides over the thickness of an element.

Table 6.4: *Summary of study to the influence of a mesh gradient in a Dyneema composite plate. The result data is given at $t = 20\mu\text{s}$*

gradient ratio in-plane	$gradientratio_{max}$	V_p	u_{max}	A_{del}
1	3	243.0 m/s	3.79 mm	353 mm ²
2	4	242.3 m/s	3.61 mm	350 mm ²
4	6	N/A m/s	N/A mm	N/A mm ²

The model in which a mesh with a gradient ratio of four is applied gives heavily distorted three-dimensional elements. These elements were so heavily distorted that the results could not be computed until $20 \mu s$. Especially the elements directly under the projectile are heavily distorted because of the high pressure that they feel. If we look at the results of the simulations in which a ratio of 1 and 2 are used, we see that maximum back displacements are 3.79 mm and 3.61 mm respectively at $t = 20 \mu s$. The accompanying delamination areas are 353 mm^2 and 350 mm^2 . The results are therefore close enough for us and it is seen that as long as the value of the gradient ratio is not chosen too high, that it only has a minor influence on the results.

Size of the plate

Experiments suggest that the size of the composite plate influences the behaviour of Dyneema composite. Therefore, four square plate models are made that all have a thickness of 4.005 mm , but have sides of 20 mm , 40 mm , 80 mm and 160 mm length respectively. Again, the projectile velocity, maximum displacement and delaminated area are compared and the data is summarised in table 6.5.

Table 6.5: *Summary of study to the influence of the size of a Dyneema composite plate on the results. The result data is given at $t = 20 \mu s$*

Length/widthth	V_p	u_{max}	A_{del}
20	243.0 m/s	3.79 mm	353 mm^2
40	238.0 m/s	3.83 mm	350 mm^2
80	232.0 m/s	3.95 mm	331 mm^2
160	230.0 m/s	4.00 mm	359 mm^2

From this table, it is seen that the velocity of the projectile at $t = 20 \mu s$ varies between 230.0 and 243.0 m/s . The maximum displacement in the Dyneema composite plate lies between 3.79 and 4.00 mm and the delaminated area varies between 353 and 359 mm^2 . This means that the results differ less than 10 %, while the size is eight times bigger. From the numbers above, it indicates that this size effect on results is minor.

6.4 Simulation results

The goal of this research is to describe the physical processes in Dyneema composite in more detail than if modelled with overall replacement models. It should be noted that the simulations done with the Orthogonal layered model are the same as in the experiments described in *Chapter 3 Dyneema behaviour*, except for the projectile and the size of the model.

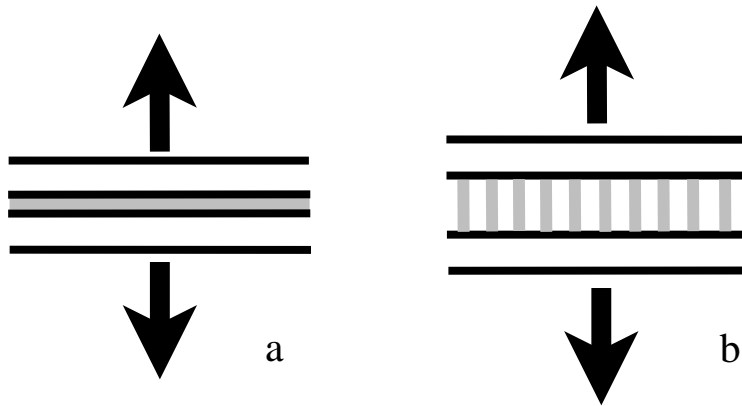


Figure 6.13: *Delamination development (schematic, not on scale) a) two Dyneema layers with matrix material in between b) Dyneema sheet in a delaminated state*

6.4.1 Physical processes observed in real composite

Filament tension and sliding

As mentioned before, the Orthogonal layered model is a so-called Layered replacement model. The information about the physical processes in the composite due to impact are therefore also on a layer level. This means that details on a smaller level, such as microcracks in the matrix material, are not described in this model. Hereafter, we summarise the most important phenomena seen in experiments.

At the point of impact, the material feels a compressive stress. In experiments, this can be seen as a kind of ‘indented’ area. If a projectile is impacted on a Dyneema composite plate, we see that filaments near the projectile are loaded in tension. Some of the filaments break, because their maximum tensile stress is reached; other filaments will just be loaded in tension. As long as the filaments are in contact with the projectile, they are loaded in tension. However, some of the filaments that are initially in contact with the projectile will slide off and so-called filament-sliding occurs.

Delamination

Because the projectile impacts on the Dyneema composite, local curvature in the composite plate is induced. The composite plate cannot cope with that and the Dyneema sheets in the composite are detached. Delamination is then the result and is schematically shown in figure 6.13.

If the delaminated area is projected on the plane perpendicular to the projectile’s trajectory, we see that the backside deformation projection on this

plane is a **starshaped area**, see also figure 3.22. If the material would be isotropic, the projected deformation area would be circle-shaped, because the properties in all directions are the same. Since Dyneema composite is an orthotropic, inhomogeneous material, it is not expected that the projected area will have a circular shape.

Other

Impact affects both the projectile and the Dyneema composite plate. Since we focus on the composite in this research, we will the behaviour of the projectile out of this discussion; the projectile is considered as a rigid body. This can also be justified by the fact that in experiments done with *FSPs* having impact velocities until about 500 m/s , the projectile is found undamaged after impact. In experiments, it is seen that using an *FSP* with a velocity of 300 m/s give a penetration. However, this can make a difference for different projectile shapes.

6.4.2 Physical processes observed in simulations

Filament tension and sliding

At the location where the projectile is first in contact with the composite plate, compressive peak stresses are found, see figure 6.14. In this figure, we see the principle maximum stresses at the front side, where the projectile impacts on the plate. The contact area feels a peak stress of about 15 MPa . In figure 6.15, maximum principle stresses are shown at the back of the plate. At the front of the plate, we see a clear ‘star-shape’ pattern and at the back of the plate that this develops later in time. We also see that when the simulation proceeds, tensile stresses occur in the composite plate. We believe that the tensile stresses in this figure mainly represent the stresses in the filaments. However, this is not explicitly shown in the simulations, because the filaments are not decoupled in the Orthogonal layered model.

In figure 6.16, the total displacements are given at the front of the plate and in figure 6.17, the total displacements are given at the back of the plate. The star-shape is, however, less prominently seen in these figures.

Delamination

In this simulation, delamination occurs between 1 and $2\ \mu\text{s}$. If delamination occurs, it is seen that the Dyneema layers move away from each other, as seen in figure 6.18. We see here, that delamination occurs near impact area, which is also what we expect from experiments.

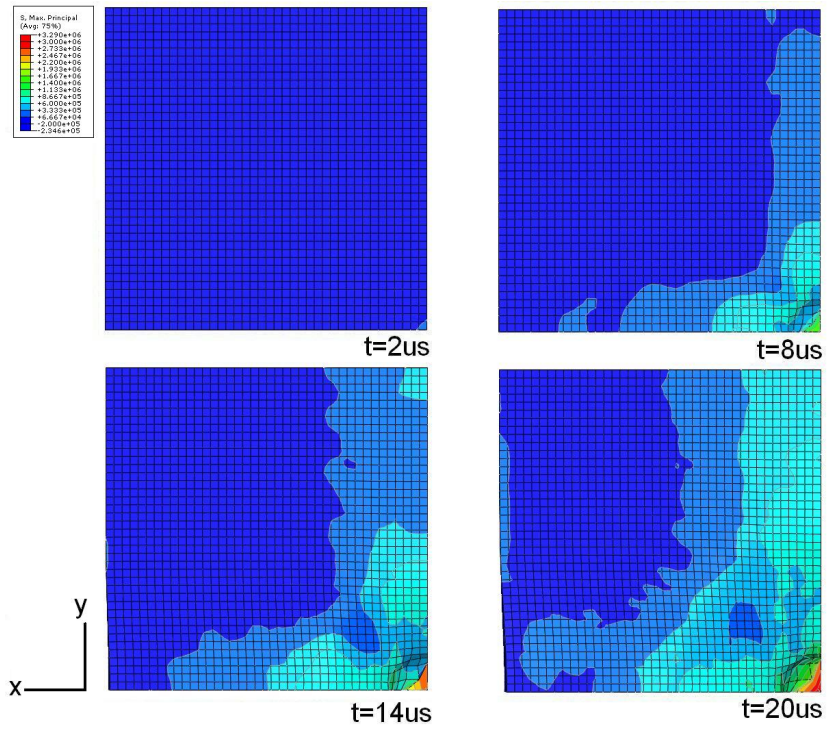


Figure 6.14: Maximum principle stresses in Orthogonal layered model at the front of the Dyneema plate. Results are given from -0.2 (blue) to 3.0 (red) GPa.

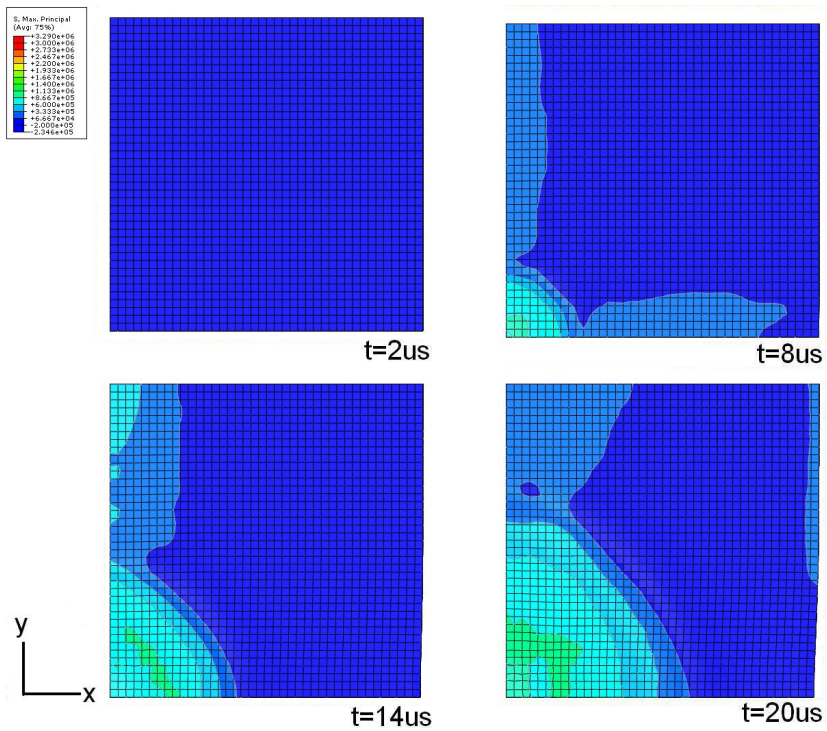


Figure 6.15: Maximum principle stresses in Orthogonal layered model at the back of the Dyncema plate. Results are given from -0.2 (blue) to 3.0 (red) GPa.

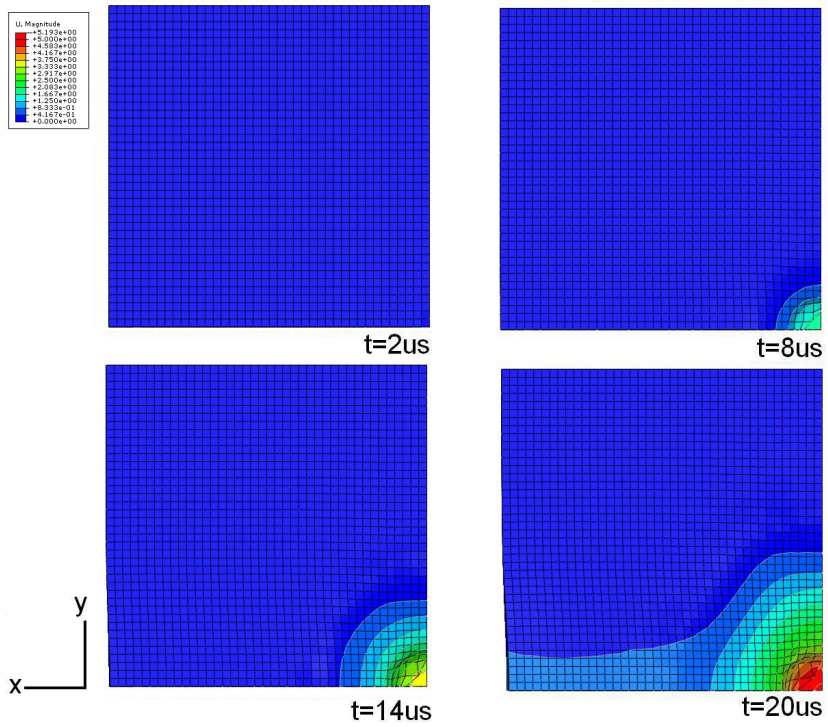


Figure 6.16: Total displacement in Orthogonal layered model at the front of the Dyneema plate. Results are given from 0 (blue) to 5.0 (red) mm.

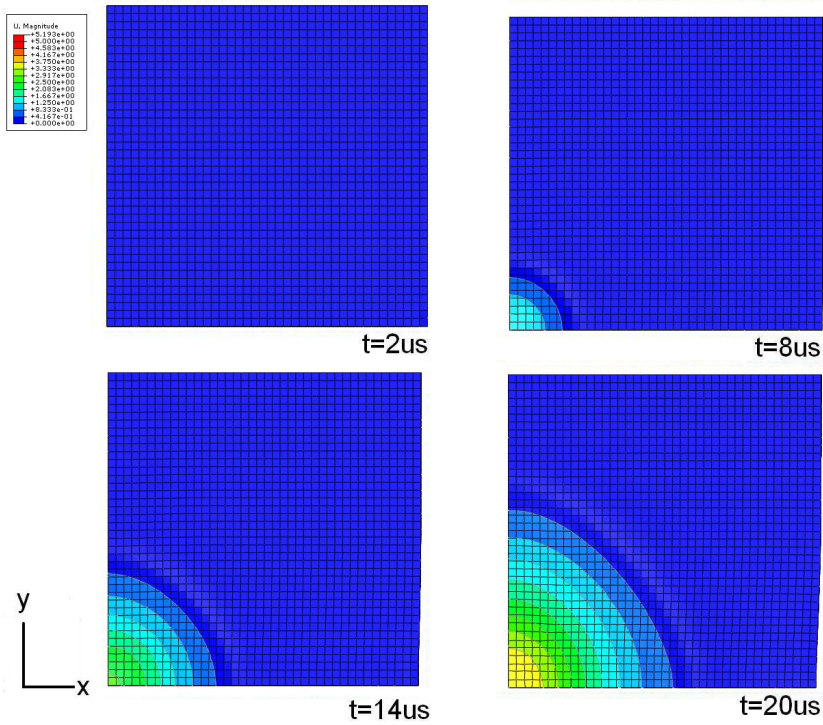


Figure 6.17: Total displacement in Orthogonal layered model at the back of the Dyneema plate. Results are given from 0 (blue) to 5.0 (red) mm.

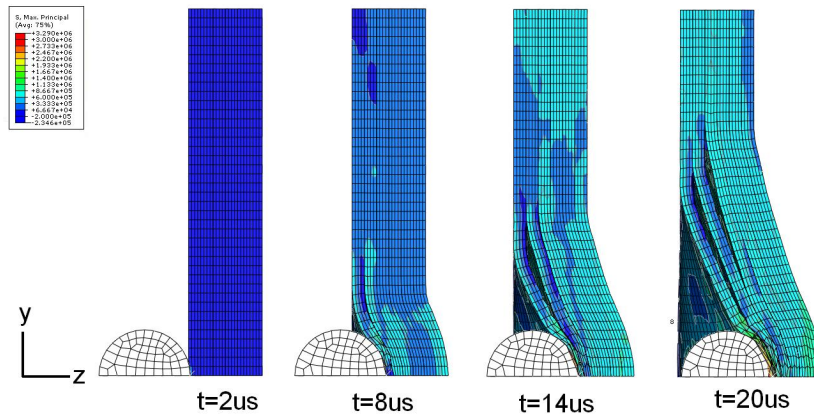


Figure 6.18: Maximum principle stresses in Orthogonal layered model at the back of the Dyneema plate. Results are given from -0.2 (blue) to 3.0 (red) GPa.

Other

As said before, the projectile can cause either a penetration or a perforation of the composite, see also *Chapter 2 Terminal ballistics*. In section 6.3, we have seen that the size of the model will have very minor influences on the results. However, the projectile may influence the impact resulting in a perforation or a penetration. The simulations, however, suffer from instabilities and hence did neither calculate a perforation nor a penetration. However, we think that the phenomena that are observed in the experiments can be qualitatively compared. In section 6.4.1, we will summarise what is seen in experiments if a Dyneema composite is impacted with a fragment. For a more extensive description, we refer to *Chapter 3 Dyneema behaviour*.

6.5 Discussion of Orthogonal layered model

Unfortunately, we encountered contact problems when modelling impact with sharp-edges projectiles on Dyneema composite. It was therefore not possible to validate the experiments with the simulation results obtained with the Orthogonal layered model. Further, due to instabilities in the computations, presumably caused by mass transfer of failed elements to neighbouring elements, the simulations do not run further than 20 μs . Hence, a penetration or perforation can currently not be predicted by this model. However, there is room for comparing the phenomena that are seen in the simulations with what is seen in experiments.

The Orthogonal layered model is a layered model and shows details on a layer level. By modelling interface behaviour with cohesive elements, we see that it is possible to make a more detailed simulation than would be possible with an overall replacement model. However, we did not decouple filaments explicitly and it is therefore not possible to directly say something about filament sliding, filament tension or filament fracture in the simulations. In the Orthogonal layered model, no distinction can be made in filament phenomena.

However, using cohesive elements results in a longer simulation run time compared to overall replacement models, as mentioned in *6.2.2 Model description*. However, we did not do a sensitivity test to the used time step. In the simulations done with the Orthogonal layered model, the stable time increment is determined by the size of the cohesive elements. Because the thickness of the interface in Dyneema composite is close to zero, the stable time increment is in the order of microseconds. If an overall replacement model would be used that has the same mesh density as the three-dimensional elements, the run time of the simulations would be ten times faster.

It is seen in the sensitivity study in this chapter that, in our opinion, the Orthogonal layered model is not so sensitive to the number of layers, mesh size, mesh distribution or size of the plate. This means that the results are not likely

to vary much if these properties are varied, which is therefore also a strength of this model.

Altogether, the Orthogonal layered model shows improvement compared to simulations done with an overall replacement model, because it is possible to explicitly show delamination. At the beginning of our research, we expected that delamination was the dominant failure mechanism. Later on, we discovered that filament phenomena, such as filament pull-out, filament sliding and filament fracture, also play an important role, especially since Dyneema composite is mainly built up from filaments. We therefore developed an additional model, namely the *Lumped filament-bundle model*. This model is described in the next chapter.

Chapter 7

Lumped filament-bundle model

The model, described in *Chapter 6 Orthogonal layered model*, is useful for modelling delamination development. In addition to the Orthogonal layered model, another discrete layered model is developed in this research, namely the *Lumped filament-bundle model*. More failure mechanisms, namely filament sliding and filament fracture, can be simulated with the Lumped filament-bundle model. The Lumped filament-bundle model and the results obtained with this model will be described in this chapter.

The principle of the Lumped filament-bundle model is described in section 7.1. Convergence tests are described in section 7.2 and the results are described in 7.3. Finally, the Orthogonal layered model and the Lumped filament-bundle model are compared in section 7.4.

7.1 Description of Lumped filament-bundle model

The Lumped filament-bundle model allows for modelling interaction between more failure mechanisms in Dyneema composite compared to an overall displacement model. In this section, the principle of the Lumped filament-bundle model, convergence and the description of this model are described.

7.1.1 Principle

Real Dyneema composite consists of a number of UD filament layers with matrix material. To be able to study filament fracture and sliding without having to model each individual component, ‘lumped’ filament bundles are used to represent several filaments.

The lumped filament bundles are, as in the real case, ordered in unidirectional layers and modelled with truss elements. The remainder of the composite properties are represented by three-dimensional elements in which the filament bundles are embedded. Note that matrix material in the composite is implicitly modelled in our model. Hereafter, the components of the Lumped filament model, namely the *Filament bundles* and the *Remainder of the composite* are described in more detail.

Filament bundles

The filament bundles in the Lumped filament-bundle model are, like in the real composite, ordered in orthogonal UD layers such as shown in figure 7.1 b). In the Lumped filament-bundle model, lumped filament bundles are represented by truss elements. Because the truss elements represent a number of filaments, the number of truss elements in the model is lower than the number of filaments in a Dyneema composite piece of the same size. This means that the space between the truss elements is larger than the space between the filaments in a real composite. The three-dimensional elements, amongst others, give coherence to the layers of filament bundles. This is done by initially tying the nodes of the truss elements to the nodes of the three-dimensional elements to which they are attached. This means that the trusses have the same displacements as the three-dimensional elements to which they are tied, as long as the elements have not failed. After one of them has failed, they are no longer connected. Because truss elements are tied to the three-dimensional elements and not to other truss elements (except to the truss elements that describe the same filament bundle), they can move with respect to other truss elements and thus filament sliding can be studied by this model.

The resistance of Dyneema filaments against tension loads is larger than in any other direction, as described in *Chapter 3 Dyneema behaviour*. Dyneema

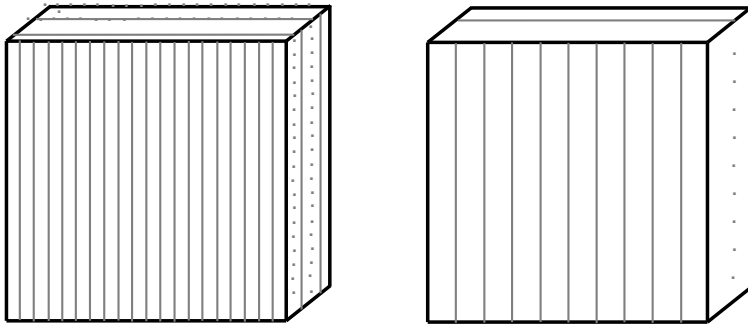


Figure 7.1: a) *Dyneema composite plate (schematic)*, b) *Lumped filament-bundle layered replacement model of Dyneema composite plate*

filaments show linear elastic behaviour up to failure in tension and this behaviour is also projected on the truss elements.

The number of truss elements (and also the number of three-dimensional elements) depend on the desired level of detail (and also on the available computational power). To be able to show filament sliding, a sufficient number of filament bundles should cover the projectile's cross section. If only one filament-bundle would be used, the effect of sliding with respect to other filaments is not visible and only filament fracture can probably be seen (provided that the projectile velocity is high enough). Determining the desired number of filament-bundles depends on engineering judgement.

The cross-sectional area of a truss element is equal to the total cross-sectional area of the filaments that is represented by this truss element. This is schematically shown in figure 7.2. Figure 7.2 a) shows a schematic section of a real piece of Dyneema composite, which contains eight filaments. In this example, the filaments all have an area A . If these filaments would be modelled by two truss elements in the Lumped filament-bundle model, each truss element would each have an area $4A$, see figure 7.2 b). More generally, the area of a truss element is equal to:

$$A_{truss} = \sum_{i=0}^{i=z} A_i \quad (7.1)$$

Here, A_i is the cross sectional area of filament i and z is the number of filaments that are represented by the truss element in question. It is assumed that the density within each filament is constant and is the same for each filament. The density of the truss element is then equal to the density of the filaments. For the properties of the filament bundles in the model, see 7.1.2.

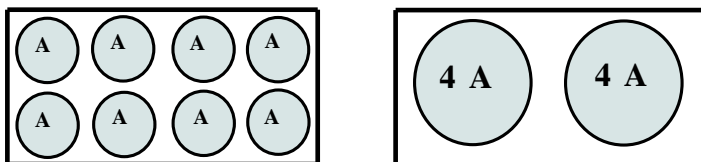


Figure 7.2: Principle of modelling filaments together in single truss element. a) a schematic view of a section of Dyneema composite b) trusses that replace the eight real filaments in the Lumped filament-bundle layered replacement model

Remainder of the composite

The remainder of the Dyneema composite is modelled by three-dimensional elements. In the real Dyneema composite, the Young's modulus of the filaments is about ten times higher than of the matrix material. This information is also used in the Lumped filament bundle model. In this model, the Young's modulus of the truss elements is ten times higher than the entries of the matrix $\overline{\overline{E}}_{mod}$. In which $\overline{\overline{E}}_{mod}$ represents the stiffness matrix of the three dimensional elements in the Lumped filament-bundle model, which contain modified values of an overall replacement model, which we will now explain.

E_{11} and E_{22} in the real Dyneema composite are dominated by the filaments and they are represented by the truss elements in the Lumped filament bundle model. This means that E_{11} and E_{22} in $\overline{\overline{E}}_{mod}$ are smaller than in $\overline{\overline{E}}_{ov}$, the stiffness matrix of the overall replacement model, and that:

$$\overline{\overline{E}}_{mod} \approx \overline{\overline{E}}_{ov} - \overline{\overline{E}}_f \quad (7.2)$$

In the direction perpendicular to the unidirectional filament-bundle layers, i.e. in thickness direction, the properties of Dyneema composite are determined by both the matrix material and the (presence of the) filaments. In that direction, the three-dimensional elements represent both the filament and matrix properties. The same can be said for the contraction and shear properties. For the values of $\overline{\overline{E}}_{mod}$ used in the Lumped filament bundle model, see 7.1.2.

The volume of the three-dimensional elements and the volume of the real Dyneema composite are, in this model, equal to each other. The truss elements have the density and (numerical) volume of the filaments that they represent. Because the three-dimensional elements represent the remainder of the composite, it is not straightforward what their density should be. In the Lumped filament-bundle model, this is calculated by equating the total mass of the composite and that of the replacement model. The volume fraction of the filaments in a real Dyneema composite is about 80% and the volume fraction of the *PUR* matrix is about 20%. The densities and volumes of the real composite and the replacement model are related as follows:

$$\rho_c V_c = (\rho_f V_f)_{real} + (\rho_m V_m)_{real} = (\rho_f V_f)_{sim} + (\rho_{cont} V_{cont})_{sim} \quad (7.3)$$

Here, ρ_c and V_c are the density and the volume of the real composite, ρ_f the density of the filaments, V_f the total volume of the filaments, ρ_m the density of the matrix and V_m the volume occupied by matrix material in the composite. In this equation, $(\rho_f V_f)_{real} = (\rho_f V_f)_{sim}$. Note that the volume of the three-dimensional elements in the model is equal to the original volume of the real composite. Therefore, the density of the three-dimensional elements becomes:

$$\rho_{cont} = \frac{\rho_c V_c - (\rho_f V_f)_{sim}}{V_{cont}} \quad (7.4)$$

For more details of the (material) properties of the three-dimensional elements in the Lumped filament bundle model, see 7.1.2.

7.1.2 Model description

Geometry

The Lumped filament-bundle model has almost the same sizes as the Orthogonal layered reference model, namely 20 mm by 20 mm by 4 mm¹. The three-dimensional elements in this reference model have sizes 0.5 mm by 0.5 mm by 0.5 mm, which means that there are eight elements through the thickness and the model has nine unidirectional filament-bundle layers that are embedded in the three-dimensional elements.

Initial conditions

Like in the Orthogonal layered model, an initial velocity of 300 m/s in z-direction is applied on the projectile. Note that the same coordinate system is applied for the Lumped filament-bundle model as for the Orthogonal layered model. This means that the z-direction is normal to the Dyneema composite plate such as shown in figure 6.3. The velocities in x-direction and y-direction are initially zero.

Boundary conditions

The same boundary conditions are used as for the Orthogonal layered model. A quarter of the plate is modelled, because the problem is symmetric about two planes, namely the xz-plane and the yz-plane such as shown in figure 6.3. Also for this model, it is assumed that the results are also symmetric. Therefore, the following boundary conditions are applied: $u_y = \theta_x = \theta_z = 0$ on the xz-plane and

¹the thickness difference with the Orthogonal layered model comes from the fact that no cohesive layers are used in the Lumped filament-bundle model

$u_x = \theta_y = \theta_z = 0$ on the yz -plane. Further, the top and bottom edges are pinned and therefore, the displacements $u_i=0$, such as shown in Chapter 6 in figure 6.3.

Material models

The properties for Dyneema filament bundles, used in the Lumped filament-bundle model, are summarised in table 7.1. The data shown in this table comes from the experiments, described in *Chapter 3 Dyneema behaviour*. It is assumed that the behaviour of a filament bundle is similar to that of a Dyneema fibre during a tensile test. This means that the filament bundle is assumed to show linear elastic behaviour up till failure, i.e. if it reaches a maximum stress of 2.8 *GPa*.

Table 7.1: *Input for truss elements*

Property	Value	Unit
ρ	981	kg/m^3
E	200	<i>GPa</i>
ν	0.3	—
σ_p^m	2.8	<i>GPa</i>
σ_{max}^m	2.801	<i>GPa</i>

The remainder of the composite uses the same constitutive model as the Dyneema layers in the Orthogonal layered model. For example, also a maximum stress criterion is used to describe failure of the remainder of the composite. Only the values of the properties are different. The stiffness matrix for this model is as follows:

$$\bar{\bar{C}} = \begin{pmatrix} 42000 & 2400 & 2700 & 0 & 0 & 0 \\ 2400 & 42000 & 2700 & 0 & 0 & 0 \\ 2700 & 2700 & 4600 & 0 & 0 & 0 \\ 0 & 0 & 0 & 900 & 0 & 0 \\ 0 & 0 & 0 & 0 & 400 & 0 \\ 0 & 0 & 0 & 0 & 0 & 400 \end{pmatrix} MPa \quad (7.5)$$

Mesh

For the lumped filament bundles, T3D2 truss elements are used. These elements have displacement degrees of freedom u_1 , u_2 and u_3 , but can only take up loads in their length direction (u_1). The elements have meshes that coincide with the surrounding three-dimensional elements. The rest of the composite is modelled with three-dimensional C3D8 elements, which means that their lengths are 0.5 *mm*. The three-dimensional elements in this model all have sizes 0.5 *mm* by 0.5 *mm* by 0.5 *mm*. In contrast to the Orthogonal layered model, no

gradient meshes are used in the Lumped filament bundle model. It is expected that using gradient meshes would speed up the calculations. However, using gradient meshes would disturb the filament bundles having continuous properties. Therefore, an equal distribution of filament bundles throughout the model is used.

Contact definition

In this model, the interaction between the projectile, the Lumped filament bundles and the remainder of the composite should be described, as well as self-interaction of the components. The contact definition in the Lumped filament-bundle model should fulfill the same set of requirements as that of the orthogonal layered model. In addition to this, the contact definition in the filament-bundle layered model is required to describe edge-to-edge contact. If edge-to-edge contact is not well described, the filament-bundles in the simulations could move through each other.

Like for the Orthogonal layered model, the general contact algorithm of ABAQUS is used for this model, because it fulfills the requirements stated above. As mentioned in *Chapter 6 Orthogonal layered model*, there are still two factors that can influence the results of the simulations, namely omission of mechanical contact damping and that of friction effects. In this research, it is assumed that these effects are minor (also indicated by experiments). See also, *Chapter 8 Conclusions and recommendations*.

Stable time increment

The stable time increment is determined by the smallest elements in the simulations. As mentioned in *Chapter 6 Orthogonal layered model*, the following inequality holds for the stable time increment:

$$\Delta t = \frac{T}{C_l} \tag{7.6}$$

with , T is the characteristic element length and C_l the longitudinal wave velocity $\sqrt{\frac{E}{\rho}}$ in the element. For the three-dimensional elements, the characteristic element length is the body diagonal and for the discrete filament bundles, this is the element length. The element length trusses has the same size as the sides of the three-dimensional elements to which they are attached. The characteristic elements length, being the body diagonal, is larger than the characteristic element length of the truss elements. This means that the minimum stable time increment is determined by the element length of the truss elements, being 0.5 mm.

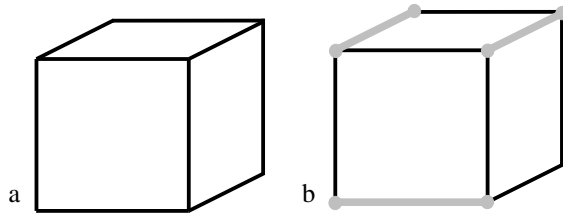


Figure 7.3: a) A three-dimensional element (schematic), b) Truss elements with their nodes tied to a three-dimensional element (schematic)

7.2 Convergence tests

For the Lumped filament-bundle model, two load cases are modelled to see if this model shows realistic behaviour and converges; a quasi-static tensile test and a ballistic experiment are modelled. Here, the ballistic test is similar to the one modelled in *Chapter 6 Orthogonal layered model* to be able to compare the Orthogonal layered model with the Lumped filament-bundle model. Because the Lumped filament-bundle model is a new model, it is not yet known if the solution converges and also a tensile test is simulated with this model to test this.

7.2.1 Tensile test

The tensile test experiment, described in *Chapter 3 Dyneema behaviour*, is modelled with the Lumped filament-bundle model. In the tensile tests described in *Chapter 3 Dyneema behaviour*, specimens with dimensions 60 mm by 10 mm by 2 mm are elongated (displacement driven). Modelling this tensile test with the Lumped filament-bundle model, allows us to see whether the quasi-static behaviour of the model describes that of a real specimen.

The results of the simulations from the Lumped filament-bundle model are compared with that of an overall replacement model of the specimen. In figure 7.3 a), a building block of the overall replacement representation of the tensile test specimen is shown; a building block consists solely of three-dimensional elements and all elements use the same material properties. The Lumped filament-bundle is built up from three-dimensional elements and embedded truss elements. The nodes of the truss elements are initially tied to adjacent three-dimensional elements and an example of this is shown in figure 7.3 b).

For the tensile test, only elastic behaviour is modelled, because the tensile test experiments did not give consistent material failure data that can be used as input for the simulation model, see also *Chapter 3 Dyneema behaviour*.

In all simulations, symmetry conditions apply and a quarter of a real specimen is modelled. The dimensions of the specimen in the simulation models are 30 mm by 5 mm by 2 mm , which is the size of a quarter of the specimen. The

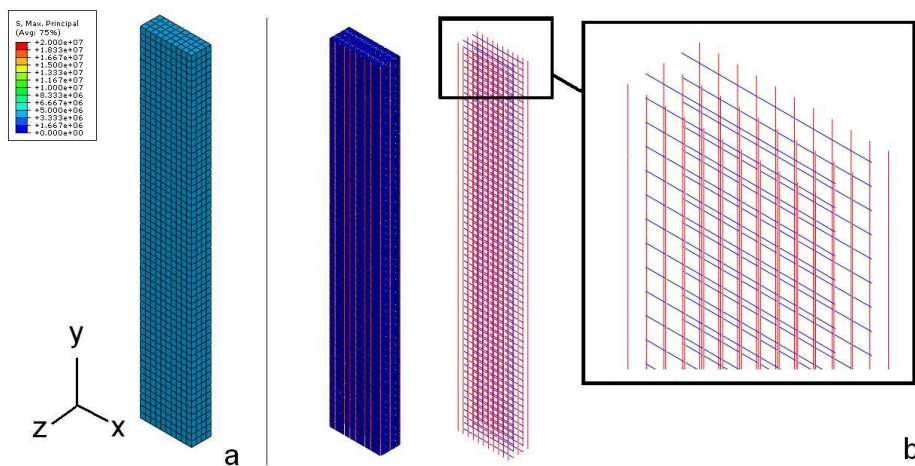


Figure 7.4: *a) Maximum principle stresses in overall replacement model, b) Maximum principle stresses in the Lumped filament-bundle model. Results are given from 0 (blue) to 20 (red) GPa.*

applied symmetry conditions are $u_y, \theta_x, \theta_z=0$ at the xz -plane and $u_x, \theta_y, \theta_z=0$ at the yz -plane. In the simulations, a 3 mm displacement (meaning $\epsilon = 0.1$) is applied to the specimen in y -direction.

The overall replacement model has the properties of the Dyneema composite that are determined with ultrasonic measurements, see reference [68]². At the moment, ultrasonic measurements are, by our knowledge, the most reliable way to determine the stiffness properties of Dyneema composite, see also reference [68].

Mesh convergence tests have been done with the Lumped filament-bundle model, in which the mesh sizes of both the trusses and of the three-dimensional elements are varied. The results obtained with different combinations of mesh size of trusses and three-dimensional elements are summarised in table 7.2. It should be noted that the three-dimensional elements have a cubic shape in all simulations. There are three simulations in which the sides of the three-dimensional elements and the truss elements have the same length and two simulations in which the mesh size of the truss elements is as big as two three-dimensional element lengths. The computation of the model in which the filament bundles are placed every other 0.125 mm and with a three-dimensional element mesh size of 0.125 mm is not feasible anymore due to lack of computational power. It turns out, however, that the maximum stresses in the truss elements are the same for all simulations and the same holds for the maximum stresses seen in the three-dimensional elements. We also noticed that

²This memo is classified and property of TNO

the qualitative results, described hereafter, are the same for all models.

Table 7.2: *Summary of mesh convergence study for Lumped filament-bundle model*

Mesh three-dimensional elements	Mesh trusses	$\sigma_{max_{cont}}$	σ_{max_f}
0.5 mm	0.5 mm	0.248 GPa	16 GPa
0.25 mm	0.25 mm	0.248 GPa	16 GPa
0.125 mm	0.125 mm	N/A	N/A
0.25 mm	0.5 mm	0.248 GPa	16 GPa
0.125 mm	0.25 mm	0.248 GPa	16 GPa

As mentioned above, a 3 mm displacement is posed in y-direction at $y = 30mm$. If we compare the stress distributions between the overall replacement model with that of the Lumped filament-bundle model, we see that the stress distribution is different for both models, see 7.4. In this figure, the maximum principle stresses are shown for the overall replacement model on the left and for the Lumped filament-bundle model on the right. In this figure, it is seen that tensile stresses only occur in the filament-bundles in y-direction; the filament-bundles perpendicular to these bundles have no tensile stresses. The maximum principle stress in the overall replacement model is the same everywhere in the model and is equal to 3.8 GPa. The maximum principle stress in the filament-bundles is 19 GPa.

In figure 7.5, we see the minimum principle stresses for both the overall replacement model and the Lumped filament-bundle model. It is seen that the filament-bundles that are orientated in x-direction are loaded in compression and that the filament-bundles in y-direction are not. It is again seen that the minimum principle stress in the overall replacement model is uniform and equal to -0.15 GPa (compression). In the Lumped filament-bundle model, the minimum principle stress in the filaments is -0.25 GPa (compression). Zooming in on the three-dimensional elements of the Lumped filament-bundle model, we see that the stress distribution, unlike in the overall replacement model, is not uniformly distributed at the free edges (right of each specimen). This is shown in figure 7.6 This can especially be said for the minimum principle stresses.

In figure 7.7, we see that the displacements in y-direction are the same for both models. This is also what we would expect, because this tells us that the application of the load is the same in both models.

However, if we look at the contraction of the specimens perpendicular to the applied load (in this case in x-direction), we see differences between the overall replacement model and the Lumped filament-bundle model, see figure 7.8. The contraction is more uniform in the overall replacement model and it is seen that contraction mainly occurs at the free edges for the Lumped filament-bundle model. Also, the total contraction is different, this is 0.01 mm for the overall

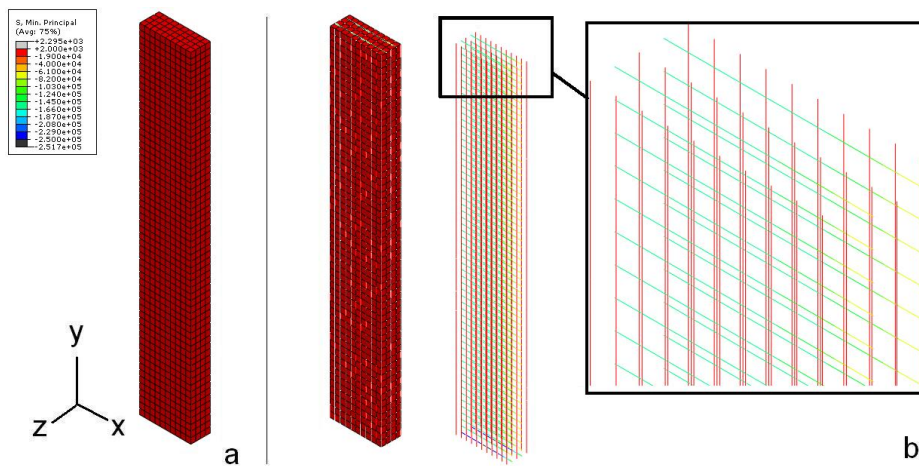


Figure 7.5: a) Minimum principle stresses in the overall replacement model, b) Maximum principle stresses in the Lumped filament-bundle model. Results are given from -0.25 GPa (blue) to 3 MPa (red).

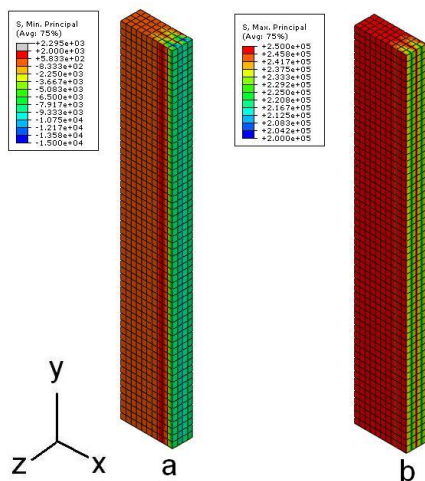


Figure 7.6: a) Minimum principle stresses in the Lumped filament-bundle model - Results are given from -15 MPa (blue) to 2 MPa (red) b) Maximum principle stresses in the Lumped filament-bundle model - Results are given from 0.2 GPa (blue) to 0.25 GPa (red).

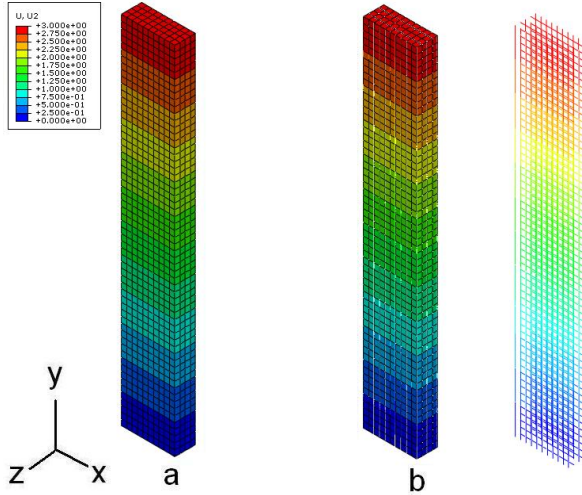


Figure 7.7: a) Displacement in y -direction of the overall replacement model, b) Displacement in y -direction of the Lumped filament-bundle model. Results are given from 0 (blue) to 3 (red) mm.

replacement model and 0.05 mm for the Lumped filament-bundle model. This difference, although small, can be explained by the decoupling of the filament-bundles from the rest of the composite. In experiments, we see indeed mainly deformation at the free edges rather than a uniform deformation, see also *Chapter 3 Dyneema behaviour* and it is hence believed that the Lumped filament-bundle model described this behaviour better than the overall replacement model.

We can conclude that deformation patterns, in the simulated tensile tests is independent of using the overall replacement model or the Lumped filament-bundle model. The stress distribution in the Lumped filament-bundle model is different from that of the overall replacement model and shows that most of the energy is absorbed by the truss elements (and thus filaments). Because the stiffness properties of the trusses and three-dimensional elements are different, this is also what we would expect. Using the Lumped filament-bundle model, it is possible to distinguish between the behaviour of the filament bundles and the remainder of the composite.

From the above, it turns out that the overall behaviour (displacements) as simulated with the Lumped filament-bundle model coincides with that of an overall replacement model and with the real case. It is seen that the stresses in the Lumped filament-bundle model are mostly taken up by the filament bundles, which is also expected from experiments, see *Chapter 3 Dyneema behaviour*. Together with the mesh convergence, this indicates that the Lumped

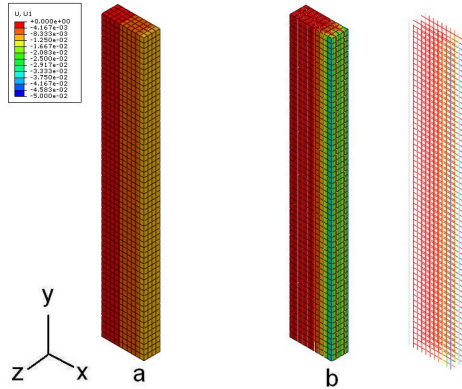


Figure 7.8: a) Contraction in the overall replacement model, b) Contraction in the Lumped filament-bundle model. Results are given from -0.05 (blue) to 0 (red) mm

filament-bundle model is suitable to model Dyneema composite for quasi-static applications.

7.2.2 Ballistic test

This research focuses on the development of replacement models that can describe ballistic impact on Dyneema composite. Like for the Orthogonal layered model, convergence tests are done for ballistic simulations with the Lumped filament-bundle model.

In the simulations, a ball impacts on a piece of Dyneema composite with an initial velocity of 300 m/s . In figure 7.9, the impact process of the reference model and the maximum stresses that occur in the plate are shown for the reference model. This figure shows the whole model, meaning both filament-bundles and three-dimensional elements are shown. Compared to the Orthogonal layered model, not much is seen in such a picture. This is because delamination is shown as unidirectional filament layers that move away from each other. This is described in more detail in *Section 7.3 Simulation results*. To study the effect of mesh size and size of the plate on the simulation results, models are made in which these parameters are varied. From the simulations that were used for this convergence study, differences in the projectile velocity, maximum displacement in shooting direction u_{max} and delamination area at $t = 20\mu\text{s}$ are determined as a function of mesh size, mesh pattern and size of the plate. The influence on projectile velocity, maximum displacement in shooting direction u_{max} and delamination area at $t = 20\mu\text{s}$ as a function of mesh size and size of the plate is given hereafter.

Doing the ballistic simulations, we encountered two major problems. The first

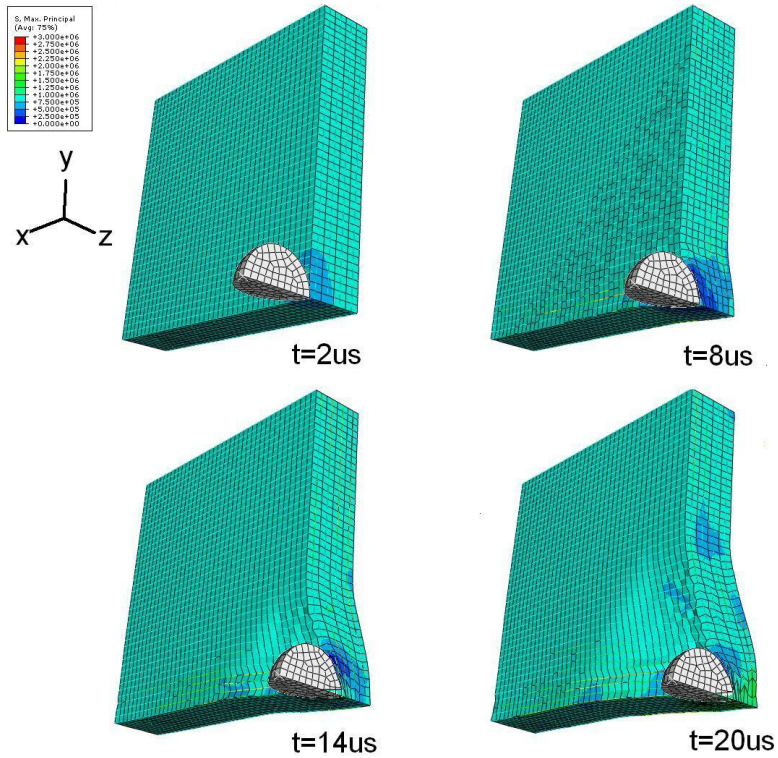


Figure 7.9: Impact of a ball on a Dyneema composite plate at $t=2, 8, 14$ and $20 \mu\text{s}$ modelled with the Lumped filament-bundle model. Results are given from 0 (blue) to 3 (red) GPa

Table 7.3: Summary of ballistic mesh convergence study for Lumped filament-bundle model 40 mm by 40 mm. The result data is given at $t = 20\mu s$

No. layers	V_p	u_{max}	A_{del}
3	226 m/s	3.0 mm	314 mm ²
5	212 m/s	2.7 mm	314 mm ²
9	210 m/s	2.7 mm	313 mm ²
15	211 m/s	2.8 mm	314 mm ²

problem relates to contact and the same contact problem with sharp-edges projectiles arises for the Lumped-filament bundle model as for the Orthogonal layered model. We did not succeed to model impact with an FSP or a cylindrical shape projectile. Therefore, we modelled the projectile impact with a ball shape projectile and analysed this case. The second problem that we encountered was the stability of the simulation. Once elements failed and were being removed from the simulation, their masses are still retained and are transferred to the elements to which they are attached. However, the simulations become very unstable and give unrealistic results after 20 μs . Because the simulations currently give no realistic results after 20 μs , a penetration or a perforation of the composite plate cannot be predicted. In table 7.3, the results are summarised for simulations in which the number of filament-bundles per unit volume is varied. It is seen that the values of the maximum backface displacements and the delaminated areas are close together for all simulations. Delamination in the Lumped filament-bundle model is shown by removing the three-dimensional elements if they reached their maximum stress. However, there is some variation, namely about 4.4 % between the lowest and the highest value, in the projectile velocity at $t = 20\mu s$.

Table 7.4: Summary of ballistic size study for Lumped filament-bundle model (nine filament layers). The result data is given at $t = 20\mu s$

Edge size	V_p	u_{max}	A_{del}
20 mm	205 m/s	2.7 mm	331 mm ²
40 mm	208 m/s	2.8 mm	332 mm ²
80 mm	205 m/s	2.7 mm	331 mm ²
160 mm	203 m/s	2.8 mm	330 mm ²

In table 7.4, it is seen that the velocities of the projectile, the maximum backface displacement and the delaminated area at $t = 20\mu s$ are very close to each other for various plate sizes. From the convergence tests, described above, it is seen that the results are close together for the test cases. Therefore, we choose to study the simulation with nine layers of filament-bundles with sizes 20

mm by 20 mm by 4 mm in more detail.

7.3 Simulation results

7.3.1 Physical processes observed in simulation

Filament tension and sliding

From the moment that the projectile and the plate are in contact, a compressive stress is found directly under the projectile in the three-dimensional elements. This compressive stress is equal to 500 MPa. At the same time, the filament-bundles are loaded in tension. The tension in the filaments, directly after impact is 2 GPa. Note that the filament-bundles cannot take up stresses in a direction other than in their length direction. The only stress that they thus feel, is the mentioned tensile stress.

The waves in the trusses, or rather filament bundles, move at a higher velocity than the waves in the three-dimensional elements. This is because the filaments have a higher modulus in that direction and thus a higher wave velocity; the wave velocity in an element is a function of, amongst others, the directional Young's modulus according to:

$$C_l = \sqrt{\frac{E}{\rho}} \quad (7.7)$$

For the three-dimensional elements, E depends on the direction in the elements, see also *Chapter 6 Orthogonal layered model*, because they have orthogonal material properties.

Directly under the projectile, the maximum stress is 19 GPa in compression. In figure 7.10, the same impact case as in figure 7.9 is shown. Here, the three-dimensional elements are removed for visualisation purposes. In this figure, only the filament-bundle layers and the projectile are shown.

In figure 7.11, we see that, apart from the fact that the filament-bundle layers move away from each other, from $t = 14\mu s$, some filament-bundles are broken. This is shown in more detail in figure 7.12. These bundles are broken, because the stress in the trusses have risen beyond the failure tensile stress.

If we look at the side view of the filament-bundle layers as shown in figure 7.11, we see at $t = 2\mu s$ that the filament-bundles form a pattern of regular, orthogonal lines. From $t = 8\mu s$ onwards, we see that this orthogonal pattern is disturbed. This is caused by filament bundles sliding away from their original position because they have to make space for the projectile. The projectile keeps 'pushing' the filament-bundles and adjacent filament-bundle layers move away from each other from $t = 8\mu s$, see figure 7.12. In this figure, the star-shape, as mentioned in *Chapter 3 Dyneema behaviour* is also seen. This is one of the mechanisms that occur in Dyneema composite, also mentioned in *Chapter 3*

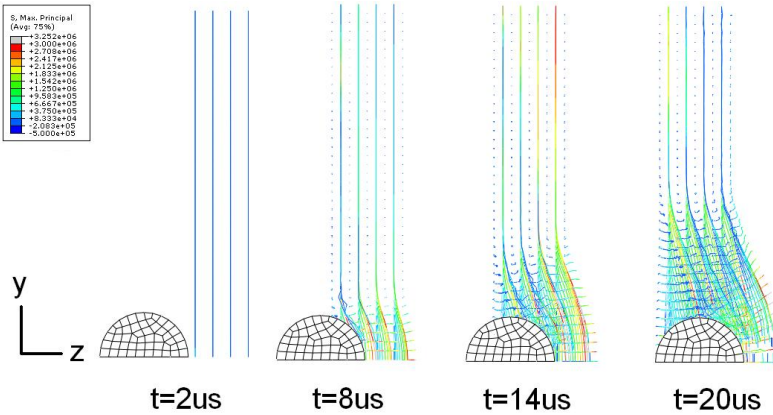


Figure 7.10: Impact of a ball on a Dyneema composite plate at $t=2, 8, 14$ and $20 \mu\text{s}$ (only filament-bundle layers are shown as seen from the side of the plate). Results are given from -0.5 (blue) to 3 (red) GPa. The maximum stress that occurred in the simulation is 3.2 GPa .

Dyneema behaviour, caused by projectile impact. Neither in overall replacement models nor in the Orthogonal layered model, was it possible to show filament sliding, filament fracture and some sort of delamination in a single simulation. In figure 7.13 the maximum principle stresses at the front of the Dyneema plate, which on the side that the projectile impacts on the plate, are shown. The same is done for the back of the plate in figure 7.14. We see that the maximum principles stresses is about ten times lower in the three-dimensional elements as for the filament-bundles. We also see that the pattern of principle stresses follow that what is found with the Orthogonal layered model.

The total displacements are shown for the front of the plate in figure 7.15 and for the back of the plate in figure 7.16. It is seen in this figure that the results are almost the same as for the Orthogonal layered model.

Delamination

Delamination could not be seen in the Lumped filament-bundle model. No three-dimensional elements were removed from the simulation, because their maximum stress criterion has not been reached. However, the displacement pattern is the same as found with the Orthogonal layered model. For the Lumped filament-bundle model, we did not adjust the criterion for delamination. We think that decoupling of the filament-bundles in the simulation, influences the delamination criterion for the three-dimensional elements. However, we did not research the influence of decoupling properties on other parts in the replacement model. We recommend to do this as a follow-up of this research.

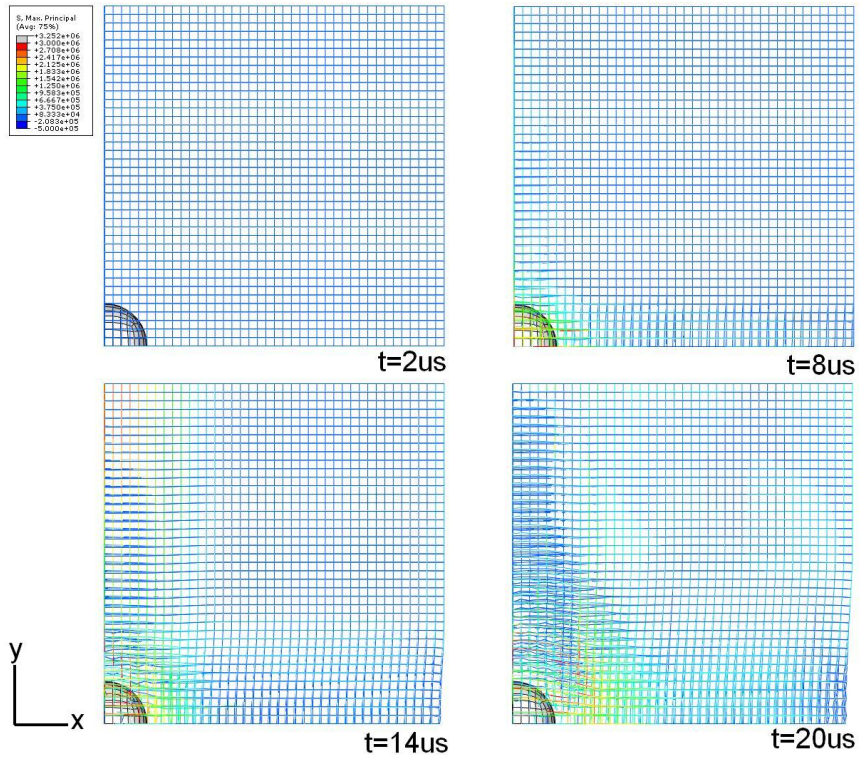


Figure 7.11: Impact of a ball on a Dyneema composite plate at $t=2, 8, 14$ and $20 \mu\text{s}$ (only filament-bundle layers are shown as seen from the back of the plate). Results are given from -0.5 (blue) to 3 (red) GPa. The maximum stress that occurred in the simulation is 3.2 GPa.

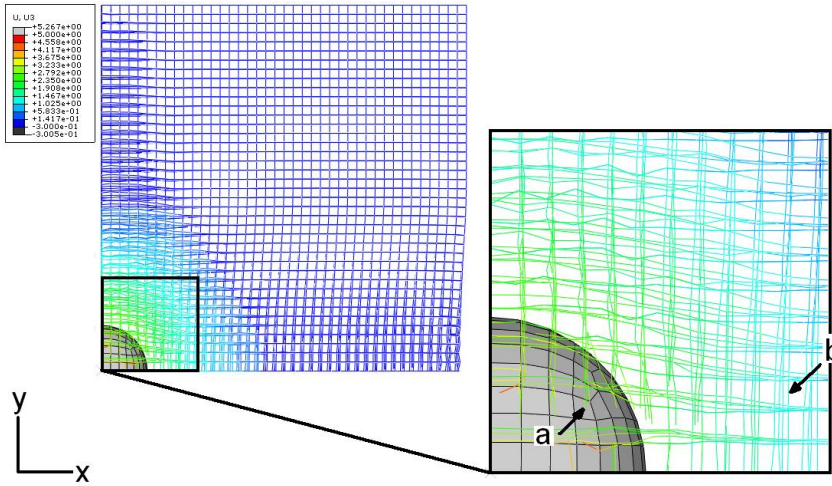


Figure 7.12: *Enlarged view of filament-bundles in the Lumped filament-bundles model at $t = 20\mu s$ a) fracture of filament-bundles b) sliding of filament-bundles. Results are given from -0.5 (blue) to 3 (red) GPa. The maximum stress that occurred in the simulation is 3.2 GPa.*

Other

Following the projectile further in time, there are two scenarios as for what can happen to the Dyneema composite, namely a penetration or a perforation, see also *Chapter 2 Terminal ballistics*. In the case of a perforation, the layers in the Dyneema sheet in the composite cannot absorb enough energy and the kinetic energy of the projectile is only partly taken up by the filaments and matrix material. The projectile will, in the case of a perforation, fly through the other end of the composite and still possess a non-zero velocity and has a kinetic energy, which is equal to the amount of energy absorbed by the composite plate subtracted from the projectile's initial kinetic energy. In this research, we could unfortunately not predict this, because of stability problems of the model after time $t = 20\mu s$. We think that this is caused by the mass of the failed elements that are transferred to other, neighbouring elements.

7.3.2 Discussion of Lumped filament-bundle model

We did not do experiments that represent the experiment modelled with the Lumped filament-bundle model. In our model, we used a ball-shaped projectile instead of a fragment to because we were not able to overcome contact problems that are caused when modelling sharp-edged projectiles. It is however seen from simulations that this model can describe filament sliding, filament fracture and delamination; we therefore think that this model has potential to describe

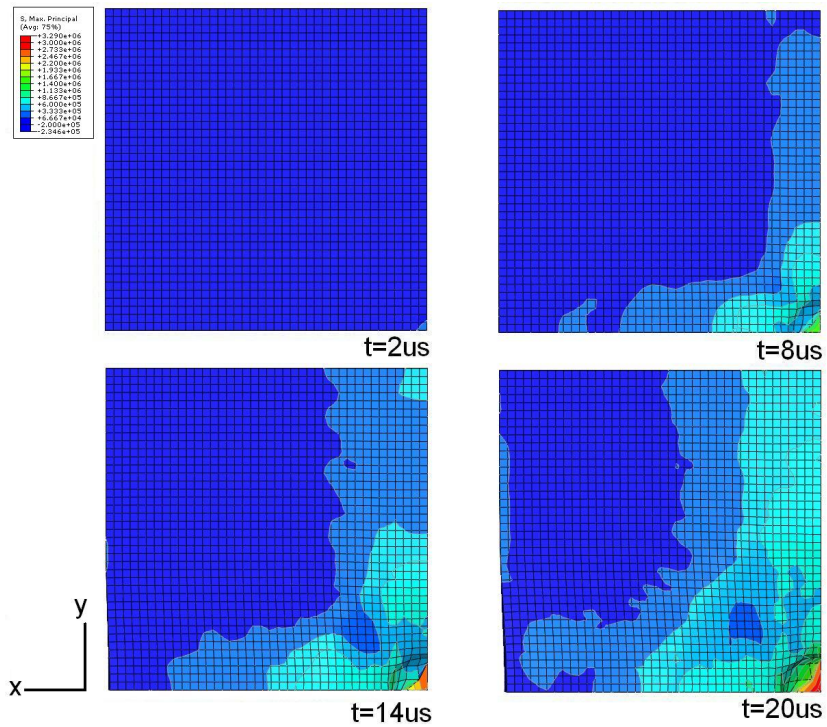


Figure 7.13: *Maximum principle stresses in three-dimensional elements of Lumped filament-bundle model at the front of the Dyneema plate. Results are given from -0.1 (red) to 0.8 (blue) GPa.*

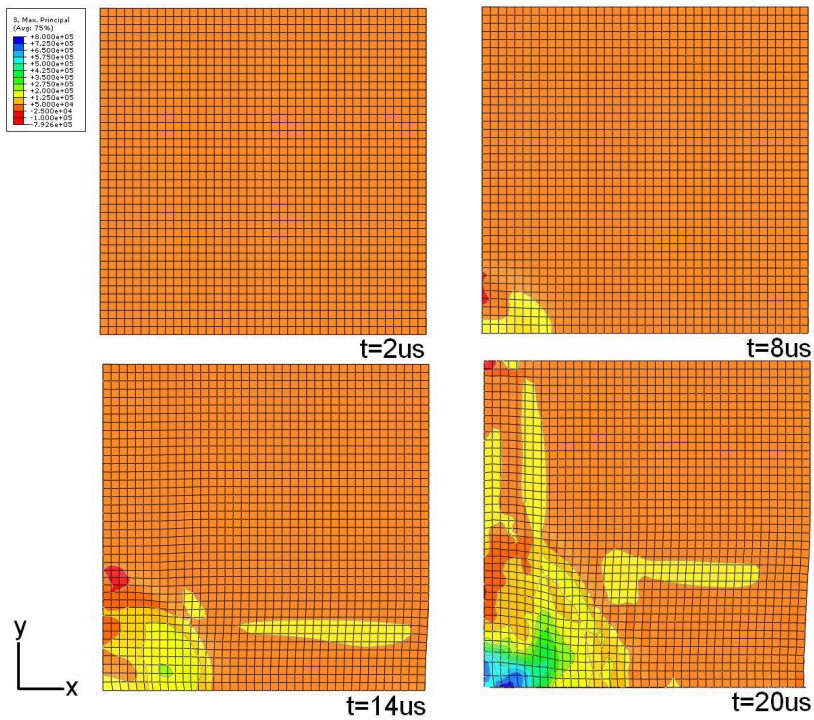


Figure 7.14: Maximum principle stresses in Lumped filament-bundle model at the back of the Dyneema plate. Results are given from -0.1 (red) to 0.8 (blue) GPa.

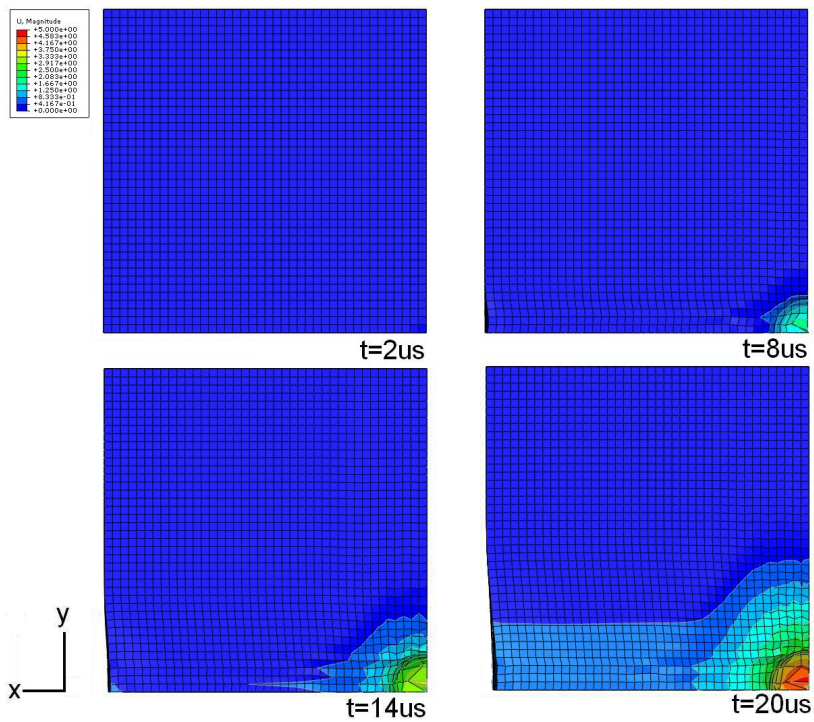


Figure 7.15: Total displacement in Lumped filament-bundle model at the front of the Dyneema plate. Results are given from 0 (blue) to 5.0 (red) mm.

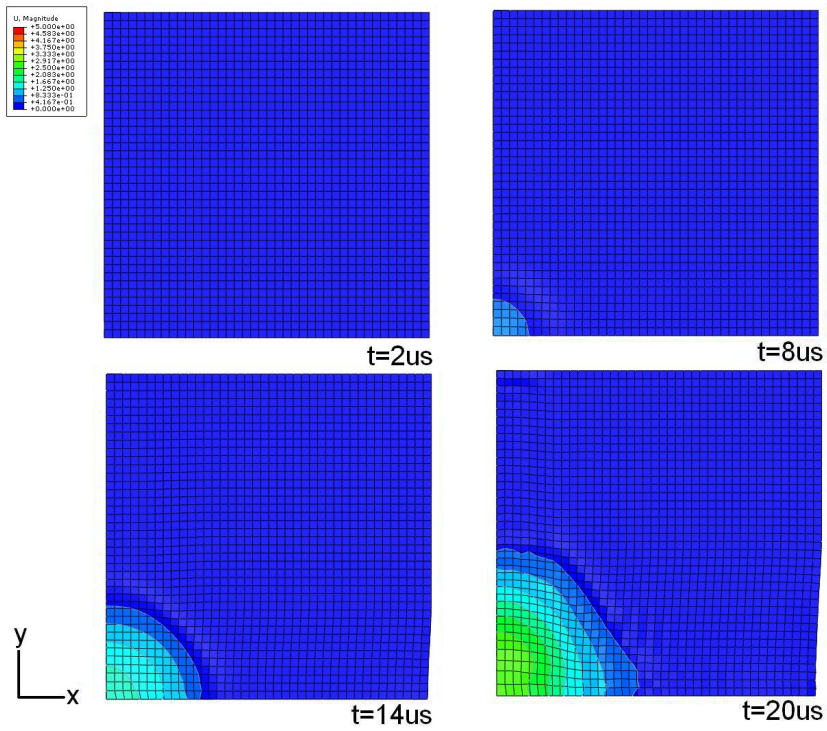


Figure 7.16: Total displacement in Lumped filament-bundle model at the back of the Dyneema plate. Results are given from 0 (blue) to 5.0 (red) mm.

impact on Dyneema composite.

The Lumped filament-layer model is, like the Orthogonal layered model, a layered model. This allows for visualisation of delamination phenomena by modelling the interface behaviour by three-dimensional elements. In addition to delamination, it is possible to study filament sliding and filament fracture with this model, which is quite a step forward. It is therefore seen that more can be described by the Lumped filament-bundle model than by the Orthogonal layered model and the Discrete filament-bundle model can therefore more realistically describe the phenomena as seen in experiments.

However, due to hardware restrictions, it is currently not possible to model the individual filaments. For this model, the stable time increment can already be very small (depending on the number of filaments that are lumped in a truss element). If a small number of filaments is lumped, this means that the stable time increment also goes down and simulation run time goes up. This means that the fineness of the mesh depends amongst others on the available computer power. We would recommend to choose the distances between the trusses as a function of the size of the projection of the projectile on the target. If too little filament-bundles are modelled, the results may not be representative, because a projectile can possibly move between the filaments. In that case, the filaments are not loaded in tension and less easily stop the projectile than if more filaments would be used.

The sensitivity study in this chapter shows that the model is not too sensitive to the number of layers, mesh size or mesh distribution. This means that the model needs not be as fine as possible. However, the greatest strength of this model remains that filament sliding and filament fracture can be visualised, something never done earlier for this specific load case and material.

7.4 Discussion

The same impact case is modelled with the Orthogonal layered model and the Lumped filament-bundle model. Both the Lumped filament-bundle model and the Orthogonal layered model are 'layered models'. The layers that are modelled are different for the two models, the Orthogonal layered model uses orthogonal layers and the Lumped filament-bundle model uses unidirectional filament-bundle layers. Below, the results of the simulations done with the Orthogonal layered model are compared to those of the Lumped filament-bundle model.

Filament tension

If the projectile impacts on the Dyneema composite, we see that -due to the introduced change in curvature- the filaments are loaded in tension. This is seen in both models. However, in the Lumped filament-bundle model, a distinction is

made between the filament-bundles and the rest of the composite and we can see that the stress in the filament-bundles is different from the remainder of the composite. Naturally, this cannot be observed in the Orthogonal layered model, because of the different modelling approach that uses orthogonal layers. The same can be said for filament fracture and filament sliding, it may be clear that this cannot be directly shown with the Orthogonal layered model. The properties of the filaments and the rest of the composite are projected onto the three-dimensional elements and the interface properties on the cohesive elements.

Delamination

Both the Lumped filament-bundle model and the Orthogonal layered model can show delamination of layers. In the Orthogonal layered model, adjacent layers are delaminated if the cohesive elements (that are placed between adjacent composite layers) fail and the three-dimensional element layers move away from each other. In the Lumped filament-bundle model, delamination of adjacent layers occurs if the maximum stress in the three-dimensional elements is reached, are removed from the simulation and the adjacent filament layers move away from each other. In the Lumped filament-bundle model, the three-dimensional elements do not only represent the interface between the filament layers, but also the shear properties of the composite. This makes the interpretation of failure of the interface, especially when the interface layer is damaged, more complex in the Lumped filament-bundle model.

Other

Both simulation models are relatively insensitive to mesh coarseness and size of the modelled plate (at least for side lengths between 20 – 160mm). There are, however, differences in results between the two models.

If we compare the results of both simulation models at $t = 20\mu s$, we see that the residual projectile velocity is 20 % less in the Lumped filament-bundle model than in the case of the Orthogonal layered model. In addition, the delaminated area is 10% more in the Lumped filament-bundle model than in the Orthogonal layered model and u_{max} is 25 % in the Lumped filament-bundle model compared to the Orthogonal layered model. We believe that this difference is caused by the presence of the discrete filament bundles in the model. Due to the presence of these discrete filament bundles, the projectile is in contact, locally, with very strong and stiff entities. This may result in a higher u_{max} . In the Orthogonal layered model, the contact between projectile and Dyneema composite plate is more of continuous nature. This may indicate that discretisation of properties is important in simulating a high fibre volume content composite, such as Dyneema.

Overall comparison

A high-level summary of overall replacement models, the Orthogonal layered model and the Lumped filament-bundle model is given in table 7.5.

Table 7.5: *Simulation methods compared*

Property	Overall	OLM	LFB
Delamination	no	yes	yes
Filament sliding	no	no	yes
Filament fracture	no	no	yes

It is seen that delamination cannot be shown by the overall replacement model, but can be described by both the Orthogonal layered model and the Lumped filament-bundle model. Filament sliding and filament fracture can only be described explicitly by the Lumped filament-bundle model, which gives a more realistic view of the way that components in a composite fail.

Conclusions and recommendations

The goal of this research is to develop a simulation tool that can predict the response of flat, square Dyneema-composite plates subjected to small projectile impact in more detail than possible with a overall replacement model. In this research, two simulation models are developed, namely the Orthogonal layered model and the Lumped filament-bundle model. Both models can describe impact phenomena of Dyneema-composite plates on a discrete layer level and thus in more detail than previously developed overall replacement models. Each of these models contribute to a better understanding of the behaviour of the composite when it is subjected to projectile impact, because they can show the development of phenomena in Dyneema composite as a function of time on a layer level. The simulations are done with an impact velocity of 300 m/s . In this velocity regime, the glassy response dominates the behaviour of the visco-elastic Dyneema material. The models could be extended to lower or higher velocities with appropriate adjustments, something that we have not done in this research.

Experimental observations

From experiments, we conclude that filament sliding, filament fracture and delamination are governing phenomena that occur in a Dyneema composite plate due to projectile impact. At the beginning of this research, we assumed -as was done by many researchers- that delamination was the dominant failure mechanism and that heat played a significant role in composite failure. From our experiments, we can conclude that only a minor part of the projectile kinetic energy is transformed into heat. This amount is so small that it can be considered negligible compared to the energy that is transformed into filament stretching, filament sliding and delamination. From experiments and simulations

together, we can conclude that filament fracture is actually the failure phenomenon that is very important.

Material properties that are needed as input for both developed models can be experimentally determined, such as the average composite properties and the filament bundle properties. For projectile impact, the material properties at a high loading speed are required. We determined this for the Dyneema fibres, but used data for the composite that are determined with ultrasonic measurements. For further research, we therefore recommend that composite properties should also be determined dynamically.

Conclusions on Orthogonal layered model

The Orthogonal layered model focuses on describing *delamination development* in Dyneema composite plates due to orthogonal impact by small projectiles. The behaviour of the interfaces between Dyneema sheets in the composite is described by cohesive elements in this model. This model is suitable to study effects such as back face deformation and delaminated area. More detailed phenomena, such as filament fracture and filament sliding, cannot be shown directly in this model.

From this, we can conclude that this model is useful for studying delamination development. The stable time increment, however, is very small. This time increment decreases and thus the computation time increases with decreasing size of the cohesive elements. Since the thicknesses of the cohesive elements are close to zero, the computation time is generally high. This model is, however, less suitable for more detailed phenomena such as filament fracture. From this, we can conclude that delamination can be shown by this model (it shows phenomena on a layer level), but that it is less useful for studying phenomena that are on a more detailed level than delamination.

Conclusions on Lumped filament-bundle model

The Lumped filament-bundle model can describe the phenomena that, in our opinion, contribute most to stopping a projectile in Dyneema composite. Besides showing delamination development in the composite, it also shows *filament sliding and filament fracture* in the composite. It turns out that the stable time increment for this simulation model is larger than that of the Orthogonal layered model.

From this, we can conclude that the Lumped-filament bundle model can describe Dyneema composite behaviour on a layer level and is able to describe both filament sliding and filament fracture.

Recommendations for further research

It is expected that both models can facilitate further development of Dyneema composite in either plates or in other Dyneema (composite) applications.

However, we recommend to develop the Lumped filament-bundle model further rather than the Orthogonal layered model. By developing the Lumped filament-bundle model, filament-related phenomena can be studied such as filament stretching, fracture and sliding. The Orthogonal layered model focuses on the interaction between the Dyneema layers and cannot show these detailed phenomena directly.

In our work, we modelled a ball impacting on a Dyneema composite plate, which is not a common projectile. However, we have contact problems using a ball-shaped projectile. In a next step, it is recommended to study and solve this contact problem. This can, for example, be done by adjusting contact parameters in ABAQUS or writing a subroutine for this contact in ABAQUS. If this problem is solved, impact with other projectiles such as fragments, cylinders or bullets can then become possible, which are more common projectiles. If these projectiles are to be modelled, it is recommended to refine the mesh in order to overcome the contact problems with sharp edges. However, we expect that this will require some extra simulation run time.

It is further seen that the simulations cannot be fully run. If a three-dimensional element fails in either of the two developed models, the element is removed from the simulation, but its mass is retained. We believe that this is a cause for the stable time increment in the simulations becoming too small and does not run anymore. In order to reduce run time, one could choose to define contact for the filament-bundles that are directly in contact with the projectile, because contact is most probable to occur in that area. Another possible solution would be to develop models using other approaches, such as multi-scale models or stochastic models. By doing so, possibly, run time can be reduced. However, models may become more complicated if these models are used.

In terms of material properties, the behaviour of Dyneema composite is still not yet fully understood. For example, the pull-in effect of the filaments should be studied in more detail. We do not know whether this effect contributes significantly in the protection against projectiles. Also, much is unknown about the parameters that influence pull-in effects. From experiments, we have indications that the effect depends, amongst others, on the size of the specimen. Further, if more should be understood about Dyneema composite, we recommend to study the behaviour of individual Dyneema sheets. In this research, we have studied Dyneema fibre and Dyneema composite behaviour, but we have not studied Dyneema sheets. By studying the behaviour of Dyneema sheets, a more qualitative understanding of layer behaviour, such as delamination, is expected to be clarified.

Summary

In this research, Dyneema-fibre reinforced composite armour plates, subjected to perpendicular impact by small projectiles, are studied. Dyneema fibre can be found in all kinds of applications ranging from leisure products such as sails or kite wires to surgical cables and armour applications such as helmets, bullet proof vests, inserts or armour vehicle panels. These applications have in common that they require a low density and a high strength and stiffness at the same time. Since Dyneema fibre has a density that is slightly lower than water, has a (static) Young's modulus of more than 120 GPa and a strength of a few GPa , it is a popular material to use in applications where both lightweightness and high strength and stiffness is required such as in the aforementioned products.

Research and development goals

In this research, a flat Dyneema composite plate is subjected to perpendicular projectile impact with velocities that range from 200 m/s to 500 m/s . The models in this research are hence developed for this velocity range. As mentioned before, Dyneema-fibre reinforced composite armour plates are the subject of this research. More precisely, the behaviour of Dyneema composite that undergoes perpendicular impact of small projectiles is studied. The goals of this thesis consist of a research and a development part.

In the research part, the goal is to study Dyneema behaviour both on a qualitative and a quantitative experimental basis. In this study, not only the impact case is studied, but also its behaviour under other load cases. This study is used as input for the development of tools that can predict the behaviour of Dyneema composite caused by projectile impact.

In the development part, the goal is to develop a model that can predict Dyneema composite behaviour when it is impacted by small projectiles. This model should give more details than overall replacement models. There are, in our opinion, three different types of tools that can be developed, namely

analytical, empirical and numerical (or rather simulation) tools. Analytical methods soon become too complicated to be a practical means to predict the behaviour of composite materials and empirical methods give too little details on the processes in the material. If simulation models are used, the level of detail and the amount of detail can be balanced by the developer; they can give as much detail as is desirable and can give a good visualisation of the processes that occur in Dyneema composite caused by projectile impact. For this research, therefore, simulation tools are developed, namely the Orthogonal layered model and the Lumped filament-bundle model. These models both give detail on a layer-level.

Dyneema composite properties and behaviour

Dyneema composite consists of a number of sheets. In order to produce Dyneema composite, a number of these sheets are pressed together under elevated temperature and pressure. The performance of the Dyneema composite can, amongst others, be influenced by changing the number of layers in the composite and the applied pressure; the resistance of the Dyneema composite against projectiles increases with increasing manufacturing pressure.

A sheet consists of two (viscoelastic) components, namely Dyneema filaments¹ that are being kept together by an amount of PUR matrix. A sheet typically contains more than 75 % Dyneema filaments by volume. Dyneema is a certain grade of Ultra High Molecular Weight Polyethylene (UHMW PE). Dyneema fibre is produced by a patented gel-spinning process in which the molecular chains are oriented. This orientation gives the fibres their favourable strength and stiffness properties. From these fibres, orthogonal filament layers are made that are kept together by the PUR matrix, which gives coherence to the Dyneema filament layers. These layers together form a so-called non-woven² Dyneema sheet.

As mentioned before, experiments on Dyneema fibre and Dyneema-fibre based composite were done to determine what phenomena occur due to projectile impact. Both ballistic experiments, quasi-static and dynamic experiments are done to get an idea of the behaviour of the material subjected to different strain rates.

From experiments, it turns out that processing of the Dyneema composite is difficult, because Dyneema filaments have a high resistance to shear loads. Because of this Dyneema composite is sensitive to delamination and sliding of sheets while being processed by most mechanical processing techniques. By concentrating mechanical loads as much as possible, using e.g. abrasive water jet cutting or laser jet cutting, delamination and sheet sliding can be reduced. This property gives difficulties in preparing test samples.

¹filaments are building blocks of a fibre

²non-wovens consist of filaments that are placed on top of each other, but are not intertwined

What is also found from experiments is that the fibre modulus increases with increasing strain rate. This is also expected, since Dyneema fibre is known to be a viscoelastic material. The modulus is 120 GPa for quasi-static loading and the modulus increases to about 200 GPa for ballistic impact loads, which is near the theoretical maximum value of the Young's modulus.

After the experiments the material is analysed with (electron) microscopes to study which (failure) phenomena occurred in the material. From these analyses, the most important phenomena that occur due to projectile impact are derived. These phenomena are filament sliding, filament fracture and delamination. In addition to these phenomena, some very local heat effects (melting) were found (about a diameter of a filament, $17\ \mu\text{m}$, away from the impact point). From this, it is determined that the simulation tools should be able to describe filament sliding, filament fracture and delamination. Melting of components is not considered in the models developed in this research, because their effects are found to be negligible.

Choice of simulation code

Computer models can either be developed in a commercial code or in a code that is less widely available, like in in-house developed software. Preference is given to developing the simulation model in a commercial simulation code, because of a higher maintainability and the possibility to continue the development of the models after this research is finished.

In order to make a choice for a simulation code, a trade-off between the three most commonly used software packages, used in the ballistics field, is made. These codes are LS Dyna, Autodyn and ABAQUS. Both Autodyn and ABAQUS give the possibility to easily define a non-standard stress-strain behaviour. Although a great number of material models is available in LS Dyna, it is more labour-intensive to adjust a different stress-strain behaviour. Both ABAQUS and LS Dyna have an extensive element library. In Autodyn, not all elements were readily available³ to be able to experiment with various replacement models, for example with truss elements.

ABAQUS has the additional advantage that both implicit and explicit integration schemes are available. This can be useful if the effect of a load case that contains both a long time duration and a short time duration; an example of this is the study of the influence of pre-stress on the ballistic performance of Dyneema composite.

Because ABAQUS has the most favourable characteristics, a choice is made to develop the simulation tools in ABAQUS rather than in LS Dyna or Autodyn.

³at the moment of this research, the elements were not available. This could be changed in the newer versions, however we based our trade-off at the data available in 2004

Two simulation models

For this research, two simulation models were developed, namely the Orthogonal layered model and the Lumped filament-bundle model. At first, we focussed on delamination development, because we assumed that this was the dominant failure model. As turned out later, filament-phenomena play an important role as well.

For both models, assumptions are made of which they have a few in common. One of the most important assumptions is that the constituents of the Dyneema-fibre based composite are loaded with such a high strain rate during projectile impact that their response is glassy during the whole process. It is therefore assumed that it suffices to consider the glassy behaviour of the constituents only. Further, the constituents are assumed to have a linear stress-strain behaviour up till failure. It is also assumed that on the scales that the Orthogonal layered model and the Lumped filament-bundle model act, continuum theory still applies (so the influence of e.g. atomic forces is negligible). Finally, the influence of environmental conditions, e.g. humidity, pressure and temperature, is assumed to be negligibly small.

The first model: the Orthogonal layered model

The Orthogonal layered model is based on the discrete layered model developed by Liu e.a., see reference [28]. The Orthogonal layered model consists of a collection of layers; these layers have the properties of a number of orthogonal Dyneema composite sheets. The layers in the Orthogonal layered model are fewer in number than the layers in a real Dyneema composite. This means that a composite layer in the Orthogonal layered model represents a number of real sheets.

Before impact, the layers are kept together by a layer of cohesive elements that represent the interaction between the Dyneema filament layers. The cohesive elements simulate the interaction between the discretised Dyneema composite layers. By modelling the Dyneema composite by the Orthogonal layered model instead of using an overall replacement model, visualisation of delamination is realised. However, details such as filament sliding and filament fracture cannot be directly shown using this model.

The second model: the Lumped filament-bundle model

The Lumped filament-bundle model is also a layered model and consists of unidirectional filament-bundle layers. It may be clear that these layers of unidirectional filament-bundles represent a number of filament layers of a real Dyneema composite; this is similar to a layer in the Orthogonal layered model, which represent more sheets. The filament bundles are embedded in three-dimensional elements and the three-dimensional elements have the

property of the whole Dyneema composite, substracted by the properties of the filament bundles. The discretisation in filament bundles is done to be able to represent filament (bundle) fracture and filament (bundle) sliding. If three-dimensional elements reach their maximum stress value, they failed and are removed from the simulation. The surrounding elements can then move away from each other and in this way delamination is described in this model. The Lumped filament-bundle model is an improvement compared to the Orthogonal layered model in the sense that this model shows more details, namely filament sliding and filament fracture. Since failure due to impact in Dyneema is filament-dominated, this model can contribute to a more thorough understanding of the mechanisms in Dyneema composite caused by projectile impact.

And hence we may conclude that:

- Filament sliding and filament fracture dominate the failure mechanisms in Dyneema composite caused by projectile impact
- The Orthogonal layered model contributes to a better understanding of delamination development in Dyneema composite, but is computationally not efficient
- The Filament-bundle model contributes to a better understanding of filament fracture and filament sliding mechanisms in Dyneema composite
- Modelling impact by sharp-edged projectiles causes contact problems
- Stability problems occur due to mass transfer of failed elements to surrounding elements

Samenvatting

In dit promotieonderzoek zijn kogelwerende platen, gemaakt van Dyneema vezel versterkt kunststof, welke orthogonale projectielinslag ondergaan, onderzocht. Dyneema vezel wordt gebruikt in allerlei producten, die variëren van zeilen en vliegtouwen tot chirurgische vezels en pantsertoepassingen zoals helmen, kogelwerende vesten, ‘inserts’ of pantserplaten. Alle genoemde toepassingen hebben met elkaar gemeen dat ze liefst een zo laag mogelijke dichtheid moeten hebben en tegelijkertijd zo sterk en zo stijf mogelijk moeten zijn. Dat is ook de reden dat Dyneema vezel veelvuldig in deze toepassingen wordt gebruikt. Omdat de dichtheid van Dyneema is lager dan dat van water, een (statische) Young’s modulus van meer dan 120 GPa en een breuksterkte van enkele GPa heeft, is dit een populair materiaal in toepassingen waar zowel lichtgewicht en een hoge sterkte en stijfheid vereist is, zoals in bovengenoemde producten.

Onderzoeksdoel en ontwikkeling

In dit onderzoek is een vlakke Dyneema composiet plaat blootgesteld aan orthogonale projectielinslag met snelheden die variëren van 200 m/s tot 500 m/s . De computermodellen zijn dan ook voor deze snelheden ontworpen. Zoals eerder genoemd, zijn Dyneema-vezelversterkte composieten pantserplaten het onderwerp van dit onderzoek. Meer specifiek, wordt het gedrag van Dyneema composiet dat loodrechte projectielinslag ondervindt, bestudeerd. Deze dissertatie beslaat een onderzoeksgedeelte en een ontwikkelingsgedeelte. In het onderzoeksdeel is het doel om Dyneema gedrag te analyseren op zowel een kwalitatief als ook kwantitatief. In dit onderzoek is niet alleen projectielinslag bekeken, maar ook Dyneema gedrag onder andere belastingen. Deze studie is gebruikt als input voor het ontwikkelen van de computermodellen die het gedrag van Dyneema composiet kunnen voorspellen, wanneer er een projectiel op inslaat. In het ontwikkelingsgedeelte, is het doel om een model te ontwikkelen dat het

gedrag van Dyneema composiet kan voorspellen tijdens projectielinslag. De voorwaarde is dat dit model meer details moet geven dan mogelijk is met een ‘overall replacement model’. Ons insziens zijn er drie manieren om gedrag te voorspellen, namelijk door middel van analytische, empirische en numerieke methoden. Er is gekozen om de voorspellingen te doen aan de hand van computermodellen, omdat analytische methoden vaak te complex zijn om praktisch te blijven en empirische methoden vaak te weinig details geven over de processen in het materiaal. Als men simulaties gebruikt, is het vooral aan de ontwikkelaar om het detailniveau te bepalen; er kan zo veel detail worden gegeven als gewenst en er kan dus een goede visualisatie worden gemaakt van Dyneema composiet dat onderhevig is aan projectielinslag. Er is gekozen voor het ontwikkelen van twee computermodellen, namelijk het ‘Orthogonal layered model’ en het ‘Lumped filament-bundle model’. Deze modellen laten beiden details zien tot op lagenniveau.

Eigenschappen en gedrag van Dyneema composiet

Dyneema bestaat uit een aantal lagen. Door Dyneema-vellen onder een hoge druk te verwarmen maakt men Dyneema composiet. De eigenschappen van het zo gevormde composiet is o.a. afhankelijk van de hoogte van de druk en het aantal gebruikte vellen, de prestatie van een Dyneema en de ballistische eigenschappen (energieabsorptie per oppervlakte-eenheid) van het composiet kunnen verbeterd worden door de druk te verhogen. Een Dyneema composiet bestaat uit een aantal Dyneema-vellen, die uit twee (viscoelastische) componenten bevat, namelijk een PUR matrix en Dyneema filamenten⁴. Een Dyneema-vel bestaat uit meer dan 75 volume % Dyneema filamenten. De chemische naam voor Dyneema is ‘Ultra High Molecular Weight Polyethylene’ (UHMW PE). Dyneema vezel wordt geproduceerd door middel van een gepatenteerd gelspinning proces, waarin de molekuulketens in de filamenten georiënteerd worden. Door deze oriëntatie krijgen de filamenten hun gewenste, hoge sterkte en stijfheidseigenschappen. Dyneema filamenten worden in orthogonale lagen neergelegd en de coherentie tussen deze lagen wordt gegarandeerd door een kleine hoeveelheid PUR matrix toe te voegen.

Zoals eerder genoemd, is er experimenteel onderzoek gedaan naar het gedrag van Dyneemavezel en Dyneemacomposiet. Hierbij zijn zowel ballistische als quasi-statische en dynamische experimenten gedaan, om een beeld te krijgen van het gedrag van Dyneema onder verschillende reksnelheden.

Er ontstaat vaak delaminatie en het verschuiven van vellen in het Dyneemacomposiet tijdens mechanische bewerking, bijvoorbeeld voor het vervaardigen van testsamples. Deze effecten kunnen enigszins worden gereduceerd door de mechanische belasting zo veel mogelijk te concentreren;

⁴filamenten zijn de bouwstenen van een vezel

voorbeelden hiervan zijn abbrassief waterstraalsnijden of laserstraalsnijden. Delaminatie of verschuiven van vellen kan hierdoor drastisch worden verminderd, doch niet geheel worden voorkomen.

Wat ook uit de experimenten naar voren is gekomen is dat de vezelmodulus toeneemt met toenemende reksnelheid. Dit kan ook enigszins worden verwacht, omdat Dyneema een viscoelastisch materiaal is. Om hiervoor een gevoel te geven: de modulus bij quasi-statische belastingen is 120 GPa en deze stijgt naar 200 GPa voor reksnelheden die optreden bij een ballistische belasting, wat de theoretische grenswaarde benadert voor Dyneemavezel.

Om te bepalen wat het meest bijdraagt aan het tegenhouden van een projectiel, zijn zowel Dyneemavezel als Dyneemacomposiet na breuk geanalyseerd met een electronen-microscop. Hieruit is gebleken dat de belangrijkste bijdrage tot het tegenhouden van een projectiel (of energieabsorptie) komt filamentbreuk.

Daarnaast kan men heel lokaal wat smeltverschijnselen zien (tot ongeveer een filamentdikte, $17\ \mu\text{m}$, verwijderd van het inslagpunt). Uit de gedane experimenten blijken de dominante verschijnselen door projectielinslag naast filamentbreuk, ook filamentverschuiving en delaminatie te zijn en deze informatie is ook gebruikt bij het ontwikkelen van de eerdergenoemde computermodellen. Smeltgedrag is hierin niet meegenomen.

Keuze van simulatiecode

Er is gekozen om de ontwikkeling van de computermodellen in een commerciële code te ontwikkelen vanwege het beter kunnen onderhouden van een simulatie model in en om de mogelijkheid open te houden om het model verder te kunnen ontwikkelen na afloop van dit onderzoek. Om tot een keuze te komen, is een trade-off gemaakt tussen drie softwarepakketten, die als standaard worden gezien in het ballistische vakgebied, namelijk LS Dyna, Autodyn en ABAQUS. In zowel Autodyn als ABAQUS, kan het spannings-rekgedrag gemakkelijk worden aangepast door de gebruiker. In LS Dyna wordt voornamelijk van voorgeprogrammeerde materiaalmodellen gebruik gemaakt, wat in ons geval niet voldoet. De mogelijkheid bestaat echter wel om een subroutine te schrijven. Als we kijken naar de elementen die beschikbaar zijn, zien we dat in zowel ABAQUS als LS Dyna geschikte elementen zitten voor de ontwikkeling van de gewenste computermodellen. In Autodyn waren op het moment van dit onderzoek nog niet alle elementen beschikbaar om een goede ontwikkeling van een model op lagenniveau mogelijk te maken.

ABAQUS heeft nog een ander voordeel, namelijk dat er zowel een impliciet als een expliciet integratieschema beschikbaar is. Dit zou in de toekomst vooral van nut kunnen zijn om een combinatie van quasi-statische en ballistische belastingen te kunnen bestuderen, bijvoorbeeld als men de invloed van voorspanning op de ballistische prestatie van een Dyneema composiet wil weten. Omdat ABAQUS de meeste pluspunten heeft, is er gekozen om de modellen in

ABAQUS in plaats van in LS Dyna of in Autodyn.

Twee computermodellen

In dit onderzoek zijn er twee computermodellen ontwikkeld, namelijk het ‘Orthogonal layered model’ en het ‘Lumped filament-bundle model’. In eerste instantie, hebben we ons gefocust op delaminatie, omdat we verwachtten dat dit dominant is in het voorspellen van gedrag van Dyneema composiet. Later bleek ook filament-gedrag een belangrijke rol te spelen.

Voor beide modellen zijn er aannames gemaakt, waarvan enkele gemeenschappelijk. Een van de meest belangrijke aannames is dat de belastingssnelheid op de componenten van Dyneema composiet zodanige hoog zijn dat de respons van de componenten zich in het glas regime bevindt gedurende het gehele proces van projectielinslag. Hieruit vloeit dan voort dat het wordt aangenomen dat het in acht nemen van slechts het glas-achtige gedrag van de componenten volstaat. Dit betekent dat ook wordt aangenomen dat de componenten een lineair gedrag vertonen ten aanzien van spannings-rek gedrag tot aan breuk.

Ook wordt voor beide modellen aangenomen dat continuum theorie nog steeds opgaat. Dit betekent dat fenomenen op moleculaire of kleinere schaal niet in acht worden genomen. Verder wordt in beide modellen verondersteld dat de invloed van omgevingsfactoren zoals vocht, druk en temperatuur, verwaarloosbaar is.

Model 1: het ‘Orthogonal layered model’

Het ‘Orthogonal layered model’ is gebaseerd op het ‘Discrete layered model’ dat door Liu e.a. is ontwikkeld, zie referentie [28]. Het ‘Orthogonal layered model’ bestaat uit een samenhangend geheel van lagen; een laag stelt meerdere sheets voor en heeft dus ook de eigenschappen van een aantal van deze sheets. Het aantal lagen in het Orthogonal layered model is kleiner dan het aantal sheets in een Dyneema composiet.

Voorafgaand aan projectielinslag worden de gediscrètiseerde lagen door een laag cohesie-elementen bij elkaar gehouden en deze elementen beschrijven de interactie tussen de lagen. Door een Dyneema composiet te modeleren met het ‘Orthogonal layered model’ i.p.v. met een ‘overall replacement model’, is de visualisatie van delaminatie gerealiseerd. Echter, details zoals filament verschuivng en filamentbreuk kan niet direct door dit model worden weergegeven.

Model 2: het ‘Lumped filament-bundle model’

Het ‘Lumped filament-bundle model’ is ook een laagjesmodel en bestaat uit uni-directionele lagen van filament-bundels. Het moge duidelijk zijn dat deze

uni-directionele filament-bundel lagen ook weer meerdere, werkelijke lagen voorstellen; dit is vergelijkbaar met een laag in het ‘Orthogonal layered model’, die ook meer werkelijke sheets voorstelt. De filamentbundels liggen ingebed in drie-dimensionale elementen en de drie-dimensionale elementen hebben hier de eigenschappen van het gehele Dyneema composiet met daarvan de eigenschappen van de filamentbundels afgehaald. De reden van discretisatie van de filamentbundels is dat er op deze manier de mogelijkheid wordt gecreëerd om filament(bundel) breuk en filament(bundel) verschuiving te kunnen visualiseren. Daarnaast biedt deze lagenvisualisatie ook de mogelijkheid om delaminatie te voorspellen. Als de maximale spanning optreedt in de drie-dimensionale elementen, falen zij en worden uit de simulatie verwijderd. De omliggende elementen kunnen dan uit elkaar bewegen en op deze manier wordt delaminatie in dit model beschreven.

Het ‘Lumped filament-bundle model’ is een verbetering t.o.v. het ‘Orthogonal layered model’ in de zin dat dit model meer details, namelijk filament verschuiving en filament breuk, kan weergeven. Omdat het grootste deel van de inslagenergie wordt geabsorbeerd door de filamenten in Dyneema composiet, draagt dit model meer bij tot de begripsvorming van mechanismen in Dyneema composiet.

En daarom concluderen we dat:

- Filament breuk en filament verschuiving de dominerende faalmechanismen in Dyneema composite zijn als gevolg van projectielinslag
- Het ‘Orthogonal layered model’ contributes bijdraagt aan een beter begrip van delaminatie-ontwikkeling in Dyneema composiet, maar niet erg efficiënt is in termen van rekenkracht
- het ‘Filament-bundle layered model’ bijdraagt aan een beter begrip van filament breuk en filament verschuiving in Dyneema composite
- Het modelleren van projectielen met scherpe randen verorzaakt contactproblemen
- Er treden stabiliteitsproblemen op door massa transport van gefaalde elementen naar naburige elementen

Acknowledgements

Doing research requires patience. Writing a dissertation requires even more patience and finishing a dissertation requires both a lot of patience and a lot of discipline and these are two properties that don't come with me naturally. Fortunately, I got support from a lot of great people to cope with this and I would like to thank them on the next few pages. If I didn't mention you here, please know that I am grateful to you as well and that this certainly doesn't mean that I forgot about you. It is just for the sake of the length of this text that I don't mention everyone!

I would like to start with my supervisors Leo Ernst, Daniel Rixen and Niels van der Meer. Leo, I will start off with you. Thank you for giving me the opportunity to pursue my studies under your supervision. What I really admire in you is your ability to think broadly and focus on important details at the same time. Furthermore, you taught me that work is not the whole part of the story and that social interactions may be just as important. Thank you, also, for being so flexible, which surely helped me to finish my thesis. Daniel, thank you for your peptalks and our lively discussions. After the serious stuff, there was also time for a bit of a laugh. I hope that many more students may enjoy your supervision. Niels, thank you for the time that you took for discussing things with me. You really got me interested in some real physics stuff like relativity theory and of course binary clocks.

I would also like to thank some of the staff from Delft University of Technology. Kaspar Jansen, I would like to thank you for your help on the, let's say, more chemical part of my project. Although I did not always agree with you, we had some very fruitful discussions. Rien van de Ruijtenbeek, whenever I'll drop by, we are going to talk about 'the old days' of the finite element development again. Your stories about this really helped me to put my research in a context of time. Jan Booij, thank you very much for your help on ABAQUS matters, it saved me a lot of time being able to submit some of my jobs on the cluster. Also

thank you for your clear explanation about networks and Linux stuff, I am sure it will come in useful. This brings me to the guys from our university lab, Jos van Driel, Jan Sterk, Erik Fritz and Harry Jansen. You really helped me solving the clamping problem. Well, most of the credits go to you Harry! You are invaluable, keep on sporting to generate ideas! I would also like to thank André Hoogstrate for our good cooperation during the Bachelor project, which brought me closer to the solution of processing Dyneema composite parts. I would also like to thank professor Piet Meijers and Bertus Nijhof †⁵ for our discussions on a more theoretical approach of my research.

When I first started my research, I knew almost nothing about ballistics. I would like to thank the people at TNO that helped me to increase my knowledge in this field. I am especially grateful to Marjolein van der Jagt for teaching me about Dyneema and its properties. I benefited a great deal from the work you did before I came. Thank you, Marjolein, also for a lot of other things like your mental support, your advice and for the many papers, posters and presentations that you reviewed for me. I am still ashamed that I forgot to mention you for some things you helped me on and hope that I can make up for this by thanking you right here! Hans Broos, we were a golden team, weren't we? Especially the experiments during the 'long' days at the Ballistic Laboratory went really well. Thank you, also, for the patience you had while answering my many questions about ballistics and also for proofreading the chapter on ballistics. I started my simulations in the computer programme Autodyn, with which I never worked before. Fortunately Koen Herlaar was so kind to explain me many things about it during my research. Thank you, Koen, for the time you always made to answer my questions in a very clear way. And what would research be without experiments and analysis? What happens in Dyneema if impacted by a projectile? Well, you can try and find out using microscopy, Kees van der Wulp once said. And you were right! How exciting it was to work with you, Kees van der Wulp and Willem Duvalois. We always found new and exiting things during our, sometimes exhausting, sessions in front (Willem, especially for you!) of the microscope. Kees, enjoy your free time now and Willem, please be careful on your (racing) bike. I'd also like to express my gratitude to Frans van Wegen for giving me information that I could use for the ballistics chapter. I would also like to thank the guys from the Laboratory of Ballistic Research (LBO) for helping me with my experiments. Special thanks go to Ton van de Voorde, Walter Borsboom, Marco Huijter, Ilco Koevermans, Mark Dijkstra, Frits Hilvers, Ton Heederik, Hans Bakker, Fred Zandvliet, Michel Kok, Martin van de Voorde, Ton van de Voorde and Ruud van der Wijst, both for your help with the experiments and for the good times during some very long days. And to Ed van Riet, thanks a lot for giving me the opportunity to present my work at the ARA in Venice!

I would like to thank Roel Marissen and Martin van Es from DSM for their

⁵23 July 1938-31 July 2011

support during my research. Roel, when you heard that I was going to work on the Dyneema subject at Mechanical Engineering, you were immediately very enthusiastic about it. Once you get enthusiastic, the person who is speaking with you automatically goes along with you in that. Thanks again, Roel, for your support.

I would also like to thank Laurent Warnet and Remco Akkerman from the University of Twente. By doing experiments with your drop tower, you helped me a great deal. These tests gave me insight in the material behaviour. In addition, you also arranged for Dyneema processing using a laser cutter. Since there are only two of such machines in the Netherlands, it was really great that you could arrange it for my students and me.

Talking about experiments, some of them worked well and others, say, less well. But even the things that I eventually didn't use in my thesis contributed to a better understanding of the material. From Jaap Weerheijm, I heard that there was this great microscope in which you could actually perform a tensile test and follow it with it. Erik Schlangen and Greet Leeghwater, thank you for helping me with this apparatus. Unfortunately, we came to the conclusion that with the lay out of the machine in combination with such a difficult material, it was going to be a research on its own. Ilse Vegt, thank you for helping me with the simulation for the Hopkinson bar so that I could figure out whether the effort was worth the result.

During my Master project, I had already been working with ABAQUS. However, there always remain things to be learnt. Fortunately, one of ABAQUS's gurus, Gertjan Kloosterman, was always willing to explain things to me and help me out with ABAQUS. Thank you, Gertjan, for your interest, helpful advices and your quick responses. Many thanks as well to the supporting office of Dassault Systèmes Simulia Benelux for making the printing of this thesis possible!

I couldn't have done the work without the help of the students with whom I had the pleasure to work with. Gerard Brouwer, you did a study on the determination of delamination patterns in Dyneema using ultrasound methods. Nidhal Bettaibi, you investigated delamination patterns using infrared techniques. Thank you both for your contributions. Thijs Schraven, Benne Engelen, Thomas van het Kaar, Tobias Oberdorfer, thanks for your extensive and challenging research on processing methods of Dyneema composite. Freeke van Osch, Jurriaan Knobel, Elie Racle, I'd like to thank you for your contribution on the modelling part of my research.

My research was about a polymer material. I had only a basic knowledge of polymers, but I am not (yet) a chemist. I went to the TOP polymer course in Eindhoven to extend my knowledge about polymers. My special thanks to Piet

Lemstra and Bas Staal (but also of course to the other lecturers) for your patience with a student that knew little about polymer chemistry at the start of the course. I would like to thank all my class mates for the good times we had and I would especially like to sincerely thank Hans Dommershuijzen for his never-ending motivation to bring this course to a good end together. Thank you also, Hans, for the many discussions we had on subjects varying from atoms and energy levels to university systems and Mechanical Engineers (being Aerospace Engineers without...).

I would also like to thank the three managers at TNO, André Diederer, Jean-Pierre Pieréij and Jan Olijslager, with whom I had the pleasure to work with during my research. André, thank you for the input that you gave me on my papers. Jean-Pierre, thanks to you I had the possibility to attend all the conferences I wanted, which gave me the opportunity to present my work to a worldwide audience. Jan, thank you for the space you gave me for pursuing my research.

And what's research without inspiring people around you? I had a good time at university and not in the last place thanks to Corinne du Burck and Paul van Woerkom. Corinne, I can only hope that 'my' next secretary will be like you. Your positive attitude and your willingness to help everyone regardless of position, person or anything is greatly appreciated. Paul, thank you for many things, for guiding me during my first days, for the many discussions on various issues and also for helping me out on what to do after my PhD. You are the best mental coach a student can wish! I would also like to thank Boryana Milosheva and Michiel van Soestbergen for their good company and I am really glad that we are still in touch.

I also enjoyed my time at TNO very much, not in the last place because of my nice colleagues who were never too busy for a laugh. I would like to thank all the people with whom I spent time at TNO in building 85. First, the old 'MB' group Hans Meulman, Rob Kemper, Hans Broos and André Diederer, Marjolein van der Jagt-Deutekom who were always there for a nice cup of tea, but who could also answer the many questions that I had on ballistics and so helped me with my research. I would also like to thank Mathijs van Klink and Sander Pronk for all the fun that we had. A very special thanks, of course, to the lady with the same blood group as I have, Elly van Puffelen. Thank you for all the advices that you gave me. They are surely invaluable. Well, I could say a lot more things here, but we'll surely visit some dance performances together or some other occasion.

That brings me to my room mates. Dao Guo Yang, it was a pleasure to share rooms with you at university. All the best to you and your family. After Dao Guo left university, Jan de Vreugd kindly asked me if he could replace Dao Guo as my room mate. I will always remember our lively discussions and hope that

you keep me informed about your organ career after I leave, because I certainly plan to come and listen to one of your performances. Patrick Vercammen, you were my first room mate at TNO. I really would have liked to see many more of your performances, but unfortunately couldn't always find the time to attend all of them. I really enjoyed you as a room mate and you are certainly one of the most wonderful persons I know. Thank you for being there for me. After some departments were put together, we had to move and I shared my office with Cornelis van 't Hof. Thank you for the nice time and your advice on thesis writing. I would also like to thank my other 'zoldergenoten' Mark Tyler Street, Joke Luyten, Jesus Mediavilla Varas for the good times we spend together. In general, I would like to thank everyone from TNO and TU Delft that I connected to and made my PhD period to an unforgettable time.

I would also like to sincerely thank my direct Shell colleagues Henk Rijkens and Jean-Nicolas Desprez for their flexibility in taking over some Tuesday afternoon meetings from me, so that could meet up with Leo to finish my thesis. Also a great thank you to Jane Mercer for her help on translating the propositions into proper English.

Last but certainly not least, I would like to thank my parents, family, in-laws and friends for their support. A very special thanks to my husband, Sander Hebly, not only for his support but also for the great times together that cheered me up after the sometimes disappointing research days that every PhD student is undoubtedly familiar with. Thanks you, also, for giving me the space to finish this manuscript and hence for tolerating a messy apartment.

Thanks again to all of you and keep in touch!

Béate Hebly-Heru Utomo
Delft, November 2011

About the author



Béate Heru Utomo is born on 4 July 1981 in Dordrecht, the Netherlands. In 1993 she commenced secondary school at the Erasmus College in Zoetermeer, the Netherlands. Here, she obtained her Gymnasium degree cum laude in June 1999. In the fall of the same year, she began her study Aerospace Engineering at Delft University of Technology in Delft, the Netherlands. During her studies, she undertook an internship at the Japanese Aerospace Exploration Agency JAXA in Tsukuba, Japan. During this internship, she contributed to the development of micro satellites at the Space Demonstration Laboratory. In October 2004, she obtained her MSc degree in Aerospace Engineering after finishing her thesis entitled

‘an Inflatable wing for MATE’. This thesis is on the analytical description of and a FEM study on an inflatable wing for an Unmanned Aerial Vehicle (UAVs). Directly after her graduation, she started her PhD research at the faculty of Mechanical, Maritime and Materials Engineering at the same university under the supervision of Professor Leo Ernst and Professor Daniel Rixen. This research has been conducted in cooperation with the department of Explosion, Ballistics and Protection from the Dutch national research institute TNO. From 1 November 2008, Béate is working for Royal Dutch Shell and has been working in various technical roles. Because gaining knowledge is one of her hobbies, she started studying Chemical Engineering at the University of Eindhoven, which she expects to finish in 2013.

Bibliography

- [1] D.W. Leeming C.L. Farrar. *Military Ballistics - a Basic Manual*. Battlefield weapons and Technology Series, 1963.
- [2] S.P. Timoshenko J.M. Gere. *Mechanics of Materials, 4th SI Edition*. Stanley Thornes, 1999.
- [3] L.E. Govaert A.K. van der Vegt. *Polymeren, van keten tot kunststof (in Dutch)*. Delft University Press, 5 edition, 2003.
- [4] A.K. van der Vegt A.E. Schouten. *Plastics*. Delta Press BV, 1987.
- [5] C. van 't Hof. *Mechanical characterization and modeling of curing thermosets*. PhD thesis, Delft University of Technology, 2005.
- [6] D. Yang. *Cure-Dependent Viscoelastic Behaviour of Electronic Packaging Polymers - Modelling, Characterization, Implementation and Applications*. PhD thesis, Delft University of Technology, 2007.
- [7] L.E. Govaert. *Deformation Behaviour of Oriented Polyethylene Fibres*. PhD thesis, TU Eindhoven, 1990.
- [8] L. Mishnaevsky Jr. *Computational mesomechanics of composites, Numerical analysis of the effect of microstructures on their strength and damage resistance*. John Wiley & Sons, Ltd., 2008.
- [9] DSM Dyneema. www.dyneema.com, 2007.
- [10] A. Hameed. Gun design (lecture notes). Cranfield University, 2007.
- [11] P. Wall. A comparison of homogenization, hashin-shtrikman bounds and the halpin tsai equations. *Applications of Mathematics*, No.4:245–257, 1997.
- [12] W.D. Callister Jr. *Fundamentals of Materials Science and Engineering, an integrated Approach*, volume 2. Wiley, 2005.

-
- [13] Th. de Jong. Versterkte materialen in de vliegtuigbouw, August 1989.
- [14] J.C. Halpin and J.L. Kardos. The halpin-tsai equations: A review. *Polymer Engineering and Science*, Volume 16(5):344–352, May 1976.
- [15] J. Rodriguez I.S. Chocron Benloulou and V. Sanchez Galvez. A simple analytical model for ballistic impact in composites. *J. PhysiqueIV France*, 7:C3–821–826, August 1997.
- [16] P.K. Porwal S. Leigh Phoenix. A new membrane model for the ballistic impact response and v50 performance of multi-ply fibrous systems. *International Journal of Solids and Structures*, 40:6723–6765, 2003.
- [17] P.M. Cunniff. Dimensionless parameters for optimizations of textile-based body armor systems. In *18th International Symposium on Ballistics*, November 1999.
- [18] T.A. Bogetti B.A. Cheeseman. Ballistic impact into fabric and compliant composite laminates. *Composite Structures*, 61:161–173, 2003.
- [19] P.M. Cunniff. A semiempirical model for the ballistic impact performance. *Textile Research Journal*, 66:45–59, 1996.
- [20] I.S. Chocron Benloulou. A simple analytical model for ballistic impact in composites. *J. Phys IV France 7*, pages C3–821–C3–826, 1997.
- [21] W. Johnson. Mathematical model for predicting residual velocities of fragments after perforating helmets and body armor. Technical report, Ballistic Research Laboratories Technical Note No. 1705, 1968.
- [22] W. Kokinakis. Penetration of dupont kevlar-29 body armor material by a right circular fragment simulator. Technical report, Ballistic Research Laboratories Interim Memorandum Report no. 173, 1974.
- [23] S.L. Ogin P.A. Smith J. Tong, F.J. Guild. On matrix growth in quasi-isotropic laminates-ii: finite element analysis. *Composites Science and Technology*, pages 1537–1545, 1997.
- [24] R.S. Barsoum. Finite element application in the fracture analysis of composite materials-delamination. *Key Engineering Materials*, pages 35–58, 1989.
- [25] A.el Mahi J.F. le Corré J.M. Berthelot, P. Leblond. Transverse cracking of cross-ply laminates: Part 2. progressive widthwise cracking. *Composites Part B*, 27A:1003–1010, 1996.
- [26] J. Varna R. Joffe, A. Krasnikovs. Cos-based simulations of transverse cracking and stiffness reduction in [s/90] laminates. *Composites Science and Technology*, 61:637–656, 2001.
-

-
- [27] J.M. Berthelot. *Composite Materials, Mechanical Behavior and Structural Analysis*. Springer Verlag, 1999.
- [28] C. Liu. *On the Prediction of Damage and Fracture Strength of Notched Composites*. PhD thesis, Delft University of Technology, 2003.
- [29] L.J. Ernst B.D. Heru Utomo. Detailed modeling of projectile impact on dyneema composite using dynamic properties. In *ATEM '07, JSME-MMD*, September 2007.
- [30] B.J. van der Meer. Ph.d. high-speed impact modelling and testing of composite (himtoc). Technical report, TNO, TU Delft, 2004.
- [31] C.J. Hayhurst R.A. Clegg C.M. Wentzel S. Hiermaier, W. Riedel. Final report, advanced material models for hypervelocity impact simulations. Technical Report EMI E 43/99, Ernst Mach Institut, 1999.
- [32] D.M. White W. Riedel, W. Harwick. Final report, advanced material damage models for numerical simulation codes. Technical Report EMI I 75/03, Ernst Mach Institut, 2003.
- [33] H.F. Swift L.B. Greszczuk D.R. Curran J.A. Zukas, T. Nicholas. *Impact Dynamics*. John Wiley & Sons, 1982.
- [34] R.F. Recht T.W. Ipson. Ballistic-penetration resistance and its measurement. *Experimental Mechanics*, 15(7):249–257, July 1975.
- [35] P.J. Hazell. Fundamentals of armour design (lecture notes). Cranfield University, 2004.
- [36] I. Horsfall. Terminal ballistics 3, heavy kinetic energy projectiles (lecture notes). Cranfield University, 2007.
- [37] *Textbook of Ballistics*. Her Majesty's Office, London, 1987.
- [38] S. Champion. Terminal ballistics (lecture notes). Cranfield University, 2007.
- [39] I. Horsfall. Armour materials (lecture notes). Cranfield University, 2007.
- [40] P.A. Lovell R.J. Young. *Introduction to Polymers, 2nd edition*. CRC Press, 1991.
- [41] R.N. Boyd R.T. Morrison. *Organic Chemistry 2nd edition*. Allyn and Bacon Inc, 1966.
- [42] R. Marissen J.M.J. Jacobs J.A.P. Simmelink, J.J. Mencke. Process for making high-performance polyethylene multifilament yarn (wo2005066401). European Patent Office, 2005.
-

-
- [43] S. Bissels P. Hinkel H. Nowack R. Marissen, R.F.M. Lange. Scanning electron microscope visualisation of crack initiation and propagation under static and fatigue loading on thermoplastic elastomers. *International Journal of Fatigue*, 27:71–84, 2005.
- [44] G. van Sandwijk. Dynamische eigenschappen van de dyneema supervezel (in dutch). Master’s thesis, Delft University of Technology, 2002.
- [45] G. Fox W.K. Stone, H.F. Schiefer. Stress-strain relationships in yarns subjected to rapid impact loading. part i: Equipment, testing procedure, and typical results. *Textile Research Journal*, (520-528), June 1955.
- [46] H.F. Schiefer J.C. Smith F.L. McCrackin. Stress-strain relationships in yarns subjected rapid impact loading. part iii: Effect of wave propagation. *Textile Research Journal*, pages 701–708, August 1955.
- [47] H.F. Schiefer W.K. Stone K.M. Towne J.C. SMith, F.L. MacCrackin. Stress-strian relationships in yarns subjected to rapid impact loading: 4. transverse impact tests. *Journal of Research of the National Bureau of Standards*, 57(2):83–89, August 1956.
- [48] H.F. Schiefer J.C. Smith, F.L. McCrackin. Stress-strain relationships in yarns subjected to rapid impact loading. part v: Wave propagation in long textile yarns impacted transversely. *Textile Research Journal*, 29:288–302, April 1958.
- [49] J.M. Blandford K.M. Towne J.C. Smith, P.J. Shouse. Stress-strain relationships in yarns subjected to rapid impact loading. part vii: Stress-strain curves and breaking-energy data for textile yarns. *Textile Research Journal*, 31:721–734, August 1961.
- [50] K.M. Towne J.C. Smith, J.M. Blandford. Stress-strain relationships in yarns subjected to rapid impact loading. *Textile Research Journal*, 32:67–76, January 1962.
- [51] P.J. Shouse K.M. Towne J.C. Smith, J.M. Blandford. Stress-strain relationships in yarns subjected to rapid impact loading. part ix: Effect of yarn structure. *Textile Research Journal*, 32:472–480, June 1962.
- [52] P.J. Shouse J.C. Smith, C.A. Fenstermaker. Stress-strain relationships in yarns subjected to rapid impact loading, part x: Stress-strain curves obtained by impacts with rifle bullets. *Textile Research Journal*, pages 919–933, November 1963.
- [53] J.P.F. Broos B.D. Heru Utomo. Dynamic material behavior determination using single fiber impact. In *IMAC*, February 2007.
-

-
- [54] B.D. Heru Utomo. Dynamic young's modulus determination using single fiber impact. In *57th Meeting of the Aeroballistic Range Association*, September 2006.
- [55] J.P.F. Broos B.D. Heru Utomo. Dynamic material behavior determination using single fiber impact. In *IMAC XXV. SEM*, February 2007.
- [56] H. Brouwer R. Marissen. The significance of fibre micro buckling for the flexural strength of a composite. *Composite Science and Technology*, 59:327–330, 1999.
- [57] T.F. Walsh. Penetration failure of spectra polyethylene fiber-reinforced ballistic-grade composites. *Key Engineering Materials*, 141-143:367–382, 1998.
- [58] Vu Ngoc Pi. *Performance Enhancement of Abrasive Waterjet Cutting*. PhD thesis, TU Delft, 2008.
- [59] H.B. Chin D.C. Prevorsek. Properties of spectra fibers and composites at ballistic rates of deformation. In *21st International SAMPE Technical Conference*, pages 812–824. SAMPE, September 1989.
- [60] T. Peijs R. Frissen, L. Govaert. Modelling the ballistic impact behaviour of polyethylene-fibre-reinforced composites. In ISB, editor, *16th International symposium on ballistics*, 1996.
- [61] T.E. Tay V.B.C. Tan, V.P.W. Shim. Experimental and numerical study of the response of flexible laminates to impact loading. *International Journal of Solids and Structures*, 40:6245–6266, 2003.
- [62] C.G. Chiorean M.A.G. Silva, C. Cismasiu. Numerical simulation of ballistic impact on somposit laminates. *International Journal of Impact Engineering*, 31:289–306, 2005.
- [63] A. Simone O. Lloberas-Valls, D. J. Rixen and L. J. Sluys. Multiscale domain decomposition analysis of quasi-brittle heterogeneous materials. *International Journal of Numerical Method Engineering*, pages –, 2011.
- [64] R.R. Namburu R.R. Valisetty, P.W. Chung. Scalable computing for the transient elasto-plastic impact analysis of composite armor using the homogenization method. *Computers and Structures*, 84:49–60, 2005.
- [65] A.N. Guz J.J. Rushchitsky I.A. Guz, A.A. Rodger. Developing the mechanical models for nanomaterials. *Composites Part A: Applied Science and manufacturing*, 38:123–1250, 2007.
- [66] A.L. Kalamkarov I.V. Andrianov, V.V. Danishevskyy. Micromechanical analysis of fiber-reinforced composites on account of influence of fiber coatings. *Composites Part B: Engineering*, 39:874–881, 2008.
-

-
- [67] M. Ristinmaa N. Saabye Ottosen. *The mechanics of Constitutive Modelling*. Elsevier, Sweden, 2005.
- [68] M.J. van der Jagt. Evaluatie ultrasoon experimenten op dyneema (in dutch), 2005. Memo 05DV3/0454.
- [69] S.R. Reid G. Zhou e.a. *Impact behaviour of fibre-reinforced composite materials and structures*. Woodhead Publishing, 2000.
- [70] A. Corigliano. Formulation, identification and use of interface models in the numerical analysis of composite delamination. *International Journal of Solid Structures*, 30:2779–2811, 1993.
- [71] R. Hill. Theory of mechanical properties of fibre-strengthened materials: I elastic behaviour. *Journal of the Mechanics and Physics of Solids*, 12:199–212, 1964.
- [72] DDS Simulia. *ABAQUS Analysis User's Manual Version 6.7*, 2007.
- [73] DDS Simulia. *ABAQUS Theory manual v. 6.7*, 2007.



ISBN/EAN: 978-94-6191-023-3

TNO

Stellingen behorende bij het proefschrift

‘High-speed impact modelling and testing of Dyneema composite’

- 1) Ontkoppeling van filament-eigenschappen, zoals gedaan is in het ‘Lumped filament-bundle model’, is noodzakelijk om op realistische wijze gedrag van Dyneema composiet met simulatie modellen te beschrijven.
 - 2) Smelten is geen dominant faalmechanisme dat optreedt tijdens projectielinslag op Dyneema composiet.
 - 3) De ontwikkelde modellen in dit proefschrift zijn ook waardevol voor de ontwikkeling van kogelwerende vesten.
 - 4) Het effect van overgewicht en ondergewicht in de maatschappij is vergelijkbaar te noemen.
 - 5) Fusie van vakgebieden is een teken van vooruitgang.
 - 6) De ontwikkeling van een samenleving wordt niet alleen bepaald door de kwaliteit van het onderwijs, maar ook door het aantal behaalde diploma’s per persoon.
 - 7) De activeringsenergie bij een mens correleert in hoge mate met de (on)zekerheid van het individu.
 - 8) In het bedrijfsleven heeft eerlijkheid als basisprincipe plaatsgemaakt voor integriteit.
 - 9) Diversiteit binnen een gemeenschap kan men niet zuiver vaststellen door het kwantitatief maken van doorsnedes van deze gemeenschap.
 - 10) Zonder overschatting van mogelijkheden kan er geen vooruitgang zijn.
-

Deze stellingen orden opponeerbaar en verdedigbaar geacht en zijn als zodanig goedgekeurd door de promotoren prof. dr. ir. L.J. Ernst en prof. dr. ir. D.J. Rixen.

Béate D. Heru Utomo

Propositions accompanying the thesis

‘High-speed impact modelling and testing of Dyneema composite’

- 1) Decoupling the filament properties, as done in the Lumped filament-bundle model, is necessary to realistically describe Dyneema composite behaviour with simulation models.
 - 2) Melting is not a dominant failure mechanism that occurs during projectile impact on Dyneema composite.
 - 3) The developed models in this thesis are also valuable for the development of bulletproof vests.
 - 4) The effect of overweight and underweight in society can be assumed comparable.
 - 5) Fusion of fields of expertise is a sign of progress.
 - 6) The development of a society is not only determined by the quality of education, but also by the number of degrees obtained by an individual.
 - 7) The activation energy of a human being correlates highly with the (un)confidence of the individual.
 - 8) In the private sector, honesty as a basic principle has been replaced by integrity.
 - 9) Diversity within a community cannot be determined precisely by making quantitative cross-sections of this community only.
 - 10) Without overrating possibilities, progress cannot exist.
-

These propositions are regarded as opposable and defensible and have been approved as such by the supervisors prof. dr. ir. L.J. Ernst and prof. dr. ir. D.J. Rixen.

Béate D. Heru Utomo